On Negative Motor Areas and Response Inhibition

by

Mitchell Garant Fisher

A dissertation accepted and approved in partial fulfillment of the

requirements for the degree of

Doctor of Philosophy

in Human Physiology

Dissertation Committee:

Dr. Ian Greenhouse, Chair

Dr. Nicole Swann, Core Member

Dr. Andrew Karduna, Core Member

Dr. Ulrich Mayr, Institutional Representative

University of Oregon

Winter 2026

DISSERTATION ABSTRACT

Mitchell Garant Fisher

Doctor of Philosophy in Human Physiology

Title: On Negative Motor Areas and Response Inhibition

Inhibitory control is the cognitive ability to flexibly suppress thoughts and actions before, during or after they have been initiated. This is a crucial function known as response inhibition, which allows us to safely navigate our environments. Previous work suggests rapid action cancellation is manifested through an inhibitory neural network which exerts transient, nonselective suppression of the motor system. However, limitations with some methods make it difficult to capture the timing and duration in which inhibitory effects present in peripheral effectors (i.e. muscular activity). Specifically, the question remains: when does the 'point of no return' occur, after which an action cannot be aborted? To address this question, I designed a pair of experiments using a standard laboratory-based response inhibition task (the stop signal task; SST) combined with measures of muscle activity (electromyography; EMG) to more precisely identify inhibitory events related to successful and failed stopping. Next, I carried out a series of experiments to more directly interrogate cortical regions implicated in the response inhibition network. These regions are known as negative motor areas, are crucial for motor control, and have considerable overlap with key regions in the response inhibition network. Presently, the negative motor network has only been studied in the context of resective surgery, using electrical stimulation to map these functional areas. Stimulation of negative motor areas (e.g. inferior frontal cortex) causes interruptions and/or arrest of vocalizations or manual movements, which implies inhibitory influence on peripheral muscles. We designed a novel method of non-invasively stimulating negative motor areas with transcranial magnetic stimulation (TMS) in healthy adults that were performing sustained muscular contractions. With this method, we

recorded evoked responses in EMG signal related to the stimulation. We refined this approach by utilizing participant MRI scans to more precisely target individual anatomical structures with TMS and successfully replicated our previous findings. Finally, we compared the evoked muscular responses with stopping metrics from a response inhibition task. A primary goal for the negative motor area studies was to guide methods for improving clinical, non-invasive evaluation of the motor system.

This dissertation includes previously published co-authored material.

ACKNOWLEDGEMENTS

This thesis was only possible due to the support of many friends, family and colleagues who have helped along the way.

- First and foremost, thank you to Dr. Ian Greenhouse for your guidance, mentorship, friendship, and patience throughout my time at UO. You've given me countless opportunities and continuous support, even when there were challenges. You're a great mentor. I'm proud of the work you do, and how you do it.
- Thank you to my committee for your support and helpful guidance. Most importantly, thank you for helping me focus my ideas for these final experiments.
- My wife, Baila, for endless support, encouragement, understanding, and chai.
- Dr. Corey Wadsley, and the New Zealand research team. Thank you for collaborating with us during the Covid-19 pandemic. The final projects wouldn't have been possible without your insight, dedication, and advice.
- Former mentees that have collaborated, assisted, or taken part in this work: Hoa Trinh, Isaiah Mills, Chris Horton, Lina Gutierrez & Jessica O'Neill.
- Lab mates and collaborators: Dr. Kelsey Schultz, Hayami Nishio, Rubi Ruopp, Dr. Alex Rockhill, Dr. Sara Parmigiani. You've all made this experience about so much more than science.
- My parents, Bruce and Renee Fisher, for your encouragement, belief, and support.
- My brother, Matthew Fisher for engaging in long talks about humans, and engines, and everything in between.
- The cats at home: Belle and Monet, the best distractions.
- The rest of my family and friends for support and encouragement along the way.

DEDICATION

This thesis is dedicated to Jules and my family and friends, especially those who are no longer with us. You are all missed dearly.

TABLE OF CONTENTS

LISTS OF FIGURES

Figure Page

LIST OF TABLES

Table Page

CHAPTER I

INTRODUCTION

Background on Inhibitory Control

The ability to cancel an initiated movement is an essential aspect of daily life which allows individuals to adapt to dynamic environments. A common example would be having to quickly stop oneself from stepping into the street when a car unexpectedly appears. In this scenario, it is critical to rapidly cancel one motor plan and initiate a new plan that prioritizes safety. This rapid termination of pre-planned or ongoing actions in response to changes in the environment is known as response inhibition (Logan & Cowan, 1984). These inhibitory mechanisms may be fundamental for motor and cognitive control. Inhibitory deficits are linked to neurological and neuropsychiatric disorders ranging from attention-deficit hyperactivity disorder (Nigg, 1999) to Parkinson's disease, one of the most common motor control disorders (Bissett et al., 2015; Gauggel et al., 2004a; MacDonald & Byblow, 2015). Given the importance of response inhibition in everyday life and the impact of inhibitory control deficits, there is a need for thorough understanding of the neural mechanisms and circuitry responsible for implementation of this ability.

Response inhibition is frequently studied in separate parts: proactive and reactive inhibition. These terms are in relation to whether inhibitory control is enacted before or after stop signals used during motor control tasks, respectively (Aron, 2011; Braver, 2012). Reactive inhibition is exhibited in the car scenario above in which the person needs to quickly cancel a movement in response to a stimulus. Proactive inhibitory control on the other hand refers to regulation of behavior in anticipation of a possible need to stop (Zandbelt et al., 2013). To continue with the car and pedestrian analogy, an example of proactive inhibition could be

walking more slowly as they approach a busy intersection where cars frequently speed around a corner. Both proactive and reactive inhibition are necessary for effective inhibitory control to successfully interact with our environments. Understanding the timing, duration, and networks response for successful inhibition is vital for improving safety and implementing new clinical practices regarding motor control.

Investigating Response Inhibition

Behavioral Measures of Response Inhibition

It is difficult to assess response inhibition in real world scenarios; therefore, laboratory tasks were devised to test the mechanisms at play in a controlled setting. In fact, a considerable amount of our understanding of motor inhibition can be attributed to tasks such as the stop signal task (SST; Logan & Cowan, 1984). In these tasks, participants are instructed to make rapid responses to audio or visual stimuli. Most trials in a SST require a response (often a button press) to a "Go" signal. On a minority of trials (e.g. 25-33%), a "Stop" signal is presented shortly after the Go signal, and participants attempt to withhold their response, or cancel a movement that has been initiated. The interval between the go and stop signal, known as the stop signal delay, can be adjusted dynamically after each stop trial based on a participant's performance to ensure an equal distribution of successful and failed stop trials. Essentially, the stop-signal delay (SSD) is lengthened when participants correctly withhold a response and shortened when they inappropriately respond after a Stop signal, with the aim of identifying a SSD that results in a 50% success to failure rate. The SSD allows the derivation of a key measure known as the stop-signal reaction time (SSRT). SSRT estimates the latent speed of stopping. This is essential for comparing stopping speed between studies due to the nature of successful stopping happening as

a covert process. When a participant succeeds at stopping, there is no behavioral response recorded, making it difficult to measure how long the stopping process takes.

An alternative paradigm to SSTs is the anticipatory response inhibition task (ARI; Slater-Hammel, 1960). Trials in ARI tasks have an indicator that progresses at a steady pace towards a target. The participant's objective is to time their response (most commonly to press a button or release a button press) when the indicator reaches the target, thus stopping the indicator. This is often presented as two vertical rectangles on a computer screen that 'fill' from the bottom at a predictable rate (He et al., 2022). The stop signal trials automatically halt the indicator before it reaches the target, requiring the participant to withhold their go response. Like the SST, ARI tasks are generally designed with variable SSDs to allow for estimation of SSRT.

The variable property of SSD allows for modeling of stopping behavior with the independent race model (Logan & Cowan, 1984). This model assumes going and stopping processes are independent, and the behavioral outcome is a result of which process completes first. Successful stops by nature do not yield a response in SSTs or ARIs. Failed stops, according to the independent race model are essentially a go process that 'won' the race with over a stop process to results in a response (Band et al., 2003; Frank, 2006; Logan & Cowan, 1984). This is a suitable model for conceptualizing cognitive control of inhibition. However, violations of the independent race model contend the independence of these processes (Bissett et al., 2021). One of these violations occurs from tasks involving a short SSD (< 200 ms), where stop failure RTs become slower than go RTs. This should be impossible if go and stop processes are independent and instead suggests that the stop signal can interact with and perturb the ongoing go process during late stages of movement preparation. Rather than reflecting a simple race outcome, these

slowed stop failures may represent partially inhibited actions that escape cancellation. This violation is important for this thesis, which involves rapid cancellation of ballistic processes.

Although these tasks have been very effective for probing the mechanisms of inhibitory control, there are some shared limitations which are necessary to address. As mentioned above, these paradigms do not allow for a direct measure for the speed of stopping, and pairing behavioral methods with electrophysiological measures could improve our understanding of inhibitory timing, especially for estimates of the speed of stopping.

Physiological Measures of Stopping

One way to increase sensitivity to stopping speed is to combine response inhibition tasks with an electrophysiological measure such as electromyography (EMG) to collect activity from the muscles involved in responding to task stimuli. Stopping can occur before or after muscular activity begins. Studies over the past few decades have employed this method to more precisely analyze timing and patterns of muscle activation depending on the outcome of trials (i.e. successful stop, failed stop). When evaluating EMG from successful stop trials, authors noticed trials in which participants began to respond, as evidenced by an increase in EMG activity, yet the participants did not complete the motor response (button press). These "partial response" trials are of interest when compared to other successful stop trials in which no EMG activity was recorded, since there is a presumed inhibitory process occurring (Fisher et al., 2024; Jana et al., 2020; Raud et al., 2020, 2022). Specifically, the EMG on these partial response trials will increase and then decrease. In an important study, Jana et al., (2020) measured the time from the stop signal to this inflection point, creating a single trial metric termed 'Canceltime'. Canceltime provides a direct electrophysiological measure of the timing in which inhibitory influence arrives to a task-relevant effector.

Canceltime and inspection of partial responses with EMG are useful metrics which help address a prevailing concern with SSRT. Namely, SSRT is suspected to overestimate a person's true speed of stopping by as much as 100 ms (Bissett et al., 2021; Skippen et al., 2019). Further overestimation of SSRT is likely a result of another covert process known as "trigger failures" that is difficult to assess or build into the SSRT calculation. Trigger failures occur on stop trials in which participants fails to discern or respond to a stop signal, allowing the go process to continue uncontested from the stop process (Matzke et al., 2017, 2019). Essentially, a subset of stop trials is indistinguishable from go trials, which affects the staircasing of the SSD, the failed stop trial RT distribution, and ultimately inflates the SSRT estimate. EMG can improve our understanding of the timing of inhibition.

Finally, it is worth discussing the concept of strategic slowing in SSTs and the implication of slowing on stopping metrics (Verbruggen et al., 2019). Success on a stop trial generally requires no response, meaning participants are implicitly encouraged to proactively withhold responses until the trial type is determined (i.e. go or stop) to increase their chance of success. As a result, RTs are prolonged in tasks with stop signals, especially so when tasks have high probabilities of stop signals (Chikazoe et al., 2009; Jahfari et al., 2010). Feedback is often given to encourage participants not to wait for a stop signal. Additionally, it is common to incentivize speeded responses by awarding points for responding quickly on go trials and for successfully stopping responses on stop trials.

Response Inhibition Network

Motor inhibition tasks have provided a framework to investigate the inhibitory control system and provided significant insights into the underlying neural circuitry. A prominent current model of the inhibitory control system involves a cortico-basal ganglia thalamocortical

circuit. Integral nodes of this network include the right inferior frontal cortex (rIFC), pre-supplementary motor area (preSMA) and the primary motor cortex (M1) (Aron, Durston, et al., 2007; Aron & Poldrack, 2006; N. Swann et al., 2009; N. C. Swann et al., 2012). Imaging and invasive neurophysiological studies have identified the hyperdirect pathway as a presumably monosynaptic white matter fiber tract connecting the rIFC and preSMA with regions of the basal ganglia, specifically the subthalamic nucleus (STN), as critical for inhibiting the motor system (Aron, Durston, et al., 2007; Chen et al., 2020; Nambu et al., 2002).

Numerous studies have shown relationships between STN activity and stopping behavior (Chen et al., 2020; Diesburg et al., 2021; Forstmann et al., 2012; Isherwood et al., 2023; Singh et al., 2021). It is thought the STN functions in the response inhibition network by broadly exciting the inhibitory output nuclei of the basal ganglia to suppress the motor nuclei of the thalamus (Badry et al., 2009; Cai, Oldenkamp, et al., 2012; Greenhouse et al., 2011; Narayanan et al., 2020; Wessel & Aron, 2017). Damage to or simulated "lesioning" of rIFC with repetitive transcranial magnetic stimulation (rTMS) results in inhibitory deficits (Aron et al., 2003; Chambers et al., 2006). This implicates the rIFC as a key region that exerts control over a potent subcortical inhibitory network. The preSMA is another cortical region with hyperdirect anatomical projections to the STN and is also implicated in stopping (Aron, Behrens, et al., 2007; Yeung et al., 2021). The potentially dissociable contributions of the preSMA and rIFC to motor inhibition via the hyperdirect pathway have not been clearly delineated.

Global Motor Suppression and the Hyperdirect Pathway

Rapid action cancellation appears to engage a global inhibitory mechanism that transiently suppresses the motor system. Behavioral evidence suggests this idea using selective stopping paradigms. In bimanual ARI tasks, participants were instructed to stop one response

while continuing the other exhibited delayed responses in the continuing hand (Coxon et al., 2006). This "stopping-interference effect" has been replicated (Aron & Verbruggen, 2008; Claffey et al., 2010; MacDonald et al., 2012) and suggests rapid stopping may rely on a nonselective pause of the motor system, after which the selected action must be re-initiated.

There is converging neurophysiological evidence that this global suppression is mediated by the hyperdirect pathway connecting the rIFC and preSMA to the STN. Activation of the STN broadly excites the basal ganglia output nuclei which increases thalamic inhibition ultimately preventing movement or inhibiting actions that are underway. There is considerable evidence that STN projections are not somatotopically selective (Gillies & Willshaw, 1998; Mink, 1996; Nambu et al., 2002), meaning this pathway is well-suited to produce a rapid, widespread suppression of motor output. These findings suggest successful stopping involves a global inhibition of the motor system. Although this mechanism is generally accepted, the precise timing this inhibitory signal reaches the peripheral effectors remains unclear.

Transcranial Magnetic Stimulation During Stopping

Further support for a global stopping mechanism comes from studies using transcranial magnetic stimulation (TMS) which is a non-invasive brain stimulation technique used to induce a current in cortical regions of the brain. When TMS is applied to the motor cortex (M1), specific muscle representations are targeted to evoke a motor-evoked potential (MEP) in the EMG recorded from the targeted muscle to serve as an index of corticospinal excitability (Barker et al., 1985; Hess et al., 1987). MEPs can be recorded while a participant is performing a task such as a SST, and the amplitude of the MEP offers temporally precise insight into the state of excitability of the motor system. One of the first studies to investigate corticospinal excitability in a stop-signal context found MEPs were suppressed in task-irrelevant, muscles on stop trials that

participants successfully canceled their response (Badry et al., 2009). Interestingly, MEP suppression was also observed on successful stop trials in leg muscles that were irrelevant to the task, therefore it is likely that a nonselective, inhibitory process was able to override or interrupt the initiated go response. This widespread stopping effect was replicated in studies that involved stopping manual responses, speech and eye saccades (Cai, Oldenkamp, et al., 2012; Greenhouse et al., 2011; Majid et al., 2012; Wessel et al., 2013). Based on these results, research has focused on determining the neural mechanisms that may explain this global effect of reactive stopping on the motor system.

Electrophysiology During Stopping

Some of the most compelling evidence for a global stopping signature has come from a rodent model due to the ability to record single unit firing rates from neurons within deep brain structures such as the basal ganglia. Schmidt et al. trained rats to perform a stop-signal task and collected firing rates from neurons in the STN and the globus pallidus internal segment (GPi; 2013). It was found that STN activity always increased after a stop cue was presented, but only on trials that the rats were successful at inhibiting their movements was activity increased in the GPi. On failed trials, inhibitory activity from the cortico-striatal pathway suppressed GPi and led to initiation of movement.

It is somewhat rare to be able to record from the basal ganglia in humans, but there is an opportunity when patients with motor disorders have had deep brain stimulus (DBS) electrodes implanted in their STN to improve motor symptoms (Little et al., 2016). Wessel et al. performed a study in DBS patients with Parkinson's Disease (PD) and recorded STN firing rate activity while simultaneously stimulating M1 with TMS (targeting a task-irrelevant hand muscle) while the patients performed a vocal stop-signal task (2016). It was found that STN activity in the beta

band was increased during successful stopping and global motor suppression as inferred by suppression of MEP amplitude was correlated with higher beta power. This finding is significant because it links activity of the STN directly with an index of global motor suppression, while replicating results from Cai et al. (2012), of stopping speech.

Unfortunately, it is difficult to know the exact time that the global stopping mechanism manifests in the motor system and even more difficult to measure the full time course of suppression. Currently, one of the best methods for detecting the time of motor system inhibition is by measuring the corticospinal excitability with TMS. The primary drawback with this method is that TMS is not a continuous measure. It only gives a snapshot of the excitability at individual time points. For example, in Badry et al., the authors found MEPs to be most suppressed at a time point of 400 ms after the go stimulus, which was about 50 ms earlier than the mean go RT of participants in the experiment (2009). It is unknown whether this is the peak of the suppression or at what time point the motor system was initially suppressed without having to collect an exorbitant number of trials across many TMS stimulation time points. Therefore, mapping the full time-course of suppression in the motor system has not yet been achieved.

Negative Motor System

Positive and Negative Motor Responses Elicited with Stimulation

As described above, excitability of the corticospinal pathway can be indexed non-invasively with single-pulse TMS by stimulating M1 regions to elicit a MEP in a targeted effector (Bestmann & Krakauer, 2015; Di Lazzaro et al., 2004; Sauv & Crowther, 2014). When magnetic or electrical stimulation of the cortex activates peripheral muscles leading to vocalizations, movements or twitches (such as MEPs), these are categorized as positive motor responses (PMRs).

Direct electrical stimulation (DES) of the brain is a standard method during intracranial resective surgery useful for mapping areas of the cortex that are responsible for eloquent functions such as speech and fine motor control. The field of DES mapping was pioneered in humans in the 1930s and 1940s when it was discovered electrically stimulating portions of the sensorimotor cortex produced vocalizations and overt movements (Foerster, 1931, 1936; Penfield, 1938, 1949; Penfield & Jasper, 1954). When these cortical areas (primarily sensorimotor cortex) are stimulated and produce movement or vocalizations, they are labeled as positive motor areas (PMA) (Penfield, 1938). While mapping areas of the inferior frontal gyrus and supplementary motor area, Penfield and colleagues noticed a peculiar phenomenon of speech arrest. These observations were some of the first characterizations of what are now known as negative motor responses (NMRs) caused by the stimulation of negative motor areas (NMA) of the frontal cortex. The function of these areas and how they were connected to the motor system were unclear. Since this original characterization of NMRs, the negative motor system has only been opportunistically studied, primarily from PMR mapping during intraoperative surgery for tumor or epileptogenic zone resection (Ikeda et al., 1993, 1995; Lim et al., 1994; Luders, 1987).

As technology improved for monitoring epileptic patients, Lüders et al. (1988) collected extraoperative recordings and performed more extensive mapping which resulted in more reproducible studies with improved patient comfort. Lüders and colleagues (1995) offered a more concrete definition of NMRs: the complete inhibition of movement without loss of muscle tone or consciousness. In most cases, DES of the cortex is the gold standard method of mapping functional cortical regions, including NMAs. Unfortunately, aspects of DES are somewhat poorly understood and this method of stimulation can result in contradictory behavioral effects and often, unpredictable results (Borchers et al., 2012). It appears that the result of cortical DES

is a complex computation which includes factors such as the strength of current, and pre-stimulation firing rate of neurons at the stimulation site. These factors make it difficult to predict whether stimulation will yield excitatory or inhibitory effects Furthermore, cortical mapping during surgery is more of a practical matter in which overt behaviors or inhibition of behaviors are observed to determine functionality in lieu of measured physiological output. Regardless, this has been a worthwhile endeavor as aspects of the negative motor system come into focus including NMA laterality (Borggraefe et al., 2016), connections based on tractography (Rech et al., 2019; Viganò et al., 2019; Yokoyama et al., 2020), and some insight into reduced bimanual control when NMAs are surgically resected (Rech et al., 2014). More recently, investigations have begun collecting EMG during mapping procedures to better understand the complex nature of negative motor functionality (Fornia et al., 2020; Viganò et al., 2021).

Negative Motor Areas and Response Inhibition

Intriguingly, there is considerable overlap between cortical regions implicated in the response inhibition network and regions that have been identified as NMAs. Specifically, preSMA and rIFC have been frequently identified as NMAs, and have substantial evidence linked to the inhibitory motor control system. To date, NMRs and reactive inhibition have not been studied together. Nearly the entire body of literature associated with NMAs is collected from surgical mapping using DES. These studies are niche, expensive, and only performed with clinical populations. Determining if NMRs can be elicited with non-invasive methods, and if there is a link between NMRs and response inhibition could open exciting new avenues to study the motor system.

Summary

Candidate neural inhibitory control mechanisms have been identified but specifics on their functionality remain. Considering the evidence regarding global suppression of corticomotor excitability is primarily established with TMS and MR methods, the precise timing in which inhibitory drive reaches peripheral effectors and the duration of the associated muscular inhibition have yet to be established. There also remain many open questions regarding NMAs, NMRs in healthy populations. Specifically, whether there are non-invasive methods to investigate the negative motor system (i.e. elicit NMRs). Finally, if characteristics of NMRs are related to metrics of response inhibition.

To address these questions, I designed a novel EMG setup paired with a SST to identify peripheral measures of inhibitory influence. In Chapter II, I address the gap in knowledge regarding the timing and duration of motoric inhibition in peripheral muscles during a SST. We examined the EMG during successful and failed stops to determine whether there is a point of no return in which the magnitude and rate of EMG onset determine success or failure in stopping. Chapter II was previously published in the Journal of Cognitive Neuroscience with Hoa Trinh, Jessica O'Neill, and Ian Greenhouse. This experiment led to a follow-up study led by an undergraduate student, Isaiah Mills, who I co-mentored. That study mirrored my setup using an ARI task to address a similar hypothesis. Isaiah's work was submitted for his honor's thesis, and subsequently published in eNeuro (Mills et al., 2025) Isaiah's findings are briefly described in the bridge between Chapters II and III.

In Chapter III, we collaborated with the University of Auckland to collect human subjects' data during the COVID-19 pandemic. We collectively designed a novel method to stimulate NMAs with non-invasive TMS delivered to frontal cortical regions of the brain. We

examined whether stimulation over frontal targets evoked EMG responses in tonically active muscles. In Chapter IV, we refined these methods by utilizing neuro-navigation to guide our stimulation based on individual anatomy to more precisely stimulate regions of interest. We then compared the results of our stimulation with metrics of stopping from SSTs to determine if stimulation effects of candidate NMAs relate to response inhibition. One goal of the work presented in Chapters III and IV is to guide methods for improving clinical evaluation of the motor system using non-invasive approaches.

REFERENCES CITED

Aron, A. R. (2011). From reactive to proactive and selective control: Developing a richer model for stopping inappropriate responses. *Biological Psychiatry*, *69*(12), e55–e68.

Aron, A. R., Behrens, T. E., Smith, S., Frank, M. J., & Poldrack, R. A. (2007). Triangulating a cognitive control network using diffusion-weighted magnetic resonance imaging (MRI) and functional MRI. *Journal of Neuroscience*, *27*(14), 3743–3752.

Aron, A. R., Durston, S., Eagle, D. M., Logan, G. D., Stinear, C. M., & Stuphorn, V. (2007). Converging Evidence for a Fronto-Basal-Ganglia Network for Inhibitory Control of Action and Cognition. *Journal of Neuroscience*, *27*(44), 11860–11864. https://doi.org/10.1523/JNEUROSCI.3644-07.2007

Aron, A. R., Fletcher, P. C., Bullmore, E. T., Sahakian, B. J., & Robbins, T. W. (2003). Stop-signal inhibition disrupted by damage to right inferior frontal gyrus in humans. *Nature Neuroscience*, *6*(2), 115–116.

Aron, A. R., & Poldrack, R. A. (2006). Cortical and Subcortical Contributions to Stop Signal Response Inhibition: Role of the Subthalamic Nucleus. *The Journal of Neuroscience*, *26*(9), 2424–2433. https://doi.org/10.1523/JNEUROSCI.4682-05.2006

Aron, A. R., & Verbruggen, F. (2008). Stop the Presses: Dissociating a Selective From a Global Mechanism for Stopping. *Psychological Science*, *19*(11), 1146–1153. https://doi.org/10.1111/j.1467-9280.2008.02216.x

Badry, R., Mima, T., Aso, T., Nakatsuka, M., Abe, M., Fathi, D., Foly, N., Nagiub, H., Nagamine, T., & Fukuyama, H. (2009). Suppression of human cortico-motoneuronal excitability during the Stop-signal task. *Clinical Neurophysiology*, *120*(9), 1717–1723.

Band, G. P. H., van der Molen, M. W., & Logan, G. D. (2003). Horse-race model simulations of the stop-signal procedure. *Acta Psychologica*, *112*(2), 105–142. https://doi.org/10.1016/S0001-6918(02)00079-3

Barker, A. T., Jalinous, R., & Freeston, I. L. (1985). Non-invasive magnetic stimulation of human motor cortex. *The Lancet*, *325*(8437), 1106–1107.

Bekker, E. M., Kenemans, J. L., Hoeksma, M. R., Talsma, D., & Verbaten, M. N. (2005). The pure electrophysiology of stopping. *International Journal of Psychophysiology*, *55*(2), 191–198.

Bestmann, S., & Krakauer, J. W. (2015). The uses and interpretations of the motor-evoked potential for understanding behaviour. *Experimental Brain Research*, *233*(3), 679–689. https://doi.org/10.1007/s00221-014-4183-7

Bissett, P. G., Jones, H. M., Poldrack, R. A., & Logan, G. D. (2021). Severe violations of independence in response inhibition tasks. *Science Advances*, *7*(12), eabf4355. https://doi.org/10.1126/sciadv.abf4355

Bissett, P. G., Logan, G. D., van Wouwe, N. C., Tolleson, C. M., Phibbs, F. T., Claassen, D. O., & Wylie, S. A. (2015). Generalized Motor Inhibitory Deficit in Parkinson's Disease Patients who Freeze. *Journal of Neural Transmission (Vienna, Austria : 1996)*, *122*(12), 1693–1701. https://doi.org/10.1007/s00702-015-1454-9

Borggraefe, I., Catarino, C. B., Rémi, J., Vollmar, C., Peraud, A., Winkler, P. A., & Noachtar, S. (2016). Lateralization of cortical negative motor areas. *Clinical Neurophysiology*, *127*(10), 3314–3321.

Braver, T. S. (2012). The variable nature of cognitive control: A dual mechanisms framework. *Trends in Cognitive Sciences*, *16*(2), 106–113.

Cai, W., Oldenkamp, C. L., & Aron, A. R. (2012). Stopping speech suppresses the task-irrelevant hand. *Brain and Language*, *120*(3), 412–415.

Chambers, C. D., Bellgrove, M. A., Stokes, M. G., Henderson, T. R., Garavan, H., Robertson, I. H., Morris, A. P., & Mattingley, J. B. (2006). Executive "brake failure" following deactivation of human frontal lobe. *Journal of Cognitive Neuroscience*, *18*(3), 444–455.

Chen, W., Hemptinne, C. de, Miller, A. M., Leibbrand, M., Little, S. J., Lim, D. A., Larson, P. S., & Starr, P. A. (2020). Prefrontal-Subthalamic Hyperdirect Pathway Modulates Movement Inhibition in Humans. *Neuron*, *106*(4), 579-588.e3. https://doi.org/10.1016/j.neuron.2020.02.012

Chikazoe, J., Jimura, K., Hirose, S., Yamashita, K., Miyashita, Y., & Konishi, S. (2009). Preparation to inhibit a response complements response inhibition during performance of a stop-signal task. *Journal of Neuroscience*, *29*(50), 15870–15877.

Claffey, M. P., Sheldon, S., Stinear, C. M., Verbruggen, F., & Aron, A. R. (2010). Having a goal to stop action is associated with advance control of specific motor representations. *Neuropsychologia*, *48*(2), 541–548.

Coxon, J. P., Stinear, C. M., & Byblow, W. D. (2006). Intracortical inhibition during volitional inhibition of prepared action. *Journal of Neurophysiology*, *95*(6), 3371–3383.

Di Lazzaro, V., Oliviero, A., Pilato, F., Saturno, E., Dileone, M., Mazzone, P., Insola, A., Tonali, P. A., & Rothwell, J. C. (2004). The physiological basis of transcranial motor cortex stimulation in conscious humans. *Clinical Neurophysiology*, *115*(2), 255–266. https://doi.org/10.1016/j.clinph.2003.10.009

Diesburg, D. A., Greenlee, J. D., & Wessel, J. R. (2021). Cortico-subcortical β burst dynamics underlying movement cancellation in humans. *Elife*, *10*, e70270.

Fisher, M., Trinh, H., O'Neill, J., & Greenhouse, I. (2024). Early rise and persistent inhibition of electromyography during failed stopping. *Journal of Cognitive Neuroscience*, *36*(7), 1412–1426.

Foerster, O. (1931). The cerebral cortex in man. *Lancet*, *2*, 309–312.

Foerster, O. (1936). The motor cortex in man in the light of Hughlings Jackson's doctrines. *Brain*, *59*(2), 135–159.

Fornia, L., Puglisi, G., Leonetti, A., Bello, L., Berti, A., Cerri, G., & Garbarini, F. (2020). Direct electrical stimulation of the premotor cortex shuts down awareness of voluntary actions. *Nature Communications*, *11*(1), 705.

Forstmann, B. U., Keuken, M. C., Jahfari, S., Bazin, P.-L., Neumann, J., Schäfer, A., Anwander, A., & Turner, R. (2012). Cortico-subthalamic white matter tract strength predicts interindividual efficacy in stopping a motor response. *NeuroImage*, *60*(1), 370–375. https://doi.org/10.1016/j.neuroimage.2011.12.044

Frank, M. J. (2006). Hold your horses: A dynamic computational role for the subthalamic nucleus in decision making. *Neural Networks*, *19*(8), 1120–1136.

Gillies, A. J., & Willshaw, D. J. (1998). A massively connected subthalamic nucleus leads to the generation of widespread pulses. *Proceedings. Biological Sciences*, *265*(1410), 2101–2109. https://doi.org/10.1098/rspb.1998.0546

Greenhouse, I., Oldenkamp, C. L., & Aron, A. R. (2011). Stopping a response has global or nonglobal effects on the motor system depending on preparation. *Journal of Neurophysiology*, *107*(1), 384–392.

Greenhouse, I., & Wessel, J. R. (2013). EEG signatures associated with stopping are sensitive to preparation. *Psychophysiology*, *50*(9), 900–908.

He, J. L., Hirst, R. J., Puri, R., Coxon, J., Byblow, W., Hinder, M., Skippen, P., Matzke, D., Heathcote, A., Wadsley, C. G., Silk, T., Hyde, C., Parmar, D., Pedapati, E., Gilbert, D. L., Huddleston, D. A., Mostofsky, S., Leunissen, I., MacDonald, H. J., … Puts, N. A. J. (2022). OSARI, an Open-Source Anticipated Response Inhibition Task. *Behavior Research Methods*, *54*(3), 1530–1540. https://doi.org/10.3758/s13428-021-01680-9

Hess, C. W., Mills, K. R., Murray, N. M. F., & Schriefer, T. N. (1987). Magnetic brain stimulation: Central motor conduction studies in multiple sclerosis. *Annals of Neurology*, *22*(6), 744–752. https://doi.org/10.1002/ana.410220611

Ikeda, A., Lüders, H. O., Burgess, R. C., & Shibasaki, H. (1993). Movement-related potentials associated with single and repetitive movements recorded from human supplementary

motor area. *Electroencephalography and Clinical Neurophysiology*, *89*(4), 269–277. https://doi.org/10.1016/0168-5597(93)90106-y

Isherwood, S. J. S., Kemp, S., Miletic, S., Stevenson, N., Bazin, P.-L., & Forstmann, B. (2023). The canonical stopping network: Revisiting the role of the subcortex in response inhibition. *bioRxiv*, 2023–06.

Jahfari, S., Stinear, C. M., Claffey, M., Verbruggen, F., & Aron, A. R. (2010). Responding with Restraint: What Are the Neurocognitive Mechanisms? *Journal of Cognitive Neuroscience*, *22*(7), 1479–1492. https://doi.org/10.1162/jocn.2009.21307

Jana, S., Hannah, R., Muralidharan, V., & Aron, A. R. (2020). Temporal cascade of frontal, motor and muscle processes underlying human action-stopping. *eLife*, *9*, e50371. https://doi.org/10.7554/eLife.50371

Lim, S. H., Dinner, D. S., Pillay, P. K., Lüders, H., Morris, H. H., Klem, G., Wyllie, E., & Awad, I. A. (1994). Functional anatomy of the human supplementary sensorimotor area: Results of extraoperative electrical stimulation. *Electroencephalography and Clinical Neurophysiology*, *91*(3), 179–193.

Little, S., Beudel, M., Zrinzo, L., Foltynie, T., Limousin, P., Hariz, M., Neal, S., Cheeran, B., Cagnan, H., & Gratwicke, J. (2016). Bilateral adaptive deep brain stimulation is effective in Parkinson's disease. *Journal of Neurology, Neurosurgery & Psychiatry*, *87*(7), 717–721.

Logan, G. D., & Cowan, W. B. (1984). On the ability to inhibit thought and action: A theory of an act of control. *Psychological Review*, *91*(3), 295. https://doi.org/10.1037/0033-295X.91.3.295

Luders, H. (1987). Negative motor responses elicited by stimulation of the human cortex. *Advonces in Epileptology*, *16*, 229–231.

Lüders, H. O., Dinner, D. S., Morris, H. H., Wyllie, E., & Comair, Y. G. (1995). Cortical electrical stimulation in humans. The negative motor areas. *Advances in Neurology*, *67*, 115–129.

MacDonald, H. J., & Byblow, W. D. (2015). Does Response Inhibition Have Pre- and Postdiagnostic Utility in Parkinson's Disease? *Journal of Motor Behavior*, *47*(1), 29–45. https://doi.org/10.1080/00222895.2014.941784

MacDonald, H. J., Stinear, C. M., & Byblow, W. D. (2012). Uncoupling response inhibition. *Journal of Neurophysiology*, *108*(5), 1492–1500. https://doi.org/10.1152/jn.01184.2011

Majid, D. S. A., Cai, W., George, J. S., Verbruggen, F., & Aron, A. R. (2012). Transcranial Magnetic Stimulation Reveals Dissociable Mechanisms for Global Versus Selective Corticomotor Suppression Underlying the Stopping of Action. *Cerebral Cortex*, *22*(2), 363–371. https://doi.org/10.1093/cercor/bhr112

Mills, I., Fisher, M., Wadsley, C. G., & Greenhouse, I. (2025). Failed stopping transiently suppresses the electromyogram in task-irrelevant muscles. *Eneuro*, *12*(1). https://www.eneuro.org/content/12/1/ENEURO.0166-24.2025.abstract

Mink, J. W. (1996). The basal ganglia: Focused selection and inhibition of competing motor programs. *Progress in Neurobiology*, *50*(4), 381–425.

Nambu, A., Tokuno, H., & Takada, M. (2002). Functional significance of the cortico–subthalamo–pallidal 'hyperdirect'pathway. *Neuroscience Research*, *43*(2), 111–117.

Narayanan, N. S., Wessel, J. R., & Greenlee, J. D. W. (2020). The Fastest Way to Stop: Inhibitory Control and IFG-STN Hyperdirect Connectivity. *Neuron*, *106*(4), 549–551. https://doi.org/10.1016/j.neuron.2020.04.017

Nigg, J. T. (1999). The ADHD Response-Inhibition Deficit as Measured by the Stop Task: Replication with DSM–IV Combined Type, Extension, and Qualification. *Journal of Abnormal Child Psychology*, *27*(5), 393–402. https://doi.org/10.1023/A:1021980002473

Penfield, W. (1938). The cerebral cortex in man: I. The cerebral cortex and consciousness. *Archives of Neurology & Psychiatry*, *40*(3), 417–442.

Penfield, W. (1949). VOCALIZATION AND ARREST OF SPEECH. *Archives of Neurology And Psychiatry*, *61*(1), 21. https://doi.org/10.1001/archneurpsyc.1949.02310070027002

Penfield, W. (1954). Mechanisms of voluntary movement. *Brain: A Journal of Neurology*.

Penfield, W., & Jasper, H. (1954). *Epilepsy and the functional anatomy of the human brain.*

Raud, L., Thunberg, C., & Huster, R. J. (2022). Partial response electromyography as a marker of action stopping. *eLife*, *11*, e70332. https://doi.org/10.7554/eLife.70332

Rech, F., Herbet, G., Gaudeau, Y., Mézières, S., Moureau, J.-M., Moritz-Gasser, S., & Duffau, H. (2019). A probabilistic map of negative motor areas of the upper limb and face: A brain stimulation study. *Brain*, *142*(4), 952–965. https://doi.org/10.1093/brain/awz021

Rech, F., Herbet, G., Moritz-Gasser, S., & Duffau, H. (2014). Disruption of bimanual movement by unilateral subcortical electrostimulation. *Human Brain Mapping*, *35*(7), 3439–3445.

Sauv, é W. M., & Crowther, L. J. (2014). The Science of Transcranial Magnetic Stimulation. *Psychiatric Annals*, *44*(6), 279–283. https://doi.org/10.3928/00485713-20140609-05

Schmidt, R., Leventhal, D. K., Mallet, N., Chen, F., & Berke, J. D. (2013). Canceling actions involves a race between basal ganglia pathways. *Nature Neuroscience*, *16*(8), 1118–1124.

Singh, M., Fuelscher, I., He, J., Anderson, V., Silk, T. J., & Hyde, C. (2021). Inter-individual performance differences in the stop-signal task are associated with fibre-specific microstructure of the fronto-basal-ganglia circuit in healthy children. *Cortex*, *142*, 283–295. https://doi.org/10.1016/j.cortex.2021.06.002

Skippen, P., Matzke, D., Heathcote, A., Fulham, W. R., Michie, P., & Karayanidis, F. (2019). Reliability of triggering inhibitory process is a better predictor of impulsivity than SSRT. *Acta Psychologica*, *192*, 104–117.

Slater-Hammel, A. T. (1960). Reliability, Accuracy, and Refractoriness of a Transit Reaction. *Research Quarterly. American Association for Health, Physical Education and Recreation*, *31*(2), 217–228. https://doi.org/10.1080/10671188.1960.10613098

Swann, N. C., Cai, W., Conner, C. R., Pieters, T. A., Claffey, M. P., George, J. S., Aron, A. R., & Tandon, N. (2012). Roles for the pre-supplementary motor area and the right inferior frontal gyrus in stopping action: Electrophysiological responses and functional and structural connectivity. *NeuroImage*, *59*(3), 2860–2870. https://doi.org/10.1016/j.neuroimage.2011.09.049

Swann, N., Poizner, H., Houser, M., Gould, S., Greenhouse, I., Cai, W., Strunk, J., George, J., & Aron, A. R. (2011). Deep Brain Stimulation of the Subthalamic Nucleus Alters the Cortical Profile of Response Inhibition in the Beta Frequency Band: A Scalp EEG Study in Parkinson's Disease. *Journal of Neuroscience*, *31*(15), 5721–5729. https://doi.org/10.1523/JNEUROSCI.6135-10.2011

Swann, N., Tandon, N., Canolty, R., Ellmore, T. M., McEvoy, L. K., Dreyer, S., DiSano, M., & Aron, A. R. (2009). Intracranial EEG reveals a time-and frequency-specific role for the right inferior frontal gyrus and primary motor cortex in stopping initiated responses. *Journal of Neuroscience*, *29*(40), 12675–12685.

Verbruggen, F., & Logan, G. D. (2009). Models of response inhibition in the stop-signal and stop-change paradigms. *Neuroscience & Biobehavioral Reviews*, *33*(5), 647–661.

Viganò, L., Fornia, L., Rossi, M., Howells, H., Leonetti, A., Puglisi, G., Conti Nibali, M., Bellacicca, A., Grimaldi, M., Bello, L., & Cerri, G. (2019). Anatomo-functional characterisation of the human "hand-knob": A direct electrophysiological study. *Cortex*, *113*, 239–254. https://doi.org/10.1016/j.cortex.2018.12.011

Viganò, L., Howells, H., Fornia, L., Rossi, M., Conti Nibali, M., Puglisi, G., Leonetti, A., Simone, L., Bello, L., & Cerri, G. (2021). Negative motor responses to direct electrical stimulation: Behavioral assessment hides different effects on muscles. *Cortex; a Journal Devoted to the Study of the Nervous System and Behavior*, *137*, 194–204. https://doi.org/10.1016/j.cortex.2021.01.005

Wessel, J. R., & Aron, A. R. (2017). On the Globality of Motor Suppression: Unexpected Events and Their Influence on Behavior and Cognition. *Neuron*, *93*(2), 259–280. https://doi.org/10.1016/j.neuron.2016.12.013

Wessel, J. R., Ghahremani, A., Udupa, K., Saha, U., Kalia, S. K., Hodaie, M., Lozano, A. M., Aron, A. R., & Chen, R. (2016). Stop-related subthalamic beta activity indexes global motor suppression in Parkinson's disease. *Movement Disorders*, *31*(12), 1846–1853. https://doi.org/10.1002/mds.26732

Wessel, J. R., Reynoso, H. S., & Aron, A. R. (2013). Saccade suppression exerts global effects on the motor system. *Journal of Neurophysiology*, *110*(4), 883–890. https://doi.org/10.1152/jn.00229.2013

Yokoyama, R., Enatsu, R., Kanno, A., Suzuki, H., Suzuki, Y., Sasagawa, A., Hirano, T., Arihara, M., Kuribara, T., Ochi, S., & Mikuni, N. (2020). Negative motor networks: Electric cortical stimulation and diffusion tensor imaging. *Revue Neurologique*, *176*(7–8), 592–600. https://doi.org/10.1016/j.neurol.2019.12.005

Zandbelt, B. B., Bloemendaal, M., Neggers, S. F. W., Kahn, R. S., & Vink, M. (2013). Expectations and violations: Delineating the neural network of proactive inhibitory control. *Human Brain Mapping*, *34*(9), 2015–2024. https://doi.org/10.1002/hbm.22047

CHAPTER II

EARLY RISE AND PERSISTENT INHIBITION OF ELECTROMYOGRAPHY DURING FAILED STOPPING

Fisher, M., Trinh, H., O'Neill, J., & Greenhouse, I. (2024). Early rise and persistent inhibition of electromyography during failed stopping. *Journal of Cognitive Neuroscience*, *36*(7), 1412–1426. https://doi.org/10.1162/jocn_a_02174

Introduction

The ability to cancel an initiated movement is an essential aspect of daily life which allows individuals to adapt to dynamic environments. A common example is quickly stopping oneself from stepping into the street when a car unexpectedly appears. Stopping ongoing movements in response to an unexpected stimulus, often referred to as reactive inhibition, is one kind of response inhibition which can be studied in the laboratory with stop-signal tasks (Logan & Cowan, 1984; Verbruggen et al., 2019). During each trial of an SST, the participant rapidly responds to a go stimulus; however, on a subset of trials, a stop signal is presented, and the participant attempts to abort their initiated movement. Behavioral data from the SST can be used to calculate a latent variable referred to as the stop-signal RT (SSRT), which is an estimate of an individual's average speed of stopping (Verbruggen et al., 2019). SSRT is a useful behavioral metric but is limited as it is an indirect measure and cannot be derived on an individual trial basis. The calculation of SSRT depends on the assumption of a horse race between competing independent go and stop processes, and whichever process finishes the race first determines the behavioral outcome. This has been a practical approach and has raised many important questions about the timing and mechanisms involved in response inhibition.

SSTs are frequently paired with electromyography (EMG), which offers temporally precise measurements of muscle activity, a valuable supplement to behavioral data (de Jong et al., 1990; McGarry & Franks, 1997; van Boxtel et al., 2001). Previous studies have examined

EMG markers associated with stopping for a variety of reasons. This approach is sensitive to different types of stopping. For example, successful stopping can occur before or after responding muscle activation. De Jong et al. (1990) used this method to probe whether there was a "point of no return" at which speeded, stimulus-driven movements could not be reactively aborted. This work demonstrated that partial EMG responses, that is, EMG bursts in the absence of a button press, are a valuable measure of motoric inhibitory influence on trials in which participants successfully abort their response. These "partial responses" during successful stop trials reveal the point at which the stop process overtakes the go process at the level of the muscle and are only detectable with EMG since button presses are not registered on trials with these outcomes. However, recent behavioral evidence (Du et al., 2022) contests the traditional horse race model, which posits that the stop process is faster than the go process (2022). By suggesting go and stop processes take more or less equivalent amounts of time to complete, these newer findings call into question whether a "point of no return" might be reached prior to the initiation of the stop process. Instead, the factor that determines successful versus failed stopping is the decision to delay the initiation of the go response (Verbruggen & Logan, 2009). Delaying response initiation manifests as slowing when participants anticipate the possible presentation of a stop signal. These conflicting perspectives motivate a revisitation of the question of whether a "point of no return" exists through a careful examination of both behavior and EMG.

Others have investigated the timing and duration of the influence of inhibition within a responding effector at the single trial level through examination of partial response EMG (prEMG) during successful stop trials (Jana et al., 2020; Raud et al., 2020; Raud & Huster, 2017). A robust, single-trial electrophysiological marker of inhibition is valuable because traditional SSRT calculations, based solely on behavior, likely overestimate the speed of

stopping by as much as 100 ms (Bissett et al., 2021; Skippen et al., 2019). The overestimation of the duration of the stopping process based on behavior alone may be partially due to the presence of "trigger failures" when a participant fails to discern and respond to a stop signal, meaning the stopping process was never “triggered” (Matzke et al., 2017, 2019). In terms of the horse race model, the go process on such trials is executed uncontested despite the presentation of a stop signal. This also raises questions about the existence and ability to determine a possible “point of no return". However, EMG evidence supports the idea that stopping is faster than going. Raud & Huster (2017) observed participants would exhibit an EMG burst in response to the go cue, followed by a decrease in EMG ~150 ms after the stop signal. It is possible this decrease in EMG is a result of the stop process finishing and canceling motor output (Raud et al., 2022). Notably, this occurred approximately 50 ms earlier than the SSRT estimation in that study and may be complemented by the engagement of antagonist muscles (Goonetilleke et al., 2010). Another recent study utilized similar methodology to derive a single-trial estimate of stopping latency via EMG (Jana et al., 2020). This was accomplished by focusing on the time between the stop signal and the partial response EMG peak on successful stop trials as an estimate of the latency of stopping (termed “cancel time”), building on previous examinations of partial response EMG activity (de Jong et al., 1990; McGarry et al., 2000; van Boxtel et al., 2001).

Motivated by these recent investigations of EMG markers of stopping, we revisited the question of the “point of no return" by more closely examining EMG onset time (EMG OT) at the individual trial level. We used both simple and choice versions of the stop task to control for the possible influence of response selection. We predicted that a comparison of EMG activity relative to the stop signal would reveal a clear difference between failed stop and partial response (successful stop) trials. Rather than a fixed point in time, we tested for the existence of a

“transition zone", where the relative likelihood of successful and failed stopping inverts. This finding would be useful in understanding the speed of stopping at the muscular level and bring context to previous work. In addition, we explored whether the time between peak EMG and EMG offset may reflect the operation of inhibitory processes acting at the level of the muscle. Specifically, we predicted a faster “ramp down" of EMG activity on failed stop trials than on go trials. This finding would suggest go and stop processes both run to completion on failed stop trials, and the effect of inhibitory mechanisms may still be observable in muscle activity.

Methods

Participants

Twenty-four participants (mean age = 23.7 years, *SD* = 2.9 years, 10 female) completed simple response versions of a go task (GT) and an SST in Experiment 1. Twenty-eight participants (mean age = 23.5 years, SD = 4.1 years, 10 female) completed choice response versions of a GT and an SST in Experiment 2. Sample size was selected based on power analysis of a previous study using similar methods (Raud & Huster, 2017). That study observed a large effect size ($d = 0.94$) with a sample of 30 participants, corresponding to $1 - \beta = 1$ for a comparison of EMG burst amplitudes between task conditions. All participants were right-handed (self-reported) and provided written informed consent according to the institutional review board at the University of Oregon. All data and code are available from the Open Science Framework at this link: https://osf.io/9dp7x/

Behavioral Tasks

Participants performed visual GT and SST that were run in MATLAB using custom code (MathWorks). The tasks followed the recommendations set in Verbruggen et al. (2019), with the lone deviation that Experiment 1 did not contain a choice element. Participants were seated

approximately 60cm from the screen and responded by pressing buttons that were interfaced with a MakeyMakey (JoyLabz, LLC) circuit board. Both experiments consisted of a GT and a SST (**Figure 2.1A**).

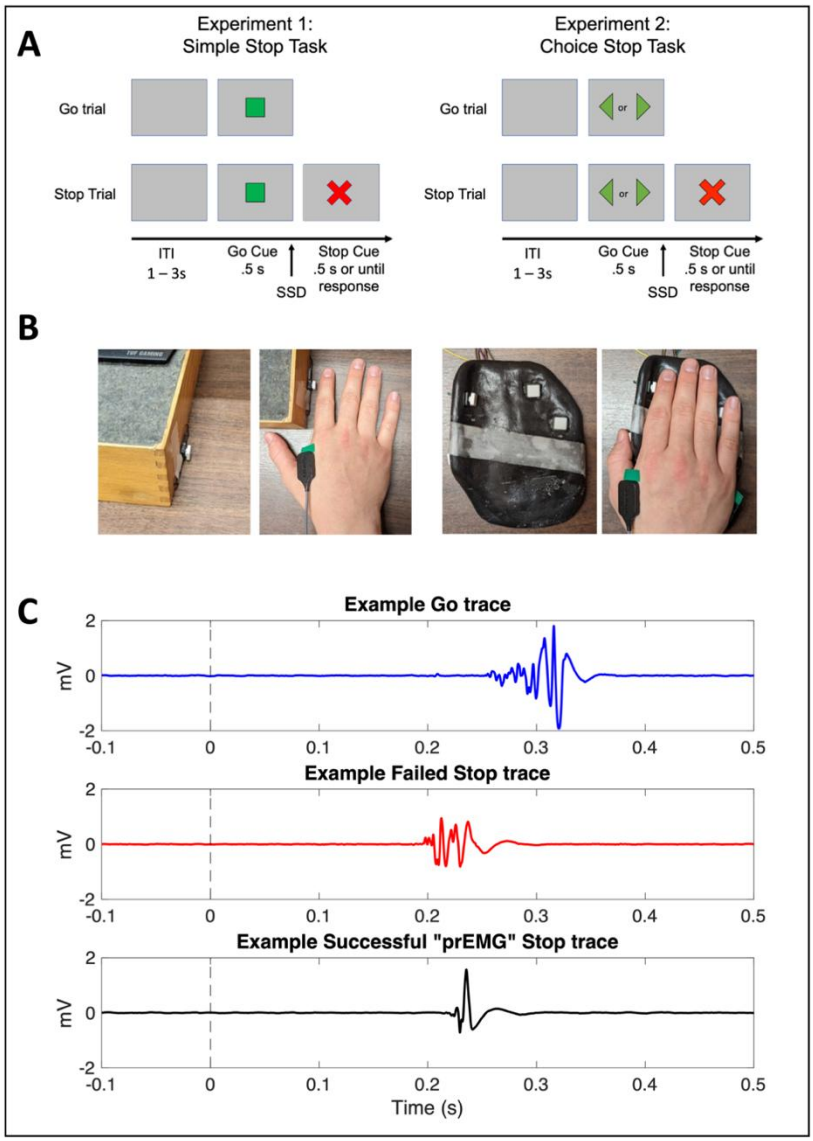

Figure 2.1. A) Visual task presentation in Experiments 1 and 2. B) Electrode placement and button configuration (left panel = Exp. 1, right panel = Exp. 2). C) Example EMG traces for 3 trial conditions that contain EMG responses: Go, Failed stop and successful stop (prEMG), with time 0 indicating go stimulus onset.

Experiment 1: Simple Go and Stop Task

Experiment 1 consisted of simple response tasks (no choice element) that participants performed with one hand and then the other in a randomized order. Participants' hands were positioned palms down, shoulder-width apart on a table in front of the visual display. Responses

were made by laterally moving the forefingers toward the midline of the body to depress a horizontally positioned button (Figure 2.1B, left images: setup was mirrored for left hand). Participants performed the GT with one hand, the GT with the other hand, the SST with the first hand, and then the SST with the second hand.

Before the GT, participants completed at least 18 trials as practice. If participants were not yet familiar, they were allowed to repeat the practice block once to ensure familiarity. Following the familiarization, participants completed one block of 30 test trials per hand. Each trial consisted of a blank screen intertrial interval (ITI) of 1-3 sec (random, uniform distribution) followed by the presentation of a go signal. The go signal on each trial was a green square presented at the center of the screen, and participants were instructed to respond as quickly as possible by depressing the response button. The go signal remained on the screen for 0.5 sec, and a correct response could be registered for 1 sec from go signal onset. No feedback was provided to participants during the GT. Average GT RT was used to determine the RT threshold for performance feedback during the SST, as described below.

In the SST, participants were informed that each trial would begin with a go signal and that, on some trials, this would be followed at a short interval by a stop signal (a red "X") that replaced the go signal. Trial duration, ITI, and jitter were the same as the GT. The go stimulus was presented for 0.5 sec, and on stop trials, the stop signal lingered for 0.5 sec. Participants were also familiarized with the SST by performing at least 18 practice trials and were once again offered a second practice block to ensure familiarity with the task. During testing, participants completed 108 trials in total with each hand, consisting of 72 go trials (66%) and 36 stop trials (33%). The stop signal was presented at a variable stop signal delay (SSD) using three independent staircases (starting at 40, 80, and 120 ms) that were adjusted according to participant

performance. Relatively short SSDs were chosen to attain high stopping success and increase the sensitivity of the planned EMG analyses (i.e., successful stop trials with partial responses). The SSD increased by 20 ms if stopping was successful and decreased by 20 ms if stopping was unsuccessful. The task was broken up into four blocks with 27 trials per block. Between blocks, participants were required to take at least a 90-sec break to prevent fatigue.

Participants were instructed to not delay their responses in anticipation of the stop signal. To enforce speeded responses, participants received a "speed up" cue on go trials when button-press RT was greater than 2.5 *SD*s above the mean GT RT. Trials that resulted in the presentation of the "speed up" cue were not analyzed, and participants were excused from the study if they received greater than 20 "speed up" cues because of inadequate performance.

Experiment 2: Choice Go and Stop task

The GT and SST in Experiment 2 consisted of a choice between left and right responses, mapped to the index and pinky fingers of the right hand, respectively. Participants' right hands were positioned on a custom-build response device with buttons positioned against the lateral portion of the distal phalanx of the index finger and beneath the tip of the pinky finger (Figure 2.1B, right images). Index finger responses were the same as the right index responses in Experiment 1 involving a lateral movement toward the midline of the body. Pinky finger responses involved a downward button press.

The GT consisted of two blocks of 30 trials (60 trials in total) with an equal number of left and right responses randomly distributed across trials. Participants completed at least 18 trials of practice before testing. The ITI was 1.2 sec, and each trial was jittered from 1 to 3 sec (random, uniform distribution). The go signal was either a right- or left-pointing green arrow for the index and pinky responses, respectively, and was displayed for 0.5 sec. Correct responses

could be registered up to 1 sec from go signal onset. As in experiment 1, no feedback was presented during the GT, but the mean GT RT was used to determine the threshold for presenting feedback during SST performance.

The SST was similar to the GT except it consisted of eight blocks of 27 trials (216 trials in total). One third of the trials (72 trials) were stop trials, with 36 stop trials per finger. The stop trials were distributed randomly across the experiment. On each stop trial, the go stimulus was replaced with a stop signal (red "X") at a variable SSD. As in Experiment 1, the SSDs were adjusted dynamically based on performance with three staircases for each response finger (six independent staircases in total). The staircases started at 100, 125, and 150 ms and increased or decreased by 20 ms after successful or failed stop trials, respectively. Participants received "speed up" feedback on go trials during the SST when they failed to respond within 2 *SD*s of their mean go RT determined from the GT. As above, if participants received 20 "speed up" cues, the experiment would end, and the data were excluded from analysis. Participants also received "try to stop" feedback on stop trials when they failed to cancel their movement.

EMG Procedure

EMG was recorded using bipolar surface electrodes connected to an eight-channel Bagnoli (Delsys) amplifier (amplification x 1000, bandpass filtered 50-450 Hz). EMG was sampled at 5000 Hz and recorded using the VETA toolbox (Jackson & Greenhouse, 2019).

In Experiment 1, EMG electrodes were placed over the left and right first dorsal interossei (FDI) muscles. In Experiment 2, EMG electrodes were placed over the left and right FDI and the abductor digiti minimi (ADM) muscle. A 4-sec EMG sweep was recorded for each trial of the task and visualized by the experimenter on a separate screen adjacent to the stimulus presentation monitor. During the practice trials, participants were coached to keep their

responding fingers close to the response buttons and to keep the EMG signal uncontaminated by noise when not responding to improve sensitivity to EMG events.

In both experiments, participants were instructed to maintain a tonic contraction of the FDI muscle of the non-responding hand throughout task performance. For Experiment 1, this means participants would maintain a contraction in their left hand while their right hand was used for responding to stimuli, and vice versa for left-hand responses. In Experiment 2, only the right hand was used for responding to the choice task, and the left hand maintained the tonic contraction through the entirety of the experiment, aside from during prescribed breaks within the task. Before testing, the maximum voluntary contraction (MVC) of the FDI in the nonresponding hand was measured, and participants were trained to maintain a tonic contraction of approximately 10% MVC. Real-time feedback displayed individualized reference lines on the EMG recording figure corresponding to 10% of the MVC and was monitored to ensure participants generated a stable contraction throughout. We consider the possible influence of these contractions on the behavioral performance and EMG in the responding hand but do not discuss the tonic EMG further in the current article.

Statistical Analyses

Behavioral Measures

Behavioral metrics of interest were calculated for each task condition in both experiments. These included means and standard deviations of button Go RT, mean SSD, mean stopping accuracy (%), integration SSRT (Verbruggen et al., 2019), and means and standard deviations of failed stop button RT.

EMG Analysis

EMG data were analyzed offline using the VETA toolbox (Jackson & Greenhouse, 2019) in MATLAB 2019a (Mathworks) in two stages. First, EMG burst onsets were identified using an automatic detection algorithm by calculating the first point from the EMG trace that exceeded 2 *SD*s of the mean for the entire trial, performed on the raw EMG signal. Second, data from each trial were visualized, and manual corrections were made where necessary. This included rejection of sweeps contaminated with artifacts and adjustments to mark the onsets and offsets of EMG bursts. EMG data were smoothed using a root mean square method (movRMS via the DSP System Toolbox) with a sliding window of 12 sample points, equivalent to 2.4 ms, and rectified. This smoothing window was selected for visualization purposes. EMG data presented in Figures 2.2 – 2.4 are group-level averaged traces that have been smoothed and rectified with the root mean square method previously described. All other metrics apart from slope calculations were collected at the individual trial level.

EMG metrics of interest were calculated using unsmoothed (raw) EMG data and included means and standard deviations of EMG burst onset, peak, and offset times. These were calculated separately for successful go trials (go EMG RT, EMG peak, go EMG offset), failed stop trials (failed EMG RT, failed EMG peak, failed EMG offset), and partial responses on successful stop trials (prEMG RT, prEMG peak, prEMG offset). In addition, EMG onset-to-peak times and EMG peak-to-offset times for all EMG bursts were calculated for each trial type and task condition. Cancel time was calculated as time elapsed from stop signal onset to EMG peak for partial responses (Jana et al., 2020).

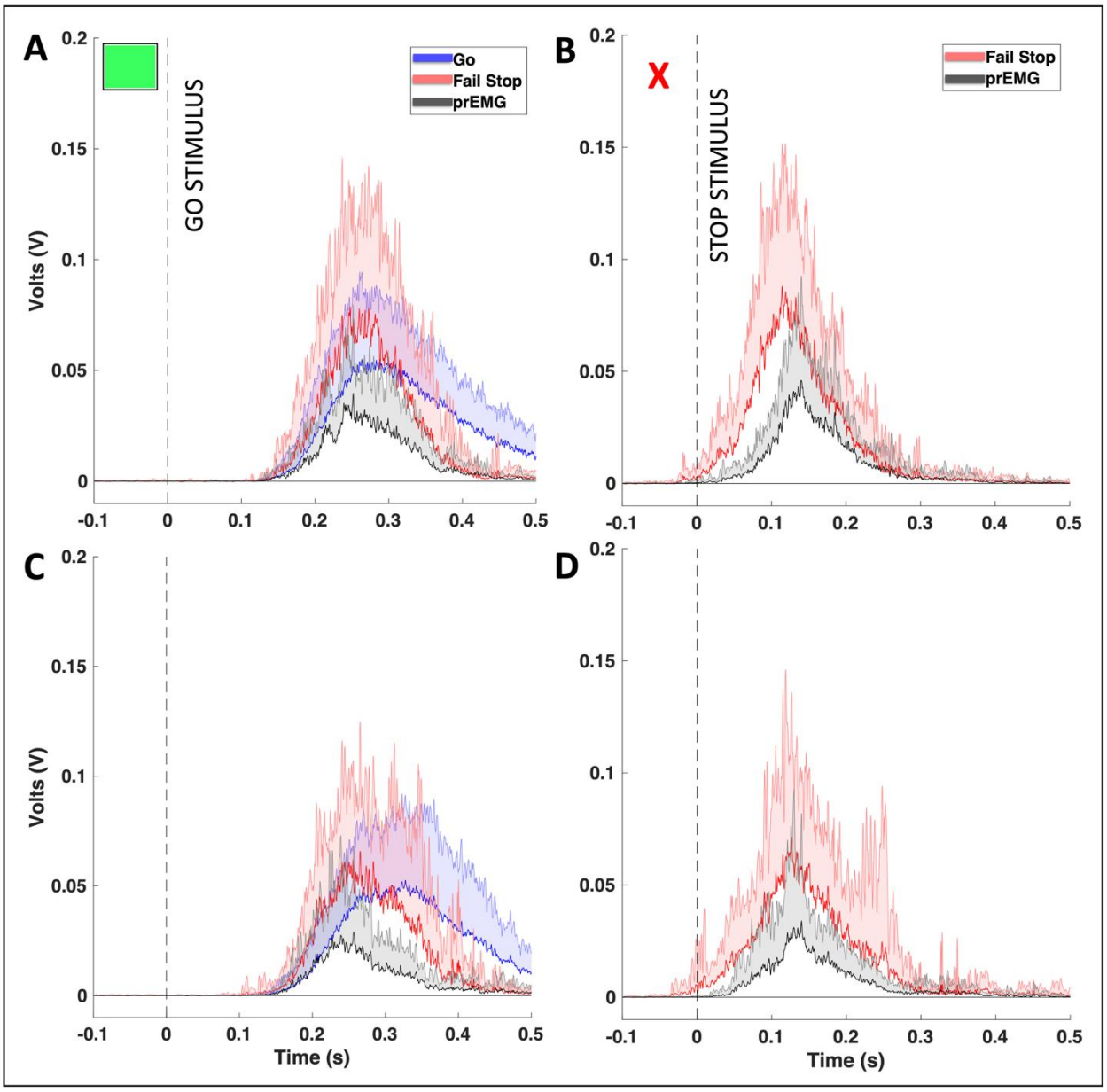

Figure 2.2. Experiment 1 (n = 24) mean ± std response EMG aligned with go stimulus (A & C) and stop stimulus (B & D). Responses from the right hand are in A & B, while responses from the left hand are in C & D. Blue traces are from go trials, while black and red traces are from successful stop trials that had a partial response (prEMG) and failed stop trials, respectively. Data are smoothed via root mean square method and rectified.

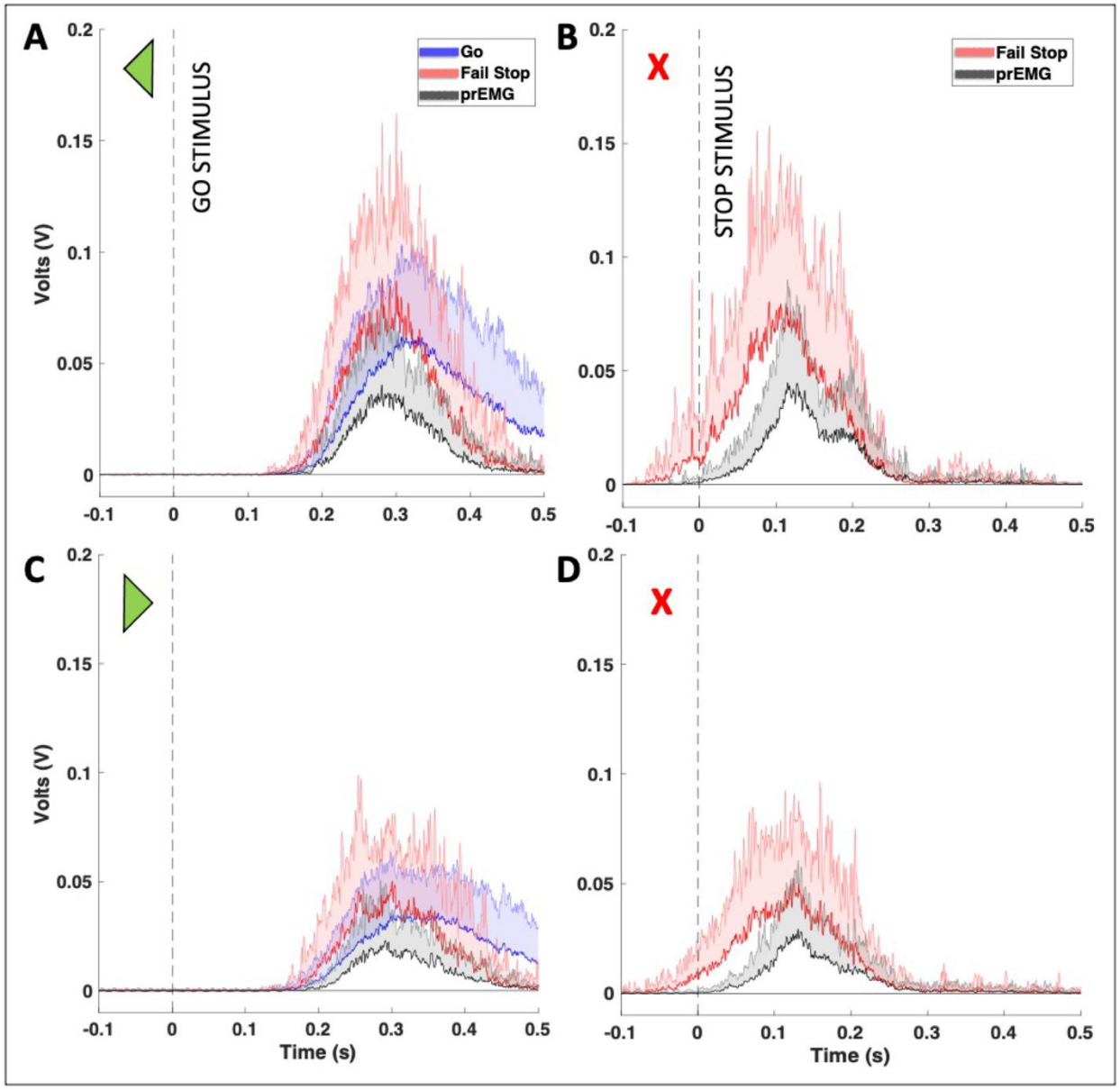

Figure 2.3. Experiment 2 (n = 28) mean ± std response EMG aligned with go stimulus (A & C) and stop stimulus (B & D). Responses from the right FDI are in A & B, while responses from the right ADM are in C & D. Blue traces are from go trials, while black and red traces are from successful stop trials that had a partial response (prEMG) and failed stop trials, respectively. Data are smoothed via root mean square method and rectified.

In addition, the electromechanical delay (EMD), that is, the time between EMG onset and button press, was calculated for go and failed stop trials. EMG peak-to-offset times were calculated along with EMG peak-to-offset slope for all response conditions. For slope calculations, EMG was deemed too noisy at the individual trial level to estimate with confidence.

Therefore, slope was calculated using a linear fit of the mean EMG peak to the mean offset of the EMG burst for each response condition for each participant. Differences in the EMG peak-to-offset times across conditions could be driven by especially slow go responses. Accordingly, we performed a separate analysis using EMG peak-to-offset times for go trials with button RTs shorter than the slowest failed stop RT for each participant, matching the maximum allowable button RT across these two conditions.

To evaluate the time at which individuals transitioned from failed to successful stopping, on a trial-wise basis, we determined successful (prEMG) and failed stop trial EMG burst onsets. Anchored relative to the stop signal, we calculated the number of trials with EMG onsets in 30-ms bins to generate a histogram for each trial type. This bin size was selected to ensure a representative sample at the group level. We predicted the ratio of fail to prEMG would shift from favoring failure to success within a time range close to the stop signal. Rather than a fixed point of no return, this would represent a transition zone for the likelihood of stopping success based on the time of response initiation.

Statistical Tests

Statistical analyses were performed in Jamovi (version 2.2, Jamovi 2021), except for Bayesian tests that were performed in JASP (version 0.14.1, JASP, 2020). For Experiment 1, a 2 x 3 repeated-measures ANOVA with the factors Hand (Left, Right) and Trial Type (GT Go, SST Go, Failed Stop) tested for differences in button RTs and EMD. Bayesian paired *t* tests to determine the likelihood of similar performance for SSD, stop accuracy, and SSRT between hands (Experiment 1) and response choices (Experiment 2), and Bayes Factors (BFs) were derived. Tests for equivalence between hands (Experiment 1) and response choices (Experiment

2) for SSD, stop accuracy, and SSRT were evaluated with two one-sided tests (TOSTs; Lakens, 2017), performed in MATLAB (Pabi, 2024).

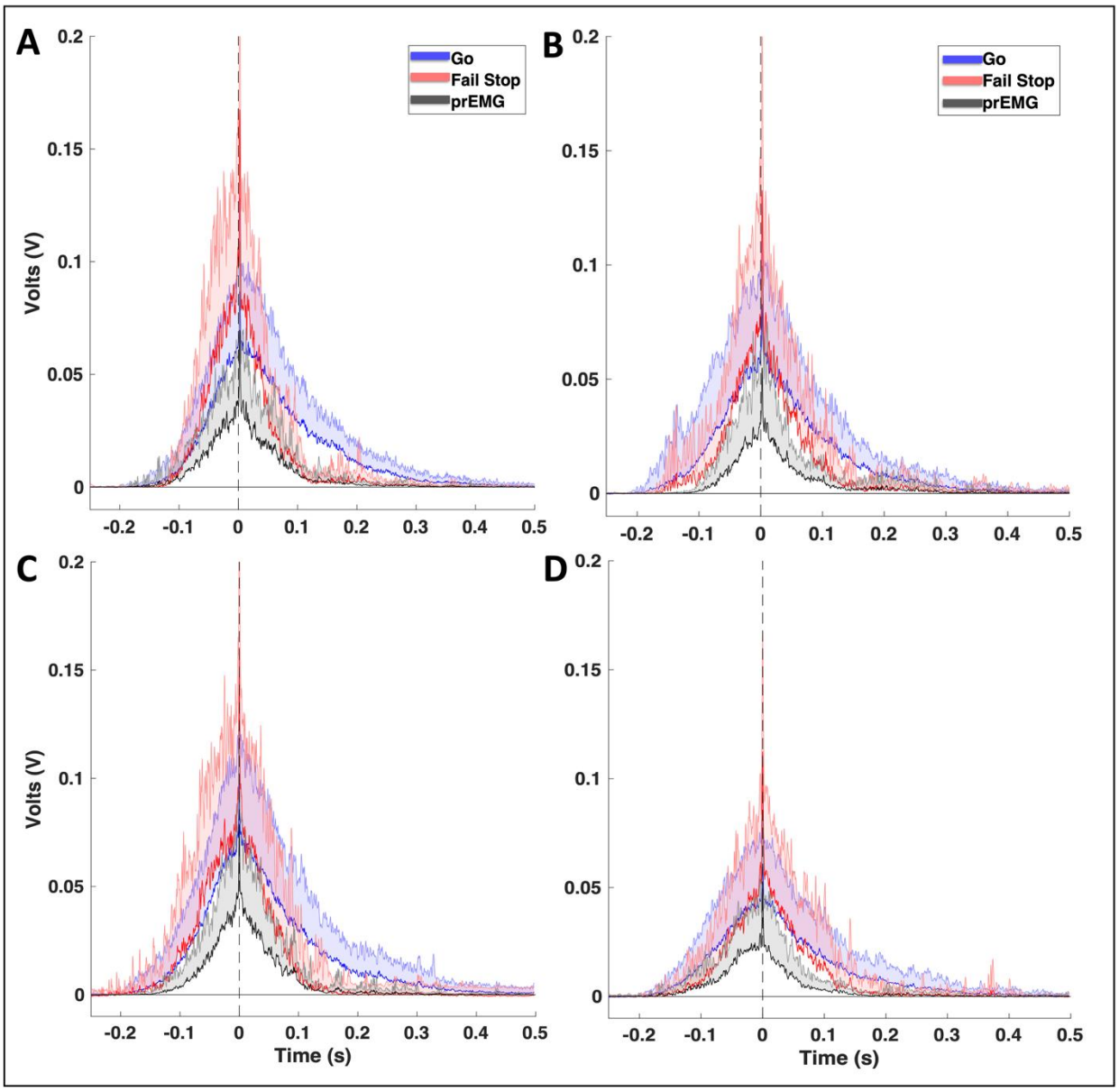

Figure 2.4. Experiment 1 (n = 24) right hand (A) and left hand (C), and Experiment 2 (n = 28) right FDI (B) and right ADM (D) mean ± std response EMG aligned to the EMG peak. Blue traces are from go trials, while black and red traces are from successful stop trials that had a partial response (prEMG) and failed stop trials, respectively. Data are smoothed via root mean square method and rectified.

A 2 x 4 repeated-measures ANOVA with the factors Hand (Left, Right) and Trial Type (GT Go, SST Go, Failed Stop, Partial Response) tested for differences in our EMG metrics of interest. A significant main effect of Trial Type would indicate that EMG activity differs across the response conditions. Here, we hypothesized that partial responses would show a later onset and possibly more gradual ramp-up than the other response conditions, based on the assumption that the likelihood of stopping increase with slower responses. Moreover, we hypothesized that there would be differences in the ramp-down in EMG activity between go and stop trials, both successful partial responses and failed responses.

The same statistical tests were conducted for Experiment 2 with the factor Hand replaced by the factor Finger (Index, Pinky). Post hoc follow-up tests were Bonferroni-corrected.

To evaluate the point of no return, that is, the point at which a button press cannot be aborted, mean EMG amplitude for the 100 ms preceding stop signal onset was compared between failed and successful stopping with a 2 x 2 repeated-measures ANOVA. The rational for this 100 ms window is based on the assumption that the go stimulus has been fully processed by this time, and EMG activity within this window is most likely associated with response initiation. Significantly greater mean EMG activity during failed than successful stopping in this time window would be consistent with the interpretation that the point of no return precedes stop signal onset.

The time between EMG peak and EMG offset provides a measure of the speed with which EMG activity resolves after the engagement of a muscle. If EMG activity decreases significantly faster on failed stop than go trials and resembles successful stop trials, this would suggest inhibition associated with stopping persists even when the stop process fails. In other words, the motor system is inhibited but too late to prevent the completion of the go response. In

this case, the rate of decline in EMG activity on failed stop trials would provide a novel marker of motor system inhibition.

A 2 x 4 repeated-measures ANOVA with the factors Hand (Left, Right) and Trial Type (GT Go, SST Go, Failed Stop, Partial Response) tested for differences in our EMG metrics of interest. A significant main effect of trial type would indicate that EMG activity differs across the response conditions. Here, we hypothesized that partial responses would show a later onset and possibly more gradual ramp up than the other response conditions, based on the assumption that the likelihood of stopping increases with slower responses. Moreover, we hypothesized that there would be differences in the ramp down in EMG activity between Go and Stop trials, both successful partial responses and failed responses.

The same statistical tests were conducted for Experiment 2 with the factor Hand replaced by the factor Finger (Index, Pinky). Post-hoc follow up tests were Bonferroni corrected.

To evaluate the point of no return, i.e. the point at which a button press cannot be aborted, mean EMG amplitude for the 100 ms preceding stop signal onset was compared between failed and successful stopping with a 2 x 2 repeated-measures ANOVA. The rationale for this 100 ms window is based on the assumption that the go stimulus has been fully processed by this time, and EMG activity within this window is most likely associated with response initiation. Significantly greater mean EMG activity during failed than successful stopping in this time window would be consistent with the interpretation that the point of no return precedes stop signal onset.

The time between EMG peak and EMG offset provides a measure of the speed with which EMG activity resolves following the engagement of a muscle. If EMG activity decreases significantly faster on failed stop trials than go trials and resembles successful stop trials, this

would suggest inhibition associated with stopping persists even when the stop process fails. In other words, the motor system is inhibited, but too late to prevent the completion of the go response. In this case, the rate of decline in EMG activity on failed stop trials would provide a novel marker of motor system inhibition.

Results

Behavioral Data

Experiment 1

Behavioral data are presented in **Table 2.1** for both experiments. Data for the right and left simple RT tasks were very closely matched. Analysis of button press RTs (GT Go, SST Go and SST failed stop trials) indicates no differences between hands [F (1,23) = .33, p = .57, η^2 = .001] and a main effect of trial type [F (2,46) = 90.28, p < .001, η^2 = .38]. Successful stop trials were not included in this analysis due to the absence of a button press. Post-hoc pairwise t-tests confirmed failed stop trial button RTs were faster than SST go trials (t = 15.3, p < .001), and GT go trial RTs were significantly faster than SST go trials (t = -10.2, p < .001). There were no differences between failed stop RT and GT go trial RT (t = -.5, p = 1.0). This confirms participants slowed their responses on go trials in the context of the SST.

Paired-samples t-tests indicated SSRT, SSD, and stopping accuracies did not differ between hands (all p's > .05). Bayesian tests for equivalence between hands for SSRT, SSD, and stopping accuracies showed anecdotal evidence for the null for all measures [all BF_{01} between 1.48 and 2.66].

Table 2.1. Means (standard deviations) for behavioral and EMG measures in Experiment 1 (n = 24) and 2 (n = 28). GT = go task, SST = stop signal task, RT = reaction time, OT = Onset time, prEMG = successful stop trials that included a partial EMG response, SSD = stop signal delay, SSRT = stop signal reaction time.

	Experiment 1 (Simple Task)		Experiment 2 (Choice Task)	
Behavioral Measures	Right (FDI)	Left (FDI)	Index (FDI)	Pinky (ADM)
GT RT (ms)	352 (32)	352 (30)	454 (58)	456 (59)
SST Go RT (ms)	410 (41)	408 (35)	453 (42)	459 (48)
SST Fail RT (ms)	357 (33)	353 (32)	390 (31)	396 (43)
GT EMG OT (ms)	203 (23)	207 (21)	258 (30)	271 (28)
SST Go EMG OT (ms)	245 (34)	246 (33)	260 (30)	281 (32)
SST Fail EMG OT (ms)	208 (31)	206 (26)	223 (25)	240 (26)
SST prEMG OT (ms)	226 (33)	222 (32)	257 (29)	278 (46)
SSRT (ms)	245 (20)	256 (29)	233 (39)	246 (41)
Cancel Time (ms)	168 (27)	166 (29)	158 (32)	161 (33)
SSD (ms)	118 (23)	113 (23)	162 (27)	167 (28)
Go trial accuracy (%)	99.9 (0.3)	99.8 (0.5)	99.4 (1.4)	99.2 (1.7)
Stop trial accuracy (%)	66.1 (8.2)	63.9 (9.5)	65.1 (8.9)	68.3 (10.8)

Experiment 2

Generally, RTs between fingers (FDI and ADM) in Experiment 2 exhibited similar RT patterns as between hands in Experiment 1. A 2 x 3 repeated measures ANOVA was used to analyze button press RTs across response types (GT go, SST go and SST failed stop trials) and between fingers. There were no differences between fingers [F (1,27) = 1.2, p = .28, η^2 = .002], however a main effect of response type was observed [F (2,54) = 63.5, p < .001, η^2 = .281]. Unlike experiment 1, post-hoc paired t-tests showed no slowing was observed between GT go

trials and SST go trials (t = -.1, p = 1.0). Post-hoc t-tests also revealed failed stop trials were significantly faster than GT go trials (t = 8.1, p < .001) and SST go trials.

Paired-samples t-tests showed that SSRT and SSD were not statistically different between fingers (all ps > .05), while stopping accuracy was higher for pinky responses than index finger responses (p < .05, d = .33). Bayesian tests for equivalence between hands for SSRT, SSD, accuracies showed anecdotal evidence for all measures [all BF_{01} between .35 and 2.89].

EMG Data

Experiment 1: EMG Onset Times and Electromechanical Delays (EMD)

Results of the 2 x 4 repeated measures ANOVA for EMG OTs (also presented in **Table 2.1**) were not significantly different between hands [F (1,23) = .01, p = .94, η^2 = .001] but showed a main effect across GT, SST go, failed stop, and successful stop (partial EMG) response types [F (3,69) = 41.63, p < .001, η^2 = .24]. Like the button-press results, post-hoc paired t-tests show SST go trial onsets were slower compared to GT go trials (t = -8.7, p < .001). GT go trial EMG OTs (205 ± 0.02 ms), and failed stop EMG OTs (207 ± 0.03 ms) had the shortest latencies and were not significantly different from each other (t = -.3, p = 1.0). Successful stopping was defined by stop trials that did not have a button response registered, however inspection of EMG data revealed that on approximately half of the stop trials (16 ± 4.7 trials per hand) EMG bursts were detected, indicating participants started to respond, but did not fully execute the button press (Jana et al., 2020; Raud et al., 2022). These trials are meaningful because there is an implied inhibitory process that prevents the completion of the button press response. Post-hoc paired t-tests showed the mean latencies of prEMG OT trials were shorter than SST go EMG OT

(t = 4.4, p < .001) and longer than failed stop trials (t = -4.6, p < .001), consistent with the idea that even early EMG activity can be successfully suppressed by the stop process.

Not statistically significant differences in EMDs were found between hands [F (1,23) = .49, p = .49, η^2 = .003]. A main effect across response type was observed for EMD [F (2,46) = 14.61, p < .001, η^2 = .096]. Post-hoc pairwise t-tests show SST go trial EMDs were significantly longer than failed stop EMD (t = 5.3, p <.001) and GT go trial EMDs (t = -4.8, p < .001). GT go trial EMDs were not significantly different from failed stop trial EMDs (t = -.5, p = 1.0).

The distribution of EMG OTs for prEMG and failed stop trials relative to the stop signal are presented in Figure 2.2 A & C (right and left hand, respectively). Visual inspection of histograms indicated a transition from a higher proportion of failed to a higher proportion of successful stopping in the range of 0.03 to 0.06 s after the stop signal. There was a significant difference in this ration between the 0.03 and 0.06 s bins χ^2 (1,24) = 13.9, p < .001. This indicates EMG onsets before 0.03 s after the stop signal are significantly more likely to be associated with failed stopping. The number of participants that contributed onset times to each bin indicates this timing is consistent across participants at the group level (unique participant counts for each bin listed below x axis).

Experiment 1: Response EMG Profiles

Further inspection of the EMG profile of the responding finger was warranted to determine how partial response EMG OTs differed from failed stop EMG OTs and how they each compared with go trial responses (Figure 2.2). To do this, we identified all trials with EMG responses and measured time epochs including: onset of EMG activity to the peak of EMG activity, peak of EMG activity to EMG offset (return to baseline), and cancel time. Cancel time is a single trial estimate of stopping latency and is the time from the stop stimulus onset to the

peak of EMG activity, as described by Jana et al. (2020). Cancel time is only appropriate to measure in successful stop trials, and as such was evaluated using paired-samples *t*-tests on prEMG trials. No statistically significant difference was observed between hands ($p = .79$, $d = .06$).

Table 2.2. Means (standard deviations) for derived EMG measures in Experiment 1 (n = 24) and Experiment 2 (n = 28). EMD = electromechanical delay, prEMG = successful stop trials that included a partial EMG response.

	Experiment 1 (Simple Task)		Experiment 2 (Choice Task)	
Derived EMG Measures	Right (FDI)	Left (FDI)	Index (FDI)	Pinky (ADM)
GT Go EMD (ms)	149 (22)	145 (23)	195 (46)	186 (43)
SST Go EMD (ms)	164 (27)	162 (23)	193 (29)	177 (36)
SST Fail EMD (ms)	150 (23)	148 (19)	165 (27)	156 (29)
GT Onset to Peak (ms)	82 (24)	83 (25)	117 (48)	101 (34)
SST Go Onset to Peak (ms)	88 (24)	95 (23)	108 (24)	95 (28)
SST Fail Onset to Peak (ms)	65 (18)	72 (17)	95 (18)	86 (24)
SST prEMG Onset to Peak (ms)	52 (14)	72 (17)	92 (18)	85 (22)
GT Peak to Offset (ms)	107 (54)	84 (41)	109 (52)	105 (37)
SST Go Peak to Offset (ms)	92 (45)	74 (21)	116 (56)	92 (33)
SST Fail Peak to Offset (ms)	78 (25)	65 (27)	104 (49)	84 (29)
SST prEMG Peak to Offset (ms)	58 (27)	48 (18)	100 (46)	80 (26)
SST Go EMG Offset Slope (mV/s)	-0.6 (0.3)	-0.7 (0.5)	-0.7 (0.4)	-0.4 (0.3)
SST Fail EMG Offset Slope (mV/s)	-2.3 (1.7)	-1.7 (1.3)	-1.7 (1.1)	-1.2 (0.8)
SST prEMG Offset Slope (mV/s)	-1.1 (0.8)	-1.0 (0.7)	-0.8 (0.6)	-0.6 (0.5)

Onset to peak times were not significantly different between hands [F (1,23) = 3.04, p = .09, η^2 = .008], but differed across conditions as expected [F (1,23) = 53.35, p < .001, η^2 = .34], (**Table 2.2**). PrEMG onset to peak times had the shortest latency and post-hoc paired *t*-tests revealed they were significantly faster than all other trial response types (all ps < .001). The short onset to peak time for prEMG trials is likely explained by the smaller peak EMG values achieved from these trials relative to other response types (peak EMG results below). All other post-hoc pairwise comparisons of EMG onset to peak times reached significance (ps < 0.05) except between GT go and SST go trials (t = -2.6, p = .09).

When observing peak EMG to EMG offset times (Figure 2.5 A & C), right hand values were significantly longer than left hand values [F (1,23) = 5.39, p = .029, η^2 = .038]. Notably, differences in peak EMG to EMG offset times across conditions were also significant [F (3,69) = 14.4, p < .001, η^2 = .148]. Post-hoc comparisons also showed peak EMG to EMG offset in prEMG trials was significantly faster than failed stop trials (t = 3.6, p < .05), SST go trials (t = 6.0, p < .001) and GT go trials (t = 5.0, p < .001). There were no significant differences found in EMG peak to offset times between GT go trials and SST go trials (t = 1.8, p = .52) and no significant differences between GT go trials and SST fail stop trials (t = 2.0, p = .079).

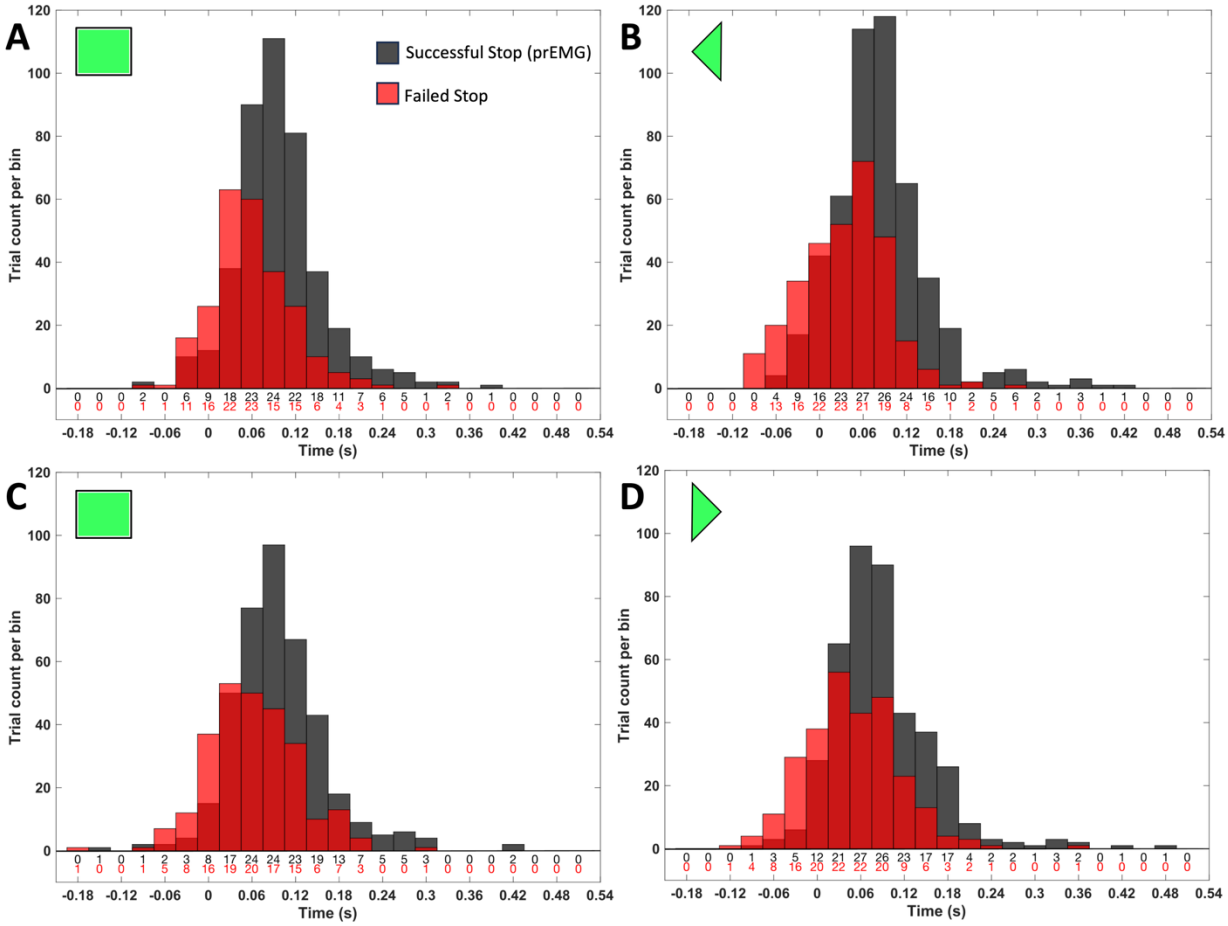

Figure 2.5. Distributions of EMG onset time differences relative to the stop signal for failed (red) and successful (prEMG, black) stops, displayed in 30 ms bins. Negative values indicate EMG onset occurred prior to stop signal and vice versa for positive values. The numbers of unique participants contributing to each bin are shown below the x axis. Experiment 1 (n = 24) data shown in A (right hand) and C (left hand). Experiment 2 (n = 28) data shown in B (FDI) and D (ADM).

Slope was also calculated to index the rate of decline from peak EMG to EMG offset for each hand and all response types (**Table 2.2**). No significant differences were found between hands [F (1,23) = .80, p = .38, η^2 = .006]. However, failed stop trials exhibited a significantly steeper slope than SST go trials and prEMG trials [F (2,46) = 32.768, p < .001, η^2 = .259], and there was a significant interaction between hands and trial type [F (2,46) = 3.658, p < .05, η^2 = .014]. Post-hoc paired t-tests were significant for all slope comparisons with failed stop trials exhibiting the steepest slope (ps < .001). These results indicate EMG burst activity declined more

quickly on failed stop trials than go and prEMG trials, despite the failure to stop, a pattern consistent with lingering inhibition on failed stop trials. Post-hoc *t*-tests showed a similar pattern for both left and right responses and the interaction is most likely explained by a greater difference between go and prEMG stop trials in the right hand ($t = 3.7$, $p < .05$) than the left hand ($t = 1.6$, $p = 1.0$).

Peak EMG values showed no statistically significant differences between hands [F (1,23) = 2.94, $p = .10$, $\eta^2 = .025$], but there was a significant difference across response types [F (3,69) = 63.52, $p < .001$, $\eta^2 = .184$]. In the right hand, the largest to smallest peak EMG values (mean ± sd) were GT go trials (180 ± 0.74V), SST go trials (1.80 ± 0.70V), failed stop trials (1.64 ± 0.79V) and finally, prEMG trials (0.97 ± 0.51V). The left hand exhibited a relatively similar pattern with the exception that go trials in the SST achieved the highest peak EMG values (1.55 ± 0.87V), followed by GT go trials (1.49 ± 0.78V), failed stop trials (1.39 ± 0.77V) and prEMG (0.69 ± 0.49V). Post-hoc paired *t*-tests showed prEMG had a significantly smaller peak EMG than all other response types (all ps < .05). This result was expected since participants successfully stopped themselves from pressing the button after initiating EMG activity.

Finally, we investigated the EMG epoch 100 ms prior to the stop stimulus for failed Stop trials and successful Stop trials with prEMG to determine if the EMG activity in this time window differentiated between successful and failed stopping (Figure 2.3 B & D). We compared the mean rectified EMG signal for each within this time window between the two response types with a 2 x 2 repeated measures ANOVA. A main effect of response type was observed [F (1,23) = 10.35, $p < .05$, $\eta^2 = .012$], and no differences found between hands [F (1,23) = 0.05, $p = .83$, $\eta^2 = .00$]. Post-hoc pairwise *t*-test indicates failed stop trials exhibited significantly more EMG in the pre-stop signal epoch ($t = 3.22$, $p < .05$).

Experiment 2: EMG Onset Times and Electromechanical Delay (EMD)

In experiment 2, EMG OTs were also evaluated with a 2 x 4 repeated measures ANOVA, raw values can be seen in **Table 2.1**. EMG OTs differed between fingers [F (1,27) = 28.805, p < .001, η^2 = .063] as well as between response types (GT go trials, SST go trials, failed stop trials and successful stop trials with prEMG) [F (3,81) = 28.363, p < .001, η^2 = .191]. Consistent with Experiment 2 button RT results, post-hoc t-tests revealed that unlike the simple SST in Experiment 1, SST Go trial EMG OTs were not significantly slower than EMG OTs from the GT, indicating participants did not slow in anticipation of stopping (t = -1.2, p = 1.0). As expected, failed stop trial EMG OTs had the shortest latencies in both fingers and were significantly faster than all other response types (all ps < .001). Participants contributed on average 17.7 ± 3.0 successful stop trials with prEMG per finger.

EMDs (mean ± sd) were calculated for GT go trials (FDI: 195 ± 46 ms, ADM: 186 ± 43 ms), SST go trials (FDI: 193 ± 29 ms, ADM: 177 ± 36 ms), and failed stop trials (FDI: 165 ± 27 ms, ADM: 156 ± 29 ms). Differences were observed between fingers [F (1,27) = 6.491, p = .017, η^2 = .023] and across conditions [F (2,54) = 27.013, p < .001, η^2 = .116]. Post-hoc paired t-tests revealed that EMDs on failed stop trials were significantly faster than both GT go trials (t = 5.6, p < .001) and SST go trials (t = 1.3, p = .58). In other words, the time between muscle activation and the button press differed between failed stop and go trials in addition to the earlier EMG onset time for failed stop than SST go trials. This suggests that there may be two distinct epochs that contribute to failed stopping: one that is prior to muscle engagement and one that occurs between muscle engagement and response completion.

The distribution of EMG OTs for prEMG and failed stop trials relative to the stop signal are presented in **figure 2.2 B & D** (FDI and ADM, respectively). Visual inspection of histograms

indicated a flip in the relative proportions of failed to successful stopping in the range of 0 to 0.03 s bins. Comparison between 0 and 0.03 s bins was not significant χ^2 (1,27) = 2.6, p = .11). Therefore, we expanded the window to compare between –0.03 and 0.03 s bins and found a significant difference χ^2 (1,24) = 18.56, p < .001). Like Experiment 1, the majority of participants (as identified by unique contributions to each bin) contribute successful and failed stop trials in this transition zone.

Experiment 2: Response EMG Profiles

As above, EMG onset to EMG peak, EMG peak to EMG offset, and cancel time were calculated for all possible response conditions (**fig. 2.4 A & C**). Cancel time did not differ between figures (p = .38, d = .17). Analysis of EMG onset to peak showed a significant main effect of finger [F (1,27) = 5.44, p < .05, η^2 = .034], with longer onset to peak durations for FDI than ADM in all response conditions. There was also a main effect of response condition [F (3,81) = 13.25, p < .001, η^2 = .78] which we explored with post-hoc t-tests. All EMG onset to peak pairwise comparisons were significant (ps < .05) with the exception of GT go trials compared with SST go trials (t = 1.5, p = .85).

EMG peak to offset time exhibited main effects of finger [F (1,27) = 5.50, p < .05, η^2 = .038] and response type [F (3,81) = 5.02, p < .05, η^2 = .025]. Post-hoc paired t-tests showed SST failed stop trials had significantly shorter peak to offset times than prEMG trials (t = 3.5, p < .05) and SST go trials (t = 4.2, p < .05). SST go trials were also found to exhibit significantly longer peak to offset times than prEMG trials (t = 5.7, p < .001). A significant interaction was present between finger and trial type [F (3,81) = 4.69, p < .005, η^2 = .008]. Post-hoc t-tests revealed a significant difference between FDI SST go trials and ADM SST prEMG (t = 3.7, p < .05). There was also a significant difference between ADM GT go trials and ADM SST prEMG (t = 3.97, p

< .05), while this pattern was not evident for the FDI GT go and FDI SST prEMG (t = .98, p = 1.0). The derived slope from peak EMG to EMG offset was steeper for FDI trials compared with ADM [F (1,27) = 9.24, p < .05, η^2 = .028] and there was also a main effect of response types [F (2,54) = 56.09, p < .001, η^2 = .025]. Post-hoc paired t-tests showed failed stop trials had significantly steeper EMG peak to offset slopes compared with SST go trials (t = 8.2, p < .001) and prEMG trials (t = -8.0, p < .001). Consistent with Experiment 1, this result suggests the influence of a persistent active inhibitory process during failed stopping.

Peak EMG (mean ± sd) values were as follows: GT go trials (FDI: 1.82 ± 0.80 V, ADM 1.15 ± 0.63 V), SST go trials (FDI: 1.84 ± 0.79 V, ADM: 1.17 ± 0.61 V), failed stop trials (FDI: 1.81 ± 0.80 V, ADM: 1.14 ± 0.56 V) and prEMG trials (FDI: 1.02 ± 0.50 V, ADM: 0.63 ± 0.33 V). Significant differences were observed between fingers [F (1,27) = 25.79, p < .001, η^2 = .157] as well as across response types [F (3,81) = 90.66, p < .001, η^2 = .145]. An interaction was observed between finger and trial type [F (3,81) = 4.75, p = .004, η^2 = .006] reflecting the proportionally smaller prEMG peak amplitudes for FDI than ADM. Similar to Experiment 1, post-hoc paired t-tests indicated that peak EMG from prEMG trials was significantly smaller than failed stop trials (t = 12.4, p < .001), SST go trials (t = 13.0, p < .001) and GT go trials (t = 11.3, p < .001). Go trials were not significantly different between GT and SST (t = -.4, p = 1.0) and failed stop trials were not significantly different from SST go trials (t = 2.0, p = .31).

As for Experiment 1, we compared rectified mean EMG amplitude within the 100 ms before the stop signal between failed stop and prEMG trials (**fig 2.4 B & D**). The 2 x 2 repeated measures ANOVA showed a main effect of response type [F (1,27) = 13.33, p < .001, η^2 = .073], and no significant differences between finger [F (1,27) = 1.03, p = .32, η^2 = .006]. The post-hoc paired t-test showed failed stop trials exhibited significantly greater EMG prior to the stop signal

than successful stops that contain partial response EMG ($t = 3.65$, $p \leq .001$). This replicated the findings of Experiment 1 and again indicates that EMG activity prior to the stop signal differed between successful and failed stop trials.

Discussion

In this study, we used simple and choice response versions of the SST paired with EMG to investigate whether muscle activity before the stop signal differentiates between successful and failed stopping and whether the decline in EMG activity at the culmination of a response reflects inhibitory processes acting at the level of the muscle. We found that EMG activity in the responding finger differentiated successful and failed stopping within the 100 ms preceding the stop signal. This revisits questions partially addressed in the previous studies regarding successful stop trials with prEMG responses (de Jong et al., 1990; Jana et al., 2020; Raud & Huster, 2017). However, here we show that this difference emerges within the first 100 ms before the stop signal in both the simple and choice stop tasks (**figs. 2.2 & 2.3**) and that EMG is sensitive to a "transition zone" during which the relative likelihoods of failed versus successful stopping invert (**fig. 2.4**). We also describe a novel marker of inhibition in the motor system when stopping fails. The time from the EMG peak to offset was consistently shorter for failed stop than go responses. This pattern is somewhat surprising and suggests that a response inhibition mechanism continues to exert an influence on motor activity throughout response execution.

An important feature of the study was the similarity between the two experiments that allowed for relative comparisons between effectors and made it possible to assess how introducing a choice response impacts elements of task performance and recruitment of muscles activity. The design afforded opportunities for internal replication and a rich data set of EMG

measures. Each experiment provided sufficient trial numbers in a relatively large sample size to measure partial responses, and the simple and choice task results indicate consistent findings. This experimental design offered high temporal resolution and precision enabling a detailed analysis of EMG signatures between conditions. The behavioral measurements were very well matched between response hands and effectors indicating tasks were performed similarly and outcomes were comparable. However, slowing was observed only in the simple version of the stop task (Experiment 1). The lack of slowing in Experiment 2 compared to Experiment 1 may be a consequence of the involvement of a choice, which inherently lengthens RTs. With our two separate samples, we cannot sufficiently address this question as the pattern may also be the consequence of interindividual differences. Nevertheless, the presence or absence of slowing did not appear to affect our EMG measures of interest related to stopping.

Previous work in this area (Jana et al., 2020; Raud & Huster, 2017) investigated aspects of EMG markers with a particular focus on trials with partial responses. However, they did not examine the extent and timing of EMG activation as a determinant of behavioral performance. Inconsistent with earlier work investigating the "point of no return" (de Jong et al., 1990), we observed that EMG increases before the stop signal led to stopping failure, regardless of whether a response choice was involved. This may be in line with more recent evidence indicating stopping is not faster than going (Du et al., 2022), as is implicit to the traditional horse race model. It was not expected that there existed a singular point of no return in which participants would be unable to inhibit a movement, especially at the group level. Instead, we have identified a transition zone that occurs near the stop signal in the choice task, ~160 ms after the go cue. This timeframe is consistent with estimates of cancel time, which we replicate here (Jana et al., 2020; Raud & Huster, 2017). In a similar vein, we show the evolution of the go process at ~160

ms after the go cue is what determines stopping success. Specifically, our data provide physiological evidence that successful cancellation of a response may not be possible if EMG activity is present before the stop signal.

We also found new evidence indicating the inhibitory process continues even when stopping fails. Our observation that EMG ramps down more quickly when stopping is unsuccessful provides a novel physiological marker of inhibition acting on the responding muscle. This inhibition is likely a manifestation of attempted stopping and may influence ensuing behavior on subsequent trials. An interesting question concerns whether or not this marker can be detected using other versions of the SST, such as the anticipatory response inhibition task, to potentially discriminate between selective and non-selective inhibitory mechanisms (MacDonald et al., 2014; Wadsley et al., 2019). This marker may be sensitive to abnormalities in inhibition in clinical populations such as Parkinson's Disease (Gauggel et al., 2004b; Obeso et al., 2008; N. Swann et al., 2011; Wessel et al., 2016). Furthermore, stopping may depend on two inhibitory mechanisms that act in sequence to pause-then-cancel a response (Diesburg & Wessel, 2021; Frank, 2006; Schmidt & Berke, 2017), and the lingering inhibition we observed during failed stopping may be a distinct marker of the second part of this two-step stopping process. These signatures may also have value for differentiating stopping-related inhibitory processes from other markers of motor inhibition, for example, those associated with unexpected and infrequent events (Iacullo et al., 2020).

Limitations

A limitation of this study was the notably high success rate at stopping in both experiments, above the typical 50% target. Although a high rate of stopping can invalidate SSRT estimates, here the higher rate of successful stopping afforded a greater number of prEMG

responses. This was helpful for attaining sufficient statistical power to compare EMG activity across response conditions. In addition, the simple stop-task design in Experiment 1 deviates from the recommended guidelines for administration of the stop task (Verbruggen et al., 2019) because the GT does not include a response choice. We specifically selected this design to assess response initiation in the absence of a choice decision because previous work suggests the process of making a response decision can interact with the stopping process (Logan, 2015; Logan & Cowan, 1984), and the convergent results between the two experiments provide validation that effects are not the result of interactions with response choice decision-related processes. We also note the peak prEMG does not reach the same level of activation as EMG on go and failed stop trials and this may partially explain differences in peak-to-offset slope. In the case of prEMG, there may be insufficient activation to necessitate suppression, or alternatively, the stopping mechanism engages early enough to provide gradual cancellation of the weaker level of activation.

Another possible limitation is that the tasks only included visual stimuli, which could leave open possible alternative outcomes for other modalities and warrants further investigation. Finally, the design of each experiment included a tonic contraction that was held for the duration of data collection. This decision was motivated by our initial intention to examine the tonic signal for EMG signatures of widespread inhibition when participants successfully canceled movements, in line with TMS experiments of similar design (Badry et al., 2009; Cai, Oldenkamp, et al., 2012; Majid et al., 2012; Wessel et al., 2013). Our initial approach to the analysis did not reveal stopping-related modulation within the tonic EMG signal, and we chose not to present these data here as follow-up investigations are underway. The additional task demands associated with sustaining a muscle contraction at a fixed level may have influenced

stop task performance. However, this does not seem likely as RTs and SSRT values are comparable to studies with similar task designs.

Conclusions

Previous work has not fully addressed whether a point of no return exists and whether inhibitory processes associated with stopping persist even during action execution. We addressed these questions in two experiments with a close examination of EMG activity. EMG activity preceding the stop signal differentiated successful and failed stop trials; moreover, we identified a transition zone where the likelihood of failing and succeeding at stopping inverts. This strongly supports the existence of a transition zone relative to the stop signal where behavioral outcomes are determined. It has been hypothesized that prEMG responses on successful stop trials indicate that the stop process runs to completion even after the responding muscle is engaged. Here, we showed the rate of decline in EMG activity on failed stop trials suggested a lingering effect of inhibition in the motor system. These two noninvasive electrophysiological markers associated with task performance may be useful for isolating specific mechanisms engaged in reactive stopping and may help to improve our understanding of inhibitory control deficits in clinical populations.

REFERENCES CITED

Badry, R., Mima, T., Aso, T., Nakatsuka, M., Abe, M., Fathi, D., Foly, N., Nagiub, H., Nagamine, T., & Fukuyama, H. (2009). Suppression of human cortico-motoneuronal excitability during the Stop-signal task. *Clinical Neurophysiology*, *120*(9), 1717–1723.

Bissett, P. G., Jones, H. M., Poldrack, R. A., & Logan, G. D. (2021). Severe violations of independence in response inhibition tasks. *Science Advances*, *7*(12), eabf4355. https://doi.org/10.1126/sciadv.abf4355

Cai, W., Oldenkamp, C. L., & Aron, A. R. (2012). Stopping speech suppresses the task-irrelevant hand. *Brain and Language*, *120*(3), 412–415.

de Jong, R., Coles, M. G. H., Logan, G. D., & Gratton, G. (1990). In search of the point of no return: The control of response processes. *Journal of Experimental Psychology: Human Perception and Performance*, *16*(1), 164. https://doi.org/10.1037/0096-1523.16.1.164

Diesburg, D. A., & Wessel, J. R. (2021). The Pause-then-Cancel model of human action-stopping: Theoretical considerations and empirical evidence. *Neuroscience & Biobehavioral Reviews*, *129*, 17–34. https://doi.org/10.1016/j.neubiorev.2021.07.019

Du, Y., Forrence, A. D., Metcalf, D. M., & Haith, A. M. (2022). *Comparing the speed of action initiation and action inhibition* [Preprint]. Neuroscience. https://doi.org/10.1101/2022.06.29.497798

Frank, M. J. (2006). Hold your horses: A dynamic computational role for the subthalamic nucleus in decision making. *Neural Networks*, *19*(8), 1120–1136.

Gauggel, S., Rieger, M., & Feghoff, T.-A. (2004). Inhibition of ongoing responses in patients with Parkinson's disease. *Journal of Neurology, Neurosurgery & Psychiatry*, *75*(4), 539–544. https://doi.org/10.1136/jnnp.2003.016469

Goonetilleke, S. C., Doherty, T. J., & Corneil, B. D. (2010). A Within Trial Measure of the Stop Signal Reaction Time in a Head-Unrestrained Oculomotor Countermanding Task. *Journal of Neurophysiology*, *104*(6), 3677–3690. https://doi.org/10.1152/jn.00495.2010

Iacullo, C., Diesburg, D. A., & Wessel, J. R. (2020). Non-selective inhibition of the motor system following unexpected and expected infrequent events. *Experimental Brain Research*, *238*(12), 2701–2710. https://doi.org/10.1007/s00221-020-05919-3

Jackson, N., & Greenhouse, I. (2019). VETA: An open-source matlab-based toolbox for the collection and analysis of electromyography combined with transcranial magnetic stimulation. *Frontiers in Neuroscience*, *13*, 975.

Jana, S., Hannah, R., Muralidharan, V., & Aron, A. R. (2020). Temporal cascade of frontal, motor and muscle processes underlying human action-stopping. *eLife*, *9*, e50371. https://doi.org/10.7554/eLife.50371

JASP Team. (2020). *JASP* (Version 0.14.1) [Computer software]. https://jasp-stats.org

Lakens, D. (2017). Equivalence tests: A practical primer for *t* tests, correlations, and meta-analyses. *Social Psychological and Personality Science*, *8*, 355-362. https://doi.oreg/10.1177/1948550617697177, PubMed: 28736600

Logan, G. D. (2015). The point of no return: A fundamental limit on the ability to control thought and action. *Quarterly Journal of Experimental Psychology*, *68*, 833-857. https://doi.org/10.1080/17470218.2015.1008020, PubMed: 25633089

Logan, G. D., & Cowan, W. B. (1984). On the ability to inhibit thought and action: A theory of an act of control. *Psychological Review*, *91*(3), 295. https://doi.org/10.1037/0033-295X.91.3.295

MacDonald, H. J., & Byblow, W. D. (2015). Does Response Inhibition Have Pre- and Postdiagnostic Utility in Parkinson's Disease? *Journal of Motor Behavior*, *47*(1), 29–45. https://doi.org/10.1080/00222895.2014.941784

MacDonald, H. J., Coxon, J. P., Stinear, C. M., & Byblow, W. D. (2014). The fall and rise of corticomotor excitability with cancellation and reinitiation of prepared action. *Journal of Neurophysiology*, *112*(11), 2707–2717. https://doi.org/10.1152/jn.00366.2014

Majid, D. S. A., Cai, W., George, J. S., Verbruggen, F., & Aron, A. R. (2012). Transcranial Magnetic Stimulation Reveals Dissociable Mechanisms for Global Versus Selective Corticomotor Suppression Underlying the Stopping of Action. *Cerebral Cortex*, *22*(2), 363–371. https://doi.org/10.1093/cercor/bhr112

Matzke, D., Curley, S., Gong, C. Q., & Heathcote, A. (2019). Inhibiting responses to difficult choices. *Journal of Experimental Psychology: General*, *148*(1), 124.

Matzke, D., Love, J., & Heathcote, A. (2017). A Bayesian approach for estimating the probability of trigger failures in the stop-signal paradigm. *Behavior Research Methods*, *49*(1), 267–281. https://doi.org/10.3758/s13428-015-0695-8

McGarry, T., & Franks, I. M. (1997). A horse race between independent processes: Evidence for a phantom point of no return in the preparation of a speeded motor response. *Journal of Experimental Psychology: Human Perception and Performance*, *23*(5), 1533.

McGarry, T., Inglis, J. T., & Franks, I. M. (2000). Against a final ballistic process in the control of voluntary action: Evidence using the Hoffmann reflex. *Motor Control*, *4*(4), 469–485.

Obeso, J. A., Rodríguez-Oroz, M. C., Benitez-Temino, B., Blesa, F. J., Guridi, J., Marin, C., & Rodriguez, M. (2008). Functional organization of the basal ganglia: Therapeutic implications for Parkinson's disease. *Movement Disorders*, *23*(S3), S548–S559. https://doi.org/10.1002/mds.22062

Pabi, G. (2024). Two one sided test (TOST) for equivalence. https://www.mathworks.com/matlabcentral/fileexchange/124560-two-one-sided-test-tost-for-equivalence

Raud, L., & Huster, R. J. (2017). The Temporal Dynamics of Response Inhibition and their Modulation by Cognitive Control. *Brain Topography*, *30*(4), 486–501. https://doi.org/10.1007/s10548-017-0566-y

Raud, L., Huster, R. J., Ivry, R. B., Labruna, L., Messel, M. S., & Greenhouse, I. (2020). A Single Mechanism for Global and Selective Response Inhibition under the Influence of Motor Preparation. *Journal of Neuroscience*, *40*(41), 7921–7935. https://doi.org/10.1523/JNEUROSCI.0607-20.2020

Raud, L., Thunberg, C., & Huster, R. J. (2022). Partial response electromyography as a marker of action stopping. *eLife*, *11*, e70332. https://doi.org/10.7554/eLife.70332

Schmidt, R., & Berke, J. D. (2017). A Pause-then-Cancel model of stopping: Evidence from basal ganglia neurophysiology. *Philosophical Transactions of the Royal Society B: Biological Sciences*, *372*(1718), 20160202. https://doi.org/10.1098/rstb.2016.0202

Skippen, P., Matzke, D., Heathcote, A., Fulham, W. R., Michie, P., & Karayanidis, F. (2019). Reliability of triggering inhibitory process is a better predictor of impulsivity than SSRT. *Acta Psychologica*, *192*, 104–117.

Swann, N., Poizner, H., Houser, M., Gould, S., Greenhouse, I., Cai, W., Strunk, J., George, J., & Aron, A. R. (2011). Deep Brain Stimulation of the Subthalamic Nucleus Alters the Cortical Profile of Response Inhibition in the Beta Frequency Band: A Scalp EEG Study in Parkinson's Disease. *Journal of Neuroscience*, *31*(15), 5721–5729. https://doi.org/10.1523/JNEUROSCI.6135-10.2011

The Jamovi Project. (2021). *Jamovi* (Version 2.2) [Computer software]. https://www.jamovi.org

van Boxtel, G. J., van der Molen, M. W., Jennings, J. R., & Brunia, C. H. (2001). A psychophysiological analysis of inhibitory motor control in the stop-signal paradigm. *Biological Psychology*, *58*(3), 229–262.

Verbruggen, F., Aron, A. R., Band, G. P., Beste, C., Bissett, P. G., Brockett, A. T., Brown, J. W., Chamberlain, S. R., Chambers, C. D., Colonius, H., Colzato, L. S., Corneil, B. D., Coxon, J. P., Dupuis, A., Eagle, D. M., Garavan, H., Greenhouse, I., Heathcote, A., Huster, R. J., … Boehler, C. N. (2019). A consensus guide to capturing the ability to inhibit actions and impulsive behaviors in the stop-signal task. *eLife*, *8*, e46323. https://doi.org/10.7554/eLife.46323

Verbruggen, F., & Logan, G. D. (2009). Models of response inhibition in the stop-signal and stop-change paradigms. *Neuroscience & Biobehavioral Reviews*, *33*(5), 647–661.

Wadsley, C. G., Cirillo, J., & Byblow, W. D. (2019). Between-hand coupling during response inhibition. *Journal of Neurophysiology*, *122*(4), 1357–1366. https://doi.org/10.1152/jn.00310.2019

Wessel, J. R., Ghahremani, A., Udupa, K., Saha, U., Kalia, S. K., Hodaie, M., Lozano, A. M., Aron, A. R., & Chen, R. (2016). Stop-related subthalamic beta activity indexes global motor suppression in Parkinson's disease. *Movement Disorders*, *31*(12), 1846–1853. https://doi.org/10.1002/mds.26732

Wessel, J. R., Reynoso, H. S., & Aron, A. R. (2013). Saccade suppression exerts global effects on the motor system. *Journal of Neurophysiology*, *110*(4), 883–890. https://doi.org/10.1152/jn.00229.2013

Bridge

The experiments presented in Chapter II yielded important insights into the timing, and duration in which inhibitory influence arrives and impacts task-relevant effectors in the context of a SST. Importantly, we showed on failed stop trials, it is likely inhibition is still arriving, but too late to terminate a process. This is shown in the increased slope angle on failed stop trials. However, a portion of this experiment that we did not observe significant results in was related to the tonic muscular contraction that participants performed throughout both SSTs. We hypothesized that a global suppressive mechanism would result in decreases in tonic EMG for task-irrelevant effectors during trials in which participants successfully stopped movements. This effect was not observed in these experiments.

We pursued a follow-up study led by an undergraduate mentee, Isaiah Mills to continue testing this idea. We designed a similar experiment with some crucial changes. Isaiah implemented a bimanual ARI task in which participants maintained a contraction in task-irrelevant effectors of both hands. Essentially participants responded to stimuli with their index fingers and maintained a steady contraction with their little fingers. Analysis of the tonic EMG signal revealed transient inhibition during failed stopping compared to go responses, indicating tonic muscle activity is sensitive to global motor suppression. This study served as Isaiah's honor's thesis in the Department of Human Physiology and was published in eNeuro (doi.org/10.1523/ENEURO.0166-24.2025).

CHAPTER III

SINGLE-PULSE TRANSCRANIAL MAGNETIC STIMULATION TO RIGHT INFERIOR FRONTAL CORTEX AND PRE-SUPPLEMENTARY MOTOR AREA ELICITS AN ELECTROMYOGRAPHIC RESPONSE

Introduction

Mapping functional and eloquent areas of the brain is an important clinical process that is routinely performed during exploratory or resective craniotomies. Electrical stimulation of the cortex has a long history and has been useful for producing a detailed functional map of the motor cortex (Krause, 1912; Penfield & Boldrey, 1937), sensory cortex (Cushing, 1909), language areas (Ojemann et al., 1989; Ojemann, 1991), and other functions (De Schotten et al., 2005; Gharabaghi et al., 2006). A standard method of cortical mapping uses direct electrical stimulation (DES) with the goal of informing neurosurgeons in real time which tissue is safe to resect while minimizing post-operative impairments with an emphasis on preserving speech and motor control (Mahon et al., 2019). During mapping, DES is often paired with resting, speech and / or repetitive movement tasks (Breshears et al., 2015; Penfield, 1949) to detect motor responses.

Depending on the site of stimulation, DES can elicit or interrupt movements and has been useful for understanding neural mechanisms for movement production and cancellation. For example, Rech et al. (2017), utilized a cortical and subcortical electrical stimulation approach to functionally map patients with frontal gliomas for resective surgery. The authors identified areas close to the central sulcus which produced movement and frontal (premotor and supplementary motor areas) that caused an arrest of movement. It is known that removal of tissue within this frontal network may result in patients developing supplementary motor area (SMA) syndrome (a

temporary neurological condition often resulting in hemiparesis, apraxia or speech difficulty, Pinson et al., 2022), and long-term bimanual motor deficits (Rech et al., 2014). Despite mechanisms of cortical and subcortical stimulations not being fully understood (Borchers et al., 2012), DES is a valuable tool for eliciting and mapping motor areas of the cortex.

When certain cortical areas (primarily sensorimotor cortex) are stimulated, they may produce vocalizations and overt movements known as positive motor responses (PMRs; Foerster, 1931, 1936; Penfield, 1938; Penfield & Jasper, 1954). Intriguingly, stimulation of various frontal cortical regions elicits negative motor responses (NMR; Penfield & Boldrey, 1937). NMRs stand in contrast to PMRs by causing a complete inhibition of movement without loss of muscle tone or consciousness (Lüders, 1987; Lüders et al., 1995). Typical NMRs include speech arrest and arrest of hand, leg and foot movements. Given the nature of NMRs, it is only possible to detect them when the negative motor area (NMA) for given effector(s) is stimulated during repetitive movement or ongoing muscular activity of the effector(s). Furthermore, cortical mapping during surgery is generally more of a practical matter in which elicitation of overt behaviors or inhibition of behaviors are observed to determine functionality, typically in the absence of electrophysiological measurements (e.g. electromyography; EMG), with some recent exceptions (Fornia, Puglisi, et al., 2020; Fornia, Rossi, et al., 2020; Rech et al., 2017; Simone et al., 2020; Viganò et al., 2019, 2021).

A separate line of research has identified a network for action stopping (Aron, Durston, et al., 2007). This cortico-basal ganglia network includes the right inferior frontal cortex (rIFC), pre-supplementary motor area (pre-SMA), motor cortex (M1) and the subthalamic nucleus (STN) (Aron et al., 2007; Aron & Poldrack, 2006; Badry et al., 2009; Nambu et al., 2002; Schaum et al., 2021; Swann et al., 2009; Swann et al., 2012). Within this network is the

hyperdirect pathway between the frontal cortex and the STN, which is implicated in widespread motor system suppression. Reactive stopping activates this network and has a widespread inhibitory influence on the motor system as demonstrated with TMS over M1 (Badry et al., 2009; Cai, Oldenkamp, et al., 2012; Wessel et al., 2013). Moreover, individuals with greater white matter integrity within this hyperdirect pathway are faster at stopping (Aron, Durston, et al., 2007; Coxon et al., 2012). Additional recent work has established the involvement of the hyperdirect pathway in humans using intraoperative approaches (Chen et al., 2020).

Intriguingly, this network overlaps with NMAs identified with DES (Breshears et al., 2019; Filevich et al., 2012; Mikuni et al., 2006; Schucht et al., 2013). Specific regions include bilateral IFC (Borggraefe et al., 2016; Breshears et al., 2015; Ikeda et al., 1995; Luders, 1987; Lüders et al., 1995; Monticelli et al., 2020; Penfield, 1949), SMA (Fried et al., 1991; Ikeda et al., 1992; Ikeda et al., 1993, 1995; Lim et al., 1994; Monticelli et al., 2020; Penfield, 1949; Penfield & Jasper, 1954; Penfield & Welch, 1951; Rech et al., 2014, 2019; Schucht et al., 2013; Yazawa et al., 2000; Zhou et al., 2021) and premotor cortices (Parmigiani & Cattaneo, 2018; Rech et al., 2019; Schluter et al., 1998; Yokoyama et al., 2020). This suggests a plausible functional role of the inhibitory stopping network and arrest of movement via stimulation of the negative motor system.

Transcranial magnetic stimulation (TMS) is another method for non-invasively eliciting PMRs while stimulating over the primary motor cortex (M1). TMS can reliably stimulate cortical populations of neurons at depths consistent with potential candidate NMAs, such as the rIFC and preSMA; (Cai, George, et al., 2012; Di Lazzaro et al., 2012; Groppa et al., 2012; Siebner et al., 2022). Like DES, several lines of evidence suggest TMS activates both inhibitory and excitatory neurons in the cortex with downstream effects on connected regions. TMS has utility for

mapping cortical representations including for clinical purposes such as pre-surgical planning (Sondergaard et al., 2021).

Traditional approaches to map or elicit NMRs have been almost exclusively performed in clinical populations with invasive procedures (i.e. surgical suite). Given that resection of NMAs may disrupt motor control (Rech et al., 2014), there is a motivation to find alternative methods for stimulating NMAs and understanding their role in the larger motor, and potentially inhibitory control network. The present research is motivated by the possibility of utilizing non-invasive brain stimulation to map non-motor regions of the cortex which are implicated in the inhibitory control network. This provides an excellent opportunity to supplement clinical populations such as Parkinson's disease or attention deficit disorders as it is thought the inhibitory control network is abnormal in such populations (Alderson et al., 2007; Bissett et al., 2015). However, we need to understand if it is feasible to elicit negative motor responses in this manner.

We set out to test whether we could elicit NMRs with single-pulse TMS over frontal targets in healthy young adults. Participants maintained tonic muscle activity and EMG was recorded while TMS was administered to the rIFC and right preSMA, or the occipital cortex (OCC) as a control. rIFC and preSMA were selected based on intraoperative results that indicated these areas produce negative motor responses most reliably (Breshears et al., 2019). We also measured the effect of M1 stimulation to identify MEP and CSP events for reference. We hypothesized stimulation over candidate NMAs would cause brief interruptions in tonically active contralateral muscles but interruptions would not be observed for OCC or M1 stimulation.

Methods

Participants

Sixteen healthy young adults were recruited for this experiment (7 male, 9 female; mean age ± std, 25.1 ± 4.8 years), all were right-handed (mean laterality quotient ± std, 0.84 ± 0.15; Veale, 2014). One participant was removed because of data quality, and M1 data from an additional participant was removed due to data quality. Therefore, we analyzed fifteen datasets of non-motor cortex stimulation, and fourteen M1 datasets. The study was approved by the University of Auckland Human Participants Ethics Committee (Ref. UAHPEC22709). Data were collected at the University of Auckland due to restrictions on human subjects research at the University of Oregon related to the COVID-19 pandemic.

Electromyography and Task Procedure

Surface EMG was recorded using Ag-AgCl surface electrodes and was sampled at 2000 Hz with a CED interface system (MICRO1401mkii, Cambridge Electronic Design Ltd.). EMG data was collected from four muscles of interest on the left hand, forearm and shoulder of the participant: first dorsal interosseous (FDI), abductor pollicis brevis (APB), extensor carpi radialis (ECR) & the anterior deltoid (Delt). Grounding electrode was positioned on the dorsum of the left hand.

Participants were comfortably seated approximately 60 cm in front of a computer screen where a live feed of their rectified EMG activity was displayed using Signal software (Version 6.05, Cambridge Electronic Design Ltd.). The maximum voluntary contraction (MVC) for each muscle was determined by asking the participants to contract the muscle as forcefully as they could four times with each contraction lasting 1 – 2 seconds. The peak value in millivolts in a 100 ms mid-contraction window was used as the MVC for each individual muscle.

The participants were then trained to simultaneously maintain a contraction equivalent to 10% of the MVC for each of the four muscles (**fig. 3.1**). To engage these muscles concurrently, the participants performed a "pinch" maneuver between their thumb and forefinger to activate FDI and APB muscles. At the same time, the participant would extend their wrist for engagement of ECR while flexing at the shoulder anteriorly in the sagittal plane to engage the anterior deltoid. To practice holding this posture in a steady manner, EMG reference lines equivalent to 10% MVC were displayed with the live rectified EMG for each muscle. Participants practiced until they could reliably sustain activation of the four muscles at or marginally above the 10% MVC threshold. EMG data was collected throughout each four second trial of the ensuing TMS protocol while participants maintained contraction at 10% MVC. Breaks were allotted throughout the session to rest the effectors.

TMS Protocol and Brainsight MNI Targeting

Single-pulse TMS was delivered over the cortex using a 70 mm figure-of-eight coil connected to a Magstim 200 stimulator (The Magstim Company Ltd, Whitland, UK). The coil was handheld and positioned over right M1 with the handle pointing backward and laterally, approximately 45° relative to midline. The optimal coil position (hotspot) for eliciting motor evoked potentials (MEPs) in the left FDI was determined and marked on the scalp. The intensity for the resting motor threshold (RMT) was used to prescribe sub- (80% RMT) and supra- (110, 120, & 130% RMT) threshold stimulation intensities for both posterior-to-anterior (PA) and anterior-to-posterior (AP) current directions during the remainder of the experiment (**Table 3.1**). These intensities were selected to ensure stimulation of the underlying targets and to assess a potential gradient of any resulting EMG events that might scale with input intensity (Seibner et al. 2022). PA and AP RMT were found to be 46.5 ± 5.7%, 60.7 ± 7.6% of max stimulator output.

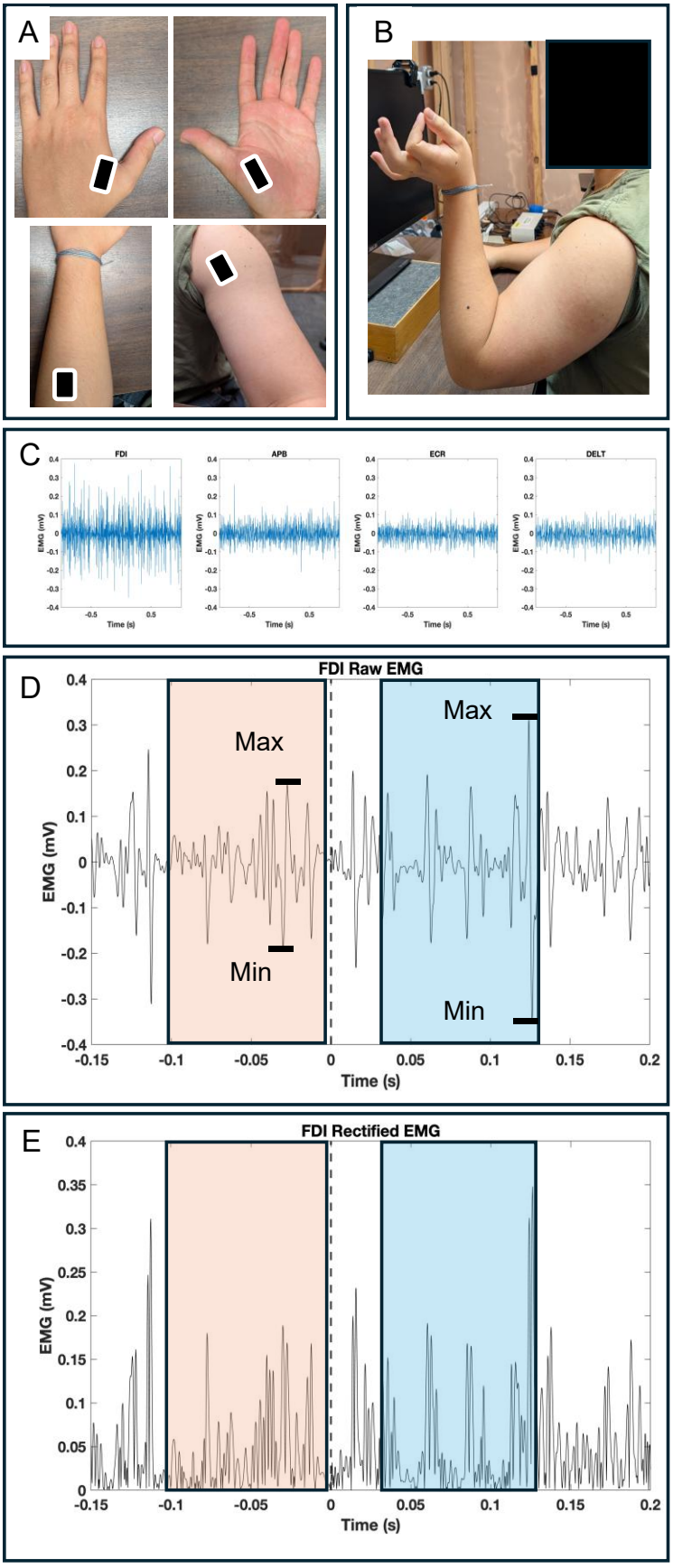

Figure 3.1. A) EMG electrode placement indicated by black rectangle. Top left photo = first dorsal interosseous (FDI), top right photo = abductor pollicis brevis (APB), bottom left photo = extensor carpi radialis (ECR), and bottom right photo = anterior deltoid (DELT). **B)** Task posture with all four muscles in a contracted status. Thumb and forefinger in a modified pinch grip, wrist extended to activate ECR and shoulder flexed to activate DELT. **C)** Example raw traces from a trial for each muscle. Time point 0 is when TMS pulse was delivered. **D)** Example calculation of peak to peak calculation (minimum subtracted from maximum) in pre- and post-stimulation time epoch of 100 ms. Pre-stimulation epoch was -105 ms to -5 ms before stimulation. Post-stimulation epoch was 25 ms to 125 ms. Calculated on a single raw trial. **E)** Example rectified EMG from a single trial. Area under the curve (AUC) was calculated in the same time epochs as peak to peak, but on rectified EMG signal.

Table 3.1. Stimulation sites, intensities as a percentage of resting motor threshold, coil orientations and trial counts for single-pulse transcranial magnetic stimulation. Stimulation intensity was set as a percentage relative to each participant's resting motor threshold (% RMT).

Stimulation Site	MNI Coordinates	Intensity (% RMT)	Coil Orientation	Trials per Orientation	Trial Total per Site
M1	(FDI hotspot)	80, 110	AP & PA	12	96
rIFC	X = 42 Y = 18 Z = -6	110, 120, 130	AP & PA	20	160
preSMA	X = 0 Y = 22 Z = 46	110, 120, 130	AP & PA	20	160
OCC	X = 6 Y = -84 Z = -1	130	AP & PA	12	48

Following hotspotting and thresholding of M1, single-pulse TMS was delivered to 4 cortical regions of interest (ROI): M1, rIFC, preSMA, and OCC. Each ROI was stimulated with the TMS coil in both PA and AP coil placements to evaluate a potential influence of current direction. The ROI order, current direction, and TMS intensities were randomized and counterbalanced across participants. Stimulation intensities and counts are listed in **Table 3.1** for each ROI.

In the present study, MNI (Montreal Neurological Institute) coordinates (Evans et al., 1994) were used for targeting rIFC (X = 42, Y = 18, Z = -6; Hampshire et al., 2010), preSMA (X = 0, Y = 22, Z = 46; Hampshire et al., 2010), and OCC pole (X = 6, Y = -84, Z = -1). M1 was stimulated on the same hotspot identified for eliciting MEPs in the FDI and served as a control target for measuring MEPs and cortical silent periods (CSPs). The MNI coordinates were co-registered into a Brainsight (Rogue Research ™) neuronavigation system for targeting all ROIs except M1. This system consists of a stereo camera, infrared trackers, and software for guiding the placement of the TMS coil relative to a participant's head based on anatomical targets. TMS

pulses were delivered 2 seconds into each 4 second trial while the participant was maintaining tonic 10% MVC contractions with each of the four selected effectors. MEPs from 110% stimulation shown in **Figure 3.2**.

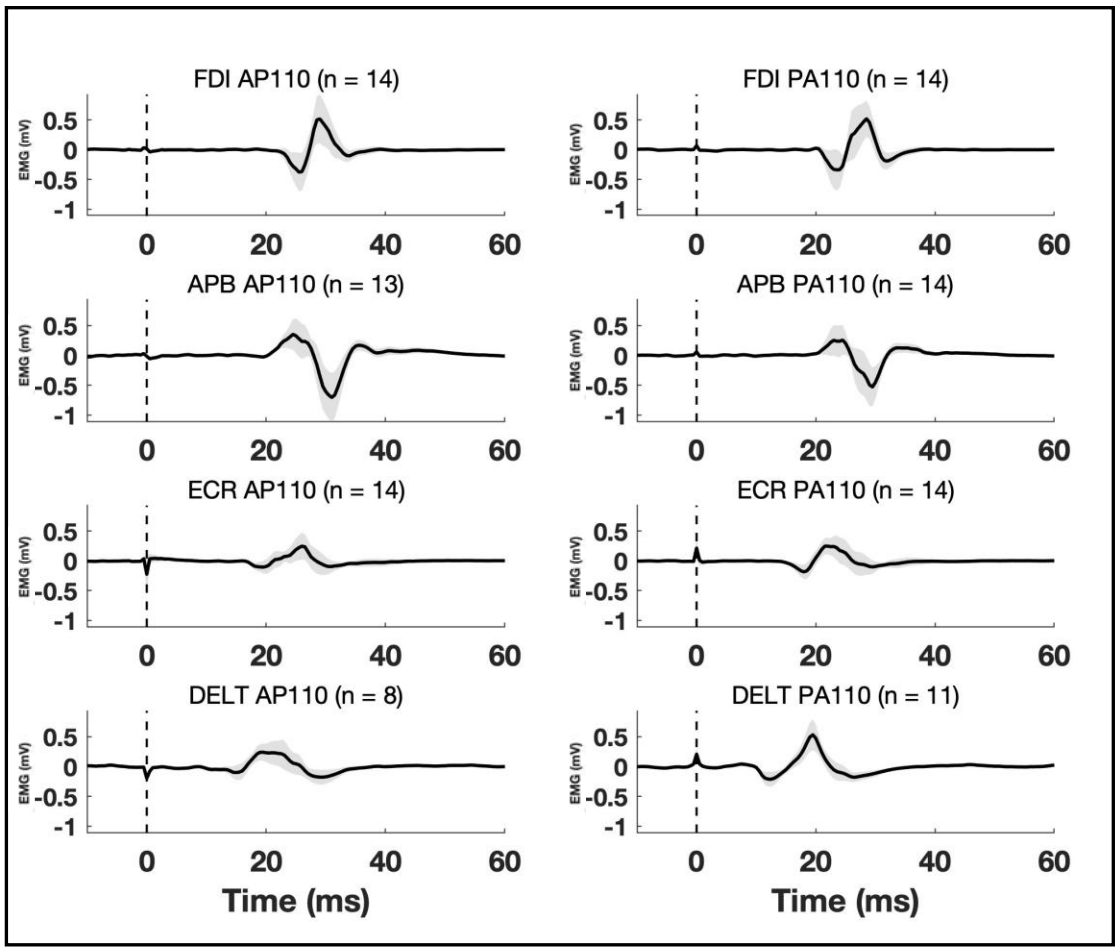

Figure 3.2. EMG signal from stimulation of the primary motor cortex (M1) over the FDI hotspot. Group averages for each muscle and coil orientation shown with shaded error. Samples are shown for each condition in parentheses since not every participant exhibited motor evoked potential (MEPs) for M1 stimulation. Note latency differences in MEPs and the EMG event indicated in Figures 3.6, 3.7, and 3.8.

EMG Data Preprocessing & Visualization

EMG data were preprocessed and visualized in two stages using the VETA toolbox (Jackson & Greenhouse, 2019) in MATLAB. First, MEPs and CSPs from the M1 condition were identified using an automatic detection algorithm. Next, data from each trial were visualized to

ensure that participants maintained sufficient levels of tonic EMG from each muscle. Whole trials or channels from a trial were removed from analysis based on visual determination of the EMG deflection outside the expected range, especially in the 500 ms window before and after stimulation. These were trials in which the participants were not sustaining a steady contraction and were removed. For rIFC stimulation, participants (n = 15) contributed an average of 18.8 ± 0.9 trials (maximum of 20) for conditions evaluated in this paper. Participants (n = 15) contributed an average of 18.9 ± 1.6 trials for the preSMA target (maximum of 20). By design, there were fewer stimulations to the OCC, and participants (n = 15) contributed an average of 11.4 ± 0.5 trials (maximum of 12) for analysis. M1 stimulation (n = 14) trial counts can be viewed in **Table 3.2** & **3.3**.

To assess the evoked responses from rIFC and preSMA, we measured the peak-to-peak amplitude and area under the curve (AUC) at the individual trial level as well as at the participant level. Measuring at the individual trial level is sensitive to patterns more similar to individual MEPs whereas averaging across trials within a participant is sensitive to features that may be hidden beneath noisier individual trial fluctuations, similar to an electroencephalographic event related potential (ERP). Peak-to-peak amplitude was assessed on raw, baseline-corrected data in a 100 ms pre-stimulation window (from 105 ms to 5 ms pre-stimulation) and a matched 100 ms post-stimulation window (from 25 ms to 125 ms post-stimulation). Example of peak-to-peak on single trial in **Figure 3.1D.** These values were used to compare if the post-stimulation window exhibited a proportionally greater EMG response than the pre-stimulation window. AUC was assessed in baseline-corrected, raw, rectified data using the trapz.m function in Matlab. AUC was performed in the same windows as peak-to-peak amplitude (see **fig 3.1E)**, and post-stimulation values were divided by pre-stimulation values to produce a proportion to compare

pre and post stimulation evoked responses. To evaluate these same measures at the subject level, the analyses were performed on the mean baseline-corrected data for all eligible trials from each condition. In the M1 condition, MEPs and CSPs were analyzed on raw data. MEPs were evaluated for peak-to-peak amplitude, onset latency and offset latency relative to stimulation, and CSPs were evaluated for duration and offset time. CSP duration was calculated by subtracting MEP offset time from CSP offset time.

Table 3.2. Motor-evoked potential amplitudes and latencies (mean ± sd) from M1 stimulation for each muscle for given coil orientation and intensity based on resting motor threshold. Mean number of trials ± sd for each condition shown in parentheses, n = 14. Note: FDI = first dorsal interosseous, APB = abductor pollicis brevis, ECR = extensor carpi radialis, DELT = anterior deltoid; AP = anterior-posterior current direction, PA = posterior-anterior current direction.

MEP Amplitudes				
	FDI	**APB**	**ECR**	**DELT**
AP 80% (mV)	1.08 ± 0.49 **(2 ± 3)**	1.08 ± 0.86 **(2 ± 3)**	0.99 ± 0.15 **(0 ± 1)**	—
AP 110% (mV)	2.83 ± 2.02 **(10 ± 3)**	2.71 ± 1.89 **(10 ± 4)**	1.56 ± 0.98 **(10 ± 3)**	1.21 ± 0.70 **(4 ± 4)**
PA 80% (mV)	0.88 ± 0.43 **(2 ± 2)**	1.02 ± 1.02 **(1 ± 1)**	0.65 ± 0.23 **(2 ± 2)**	—
PA 110% (mV)	2.79 ± 2.09 **(11 ± 1)**	2.31 ± 1.76 **(10 ± 3)**	1.79 ± 0.86 **(11 ± 1)**	1.26 ± 1.02 **(5 ± 5)**
MEP Latencies				
	FDI	**APB**	**ECR**	**DELT**
AP 80% (ms)	22.0 ± 6.1 **(2 ± 3)**	21.8 ± 5.5 **(2 ± 3)**	19.7 ± 13.8 **(0 ± 1)**	—
AP 110% (ms)	19.2 ± 4.5 **(10 ± 3)**	19.4 ± 5.9 **(10 ± 4)**	14.4 ± 4.8 **(10 ± 3)**	13.9 ± 11.0 **(4 ± 4)**
PA 80% (ms)	19.6 ± 4.6 **(2 ± 2)**	21.4 ± 11.0 **(1 ± 1)**	13.4 ± 4.1 **(2 ± 2)**	—
PA 110% (ms)	17.4 ± 4.5 **(11 ± 1)**	17.9 ± 5.0 **(10 ± 3)**	13.6 ± 4.4 **(11 ± 1)**	9.7 ± 2.5 **(5 ± 5)**

Statistical Tests

Statistical tests were performed in JASP (JASP 0.16.3, JASP, 2020). Peak-to-peak and AUC measures were represented as a proportion of the post-stimulation epoch relative to the pre-stimulation baseline. The same statistical tests were performed for the trial-wise and subject-averaged (ERP) data.

A repeated-measures ANOVA with the factors ROI (rIFC, preSMA, and OCC), coil orientation (AP and PA), and muscle (FDI, APB, ECR, and DELT) tested for differences in peak-to-peak and AUC measures. This test was performed for the 130% RMT TMS intensity as this intensity was consistent across ROI. We also performed repeated-measures ANOVA to evaluate whether there was an effect of TMS intensity with factors ROI (rIFC, preSMA), coil orientation (AP and PA), stimulation intensity (110%, 120%, and 130%), and muscle (FDI, APB, ECR, DELT). This was appropriate because only rIFC and preSMA were matched at 110, 120, and 130% RMT. Sphericity violations were corrected with Greenhouse-Geisser and significant effects were evaluated with Bonferroni-corrected post hoc tests, alpha level set to 0.05. Statistical test results are provided with the corrected non-integer degrees of freedom unless otherwise noted. Means and standard deviations were calculated for characteristics of MEPs and CSPs resulting from M1 stimulation, however no statistical comparisons were made due to relatively low trial counts (**Table 3.2 & 3.3**).

Table 3.3. Cortical silent period onset latencies and durations (mean ± sd) from M1 stimulation for each muscle for given coil orientations and intensity based on resting motor threshold. Mean ± sd number of trials shown in parentheses, n = 14. Note: FDI = first dorsal interosseous, APB = abductor pollicis brevis, ECR = extensor carpi radialis, DELT = anterior deltoid; AP = anterior-posterior current direction, PA = posterior-anterior current direction.

CSP Latencies				
	FDI	**APB**	**ECR**	**DELT**
AP 80% (ms)	35.0 ± 10.1 (**2 ± 3**)	42.1 ± 4.8 (**2 ± 4**)	33.9 ± 6.8 (**0 ± 1**)	—
AP 110% (ms)	48.2 ± 7.9 (**10 ± 2**)	50.5 ± 8.9 (**10 ± 3**)	41.7 ± 7.1 (**10 ± 3**)	39.7 ± 12.7 (**3 ± 4**)
PA 80% (ms)	45.9 ± 27.8 (**1 ± 1**)	39.7 ± 14.7 (**0 ± 1**)	28.7 ± 3.0 (**1 ± 2**)	—
PA 110% (ms)	45.5 ± 6.7 (**11 ± 1**)	46.8 ± 7.8 (**11 ± 2**)	38.8 ± 6.0 (**11 ± 1**)	31.3 ± 5.7 (**4 ± 5**)
CSP Durations				
	FDI	**APB**	**ECR**	**DELT**
AP 80% (ms)	33 ± 9 (**2 ± 3**)	34 ± 11 (**2 ± 3**)	23 ± 11 (**0 ± 3**)	—
AP 110% (ms)	76 ± 33 (**10 ± 3**)	72 ± 33 (**10 ± 3**)	61 ± 24 (**10 ± 3**)	49 ± 12 (**3 ± 5**)
PA 80% (ms)	36 ± 24 (**1 ± 3**)	43 ± 15 (**0 ± 3**)	22 ± 5 (**1 ± 3**)	—
PA 110% (ms)	68 ± 31 (**11 ± 3**)	56 ± 23 (**11 ± 3**)	57 ± 17 (**11 ± 3**)	37 ± 11 (**4 ± 5**)

Results

Trial-wise comparisons at 130% RMT

Mean peak-to-peak and AUC measures were calculated across trials within each participant and submitted to statistical tests. For peak-to-peak amplitudes, there was a significant main effect of ROI, [$F(1.456, 20.385) = 5.83$, $p < .05$, $\eta^2_p = .294$], and no significant effects of coil orientation [$F(1, 14) = 0.32$, $p = .58$, $\eta^2_p = .022$] or muscle [$F(1.955, 27.365) = 3.15$, $p = .060$, $\eta^2_p = .177$]. Post hoc t tests for ROI revealed significantly greater peak-to-peak amplitudes for rIFC compared to preSMA ($t = 2.7$, $d = .41$, $p < .05$) and OCC ($t = 3.2$, $d = .49$, $p < .05$). This

result does not agree with our initial hypothesis which predicted a reduction in tonic EMG following stimulation of rIFC and preSMA. As can be seen in (**fig. 3.3, 3.6 & 3.7**), there is a stereotyped rise in the tonic EMG signal across each muscle for most conditions following TMS. However, rIFC exhibited the greatest effect of stimulation indicating a possible link with this ROI and the motor output. Therefore, the peak-to-peak and AUC results will represent the relative increase in EMG activity compared with the pre-stimulation activity. Comparatively, OCC does not show this stereotyped rise and fall post-stimulation (**fig.** 3.**6**). Peak-to-peak results can be seen in **Figure 3.4**.

For AUC, there were significant main effects of ROI, [$F(1.348, 18.876) = 9.19$, $p < .01$, $\eta^2_p = .396$], coil orientation [$F(1,14) = 10.60$, $p < .01$, $\eta^2_p = .431$], and muscles [$F(2.068, 28.950) = 5.38$, $p = .010$, $\eta^2_p = .278$]. Bonferroni-corrected post hoc *t* tests for ROI indicated greater AUC for rIFC compared with OCC ($t = 4.3$, $d = .93$, $p < .001$), but not preSMA compared with OCC ($t = 1.7$, $d = .38$, $p = .28$). The post hoc *t* test between rIFC and preSMA was not significant ($t = 2.5$, $d = 0.55$, $p = .054$). Since coil orientation only has two levels, we observed the AP orientation had a significantly greater AUC when collapsed across muscles and ROI. For the comparisons between muscles, post hoc *t* tests showed AUC was significantly smaller for APB ($t = -3.2$, $d = -0.44$, $p < .05$) and ECR ($t = -3.7$, $d = -0.51$, $p < .01$) than DELT. The differences between DELT and other muscles are possibly related to the relatively stronger muscular activity from a larger muscle corresponding to a greater range. It is possible that scaled for muscle size, the proportional change is equivalent across muscles, but this was not investigated. AUC results can be seen in **Figure 3.5**.

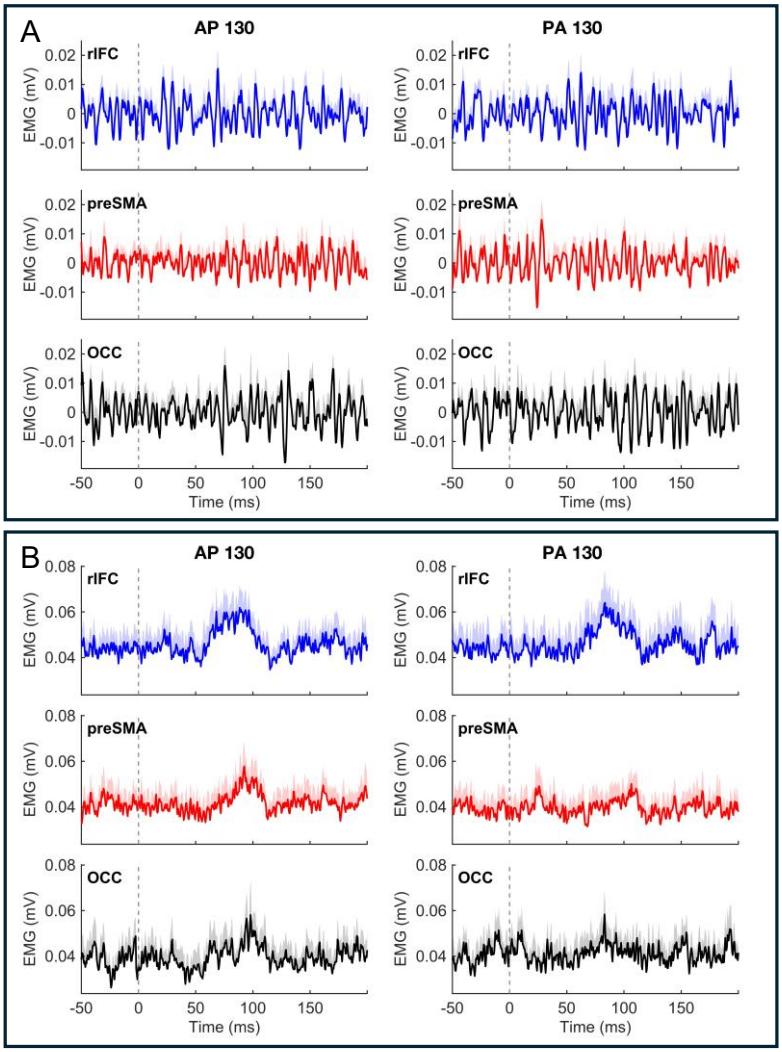

Figure 3.3. Example group level FDI raw EMG signal for AP and PA 130% RMT stimulation with positive error displayed (n = 15). **A)** The mean signal was calculated for each participant within each respective condition and then the mean was calculated at the group level. **B)** The signal was rectified at the trial level for each participant, then averaged for the participant and then the mean was calculated across the group.

Trial-wise comparisons across 110%, 120%, and 130% RMT

Next, we evaluated effects of TMS intensity (110%, 120%, and 130% RMT) over rIFC vs. preSMA. A main effect of ROI showed rIFC had a significantly greater peak-to-peak amplitude than preSMA [$F(1, 14) = 19.27$, $p < .001$, $\eta^2_p = .579$]. There was also a main effect of coil orientation with AP coil orientation producing significantly greater peak-to-peak amplitudes

than PA [$F(1.998, 27.199) = 4.71$, $p < .001$, $\eta^2_p = .576$]. There was a main effect of muscle [$F(1.998, 27.978) = 4.71$, $p < .05$, $\eta^2_p = .252$], but there was no main effect of TMS intensity [$F(1.943, 27.199) = 0.92$, $p = .41$, $\eta^2_p = .062$]. The pattern was the same for AUC with main effects of ROI [$F(1, 14) = 21.80$, $p < .001$, $\eta^2_p = .609$], coil orientation [$F(1, 14) = 19.53$, $p < .001$, $\eta^2_p = .582$], and muscle [$F(1.809, 25.331) = 14.88$, $p < .001$, $\eta^2_p = .515$], but no effect of TMS intensity [$F(1.703, 23.843) = 1.68$, $p = .21$, $\eta^2_p = .107$].

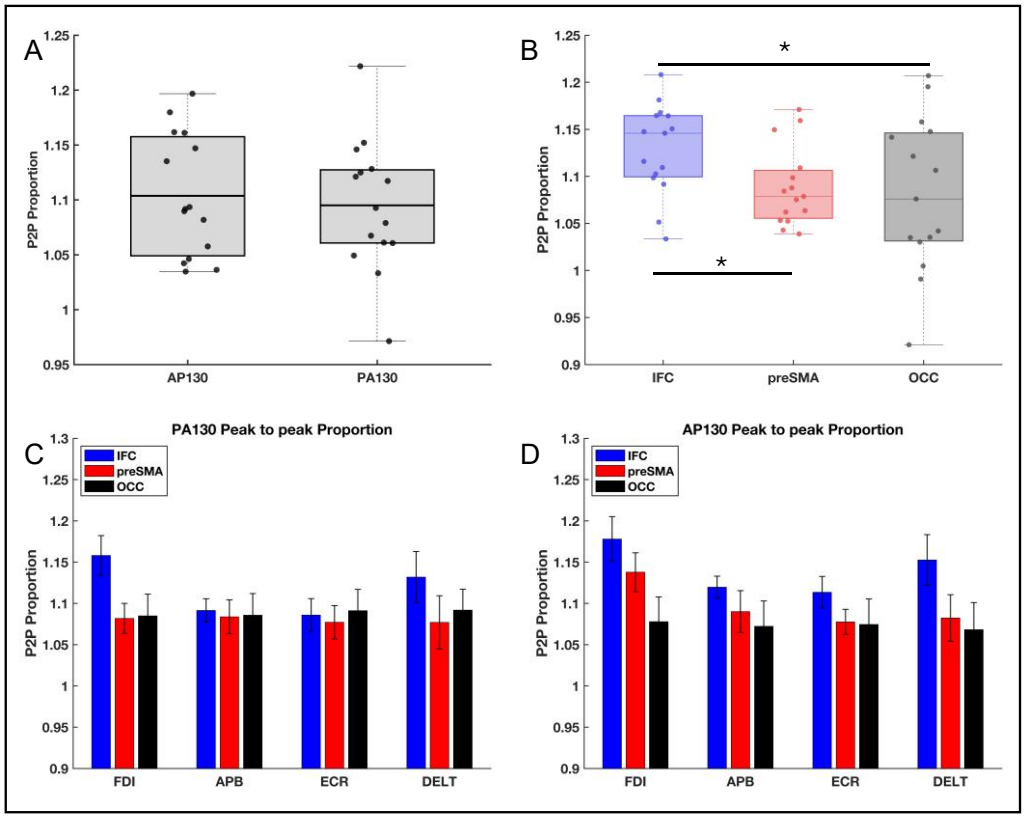

Figure 3.4. Proportion of peak-to-peak difference (P2P) post- vs. pre- stimulation calculated at the trial level (n = 15). **A)** Boxplot displaying P2P difference between AP and PA coil orientation at 130% RMT. **B)** Boxplot showing the P2P difference between ROI. **C)** PA130 AUC proportion for each ROI and muscle. **D)** AP130 P2P proportion for each ROI and muscle. * indicates p < .05.

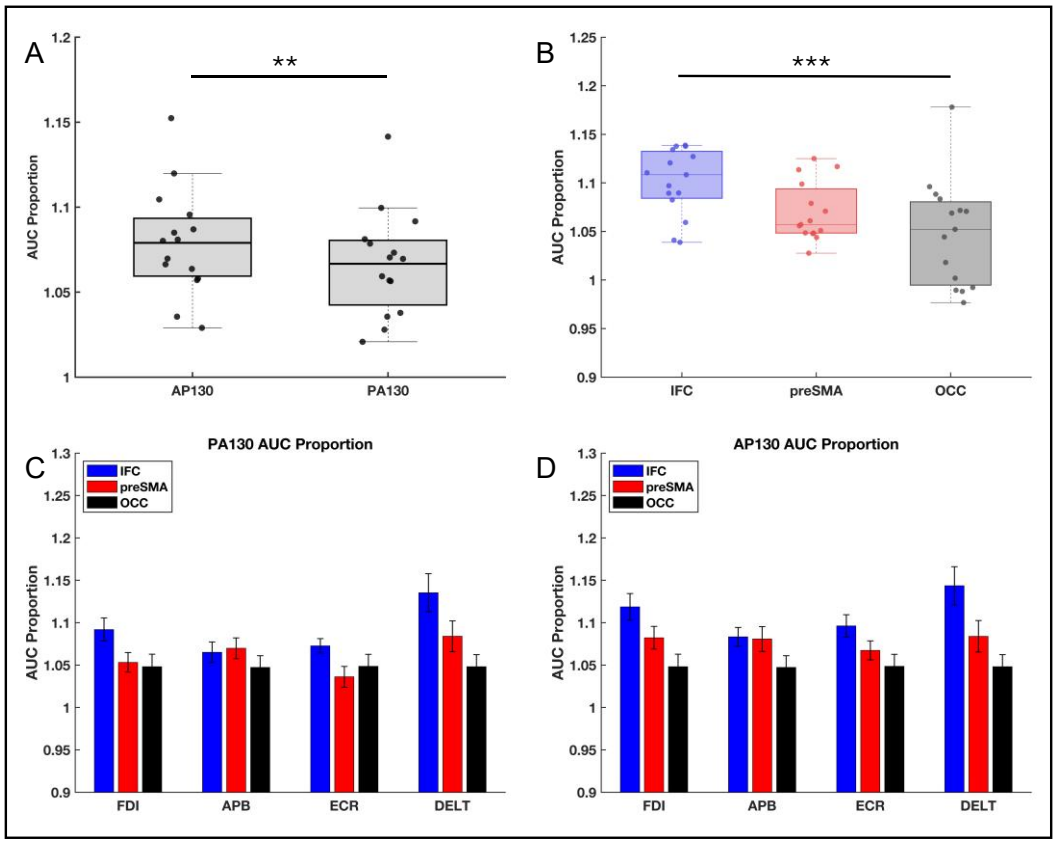

Figure 3.5. Proportion of area under curve (AUC) post- vs. pre- stimulation calculated at the trial level (n = 15). **A)** Boxplot displaying AUC difference between AP and PA coil orientation at 130% RMT collapsed across ROI and muscles. **B)** Boxplot showing the AUC difference between ROI collapsed across muscles. **C)** PA130 AUC proportion for each ROI and muscle. **D)** AP130 AUC proportion for each ROI and muscle. ** indicates $p < .01$, *** indicates $p < .001$.

Participant mean comparisons at 130% RMT

Mean timeseries were calculated at the participant level separately for each condition and the group-level mean peak-to-peak and AUC were calculated before submitting to statistical tests. For peak-to-peak amplitudes measured on raw signal, there was a significant main effect of ROI, [$F(1.428, 19.986) = 5.17$, $p < .05$, $\eta^2_p = .270$] and muscles [$F(2.452, 34.321) = 5.26$, $p < .01$, $\eta^2_p = .273$]. There was no significant difference between coil orientations [$F(1, 14) = 0.74$, $p = .40$, $\eta^2_p = .050$]. Post hoc *t* tests for ROI revealed rIFC exhibited significantly greater peak-to-peak amplitudes than preSMA ($t = 3.0$, $d = 0.54$, $p < .05$), but not greater than OCC ($t = 2.5$, $d =$

0.44, $p = .06$), and preSMA was not significantly different than OCC ($t = -0.6$, $d = -0.10$, $p = 1.00$).

AUC measures at the subject level performed on raw, rectified data also revealed significant main effects of ROI [$F(1.876, 26.176) = 7.57$, $p < .01$, $\eta^2_p = .351$], and muscle [$F(1.771, 24.800) = 11.39$, $p < .001$, $\eta^2_p = .449$], but no differences in coil orientation [$F(1, 14) = 11.39$, $p = .26$, $\eta^2_p = .092$]. Post hoc t tests for ROI showed rIFC had significantly greater AUC than preSMA ($t = 3.3$, $d = .48$, $p < .01$) and OCC ($t = 3.4$, $d = .49$, $p < .01$).

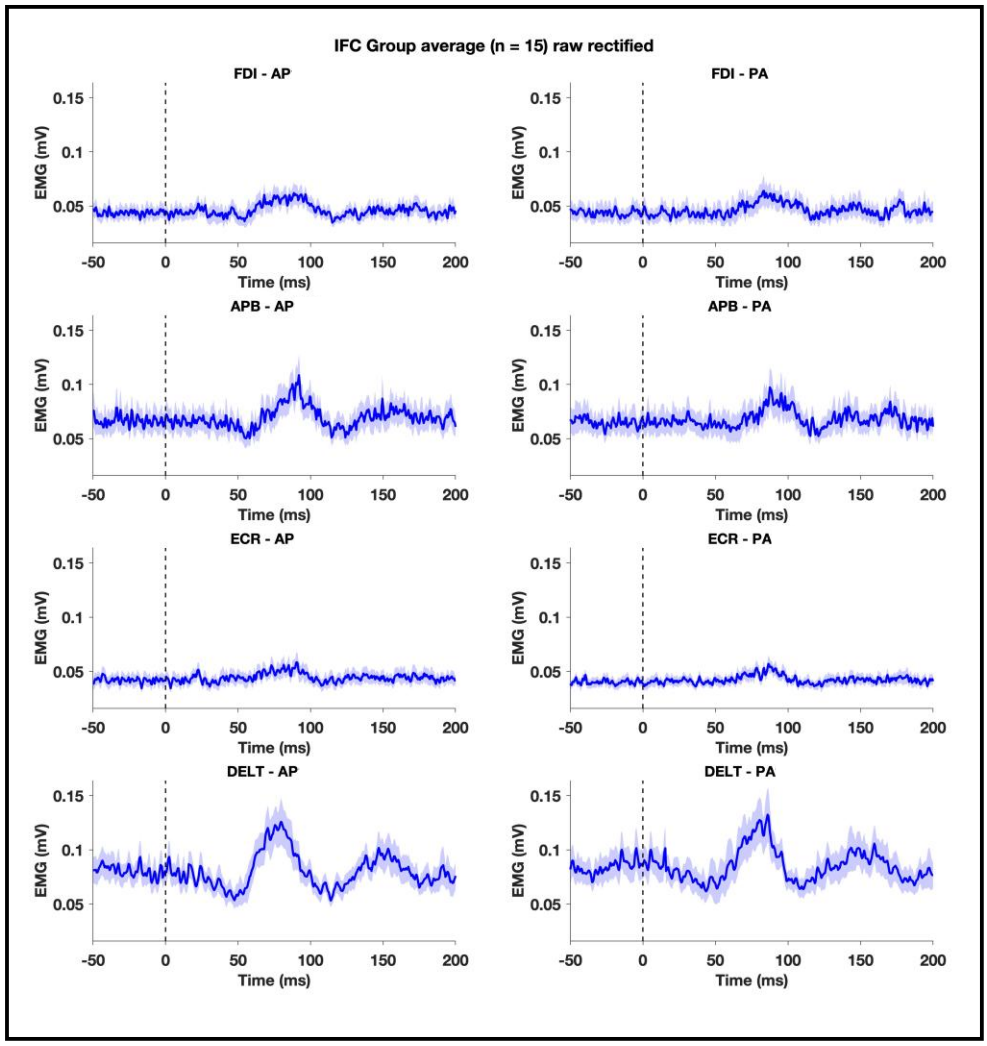

Figure 3.6. Raw rectified EMG signal time locked to TMS pulse for each muscle and coil orientation (n = 15) at 130% RMT from stimulation over the right inferior frontal cortex (rIFC). AP = anterior-to-posterior; PA = posterior-to-anterior.

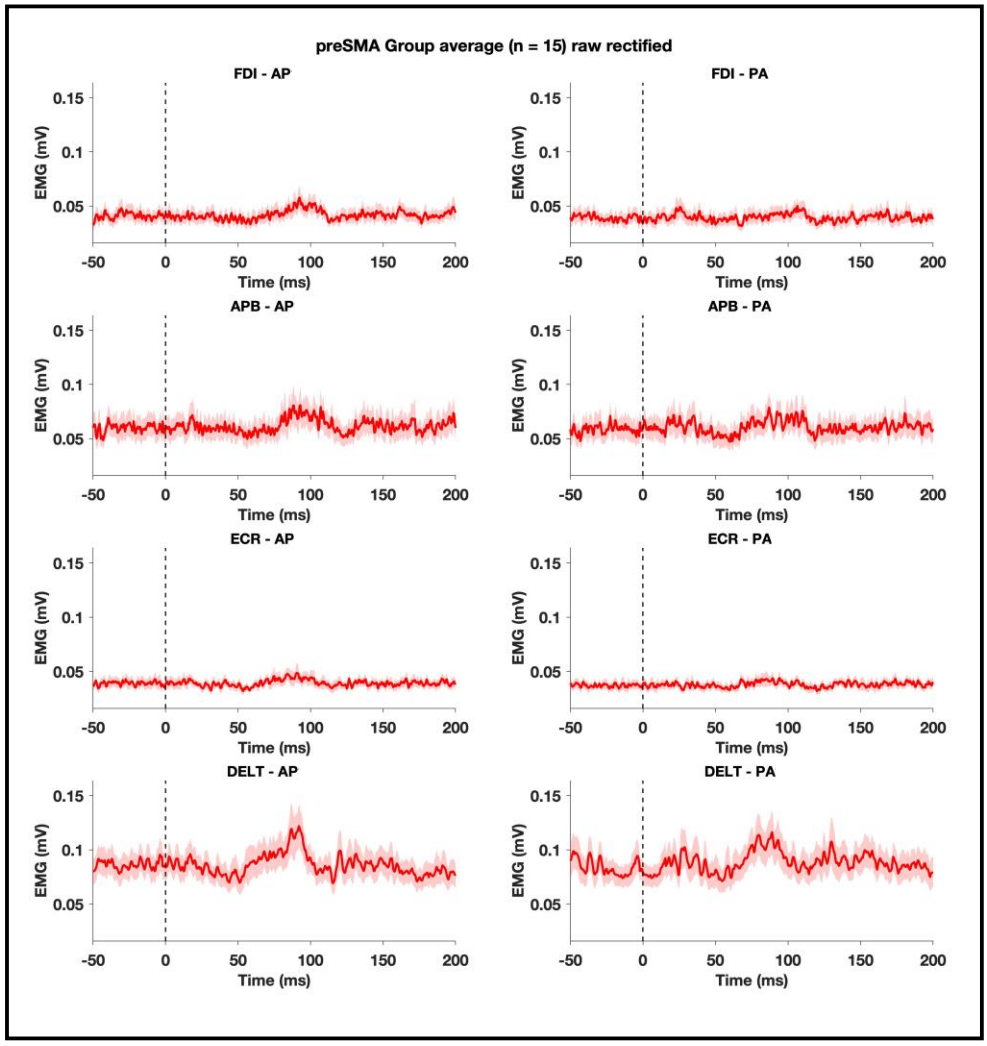

Figure 3.7. Raw rectified EMG signal time locked to TMS pulse for each muscle and coil orientation (n = 15) at 130% RMT from stimulation over the pre-supplementary motor area (preSMA).

Discussion

In the present study, we hypothesized stimulation of candidate NMAs would disrupt ongoing muscular contractions. This hypothesis was motivated by findings from DES to NMAs in the frontal cortex in clinical populations (Luders, 1987; Rech et al., 2014; Viganò et al., 2021). These studies elicited NMRs which are characterized by complete inhibition of movement without loss of muscle tone or consciousness. We tested and evaluated a novel method of frontal cortex stimulation with the aim of eliciting NMRs utilizing single-pulse TMS. We used MNI

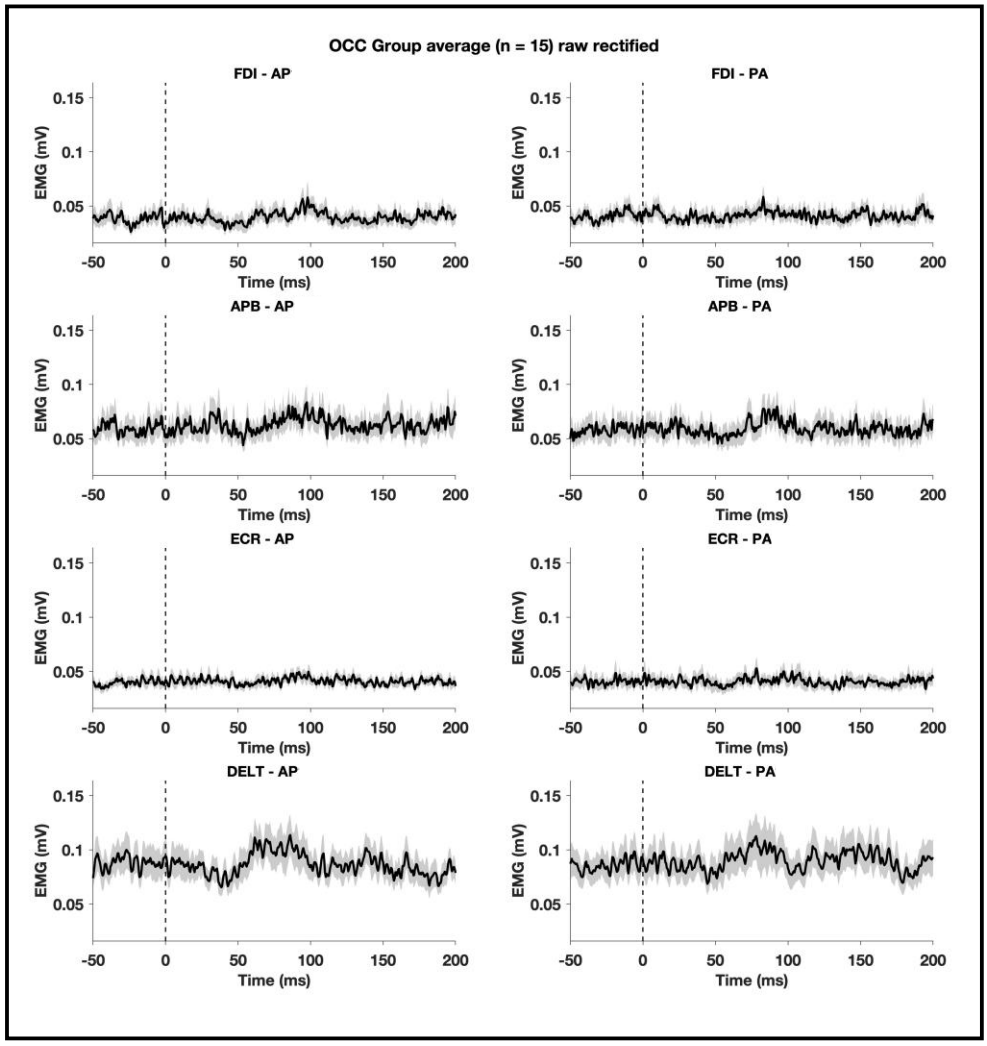

Figure 3.8. Raw rectified EMG signal time locked to TMS pulse for each muscle and coil orientation (n = 15) at 130% RMT from stimulation over the occipital cortex (OCC).

coordinates to target two non-motor ROIs (rIFC and preSMA) and used the occipital cortex (OCC) as our control. We also stimulated M1 over the FDI hotspot to serve as a reference for PMR characteristics and to set thresholds for our non-M1 targets. Since this was a novel approach, we used a variety of stimulation intensities, coil orientations, and four muscles on the contralateral upper limb. To detect NMRs, we trained participants to maintain a tonic contraction in these four muscles simultaneously. We initially hypothesized stimulation of candidate NMAs would result in a brief reduction of EMG activity following stimulation. We expected any evoked responses to exhibit qualities and latencies similar to CSPs.

However, instead of a reduction in the tonic EMG, we observed an increase in the EMG signal for both NMA targets beginning approximately 50 ms post-stimulation and ending approximately 75 ms later. This modulation was strongest for rIFC stimulation, especially in the FDI and DELT muscles, and was present in most conditions regardless of coil orientation or stimulation intensity. This finding suggests an important link between the rIFC and upper limb muscles that is not present with the more posterior and superior preSMA target. These evoked responses occurred after the typical period for MEPs (15-35ms) and do not have characteristic MEP shapes. MEPs measured and collected within this task protocol resolved within 40 ms of the stimulation. Although, the evoked responses had significant overlap with CSP epochs which began on average 48 ms post-stimulation and persisted for ~ 72 ms, which covered nearly the entire period of this positive motor response. It is not clear whether this is a coincidental overlap or if the networks involved in producing these PMRs are shared with those for CSPs.

Though we did not find evidence to support our hypothesis of a reduction in EMG activity following single-pulse TMS, we did find evidence of motor responses that we believe are related to the frontal cortex stimulation of rIFC and preSMA. It is unlikely these PMRs are a result of transcortical simulation effects due to the distance between M1 and rIFC or preSMA (Numssen et al., 2023). Additionally, the PMRs do not exhibit classic MEP timing or shape (Spampinato et al., 2023). Due to the response timing, it also seems unlikely to attribute these responses to long-latency reflexes (LLR) because of muscle perturbations. Upper extremity LLRs are rapid feedback, spinal-mediated responses resulting from unexpected perturbations and aid in motor control. LLRs are elicited peripherally and upper extremity reflexes typically occur within 50-150 ms from perturbation (Dubey et al., 2025). The frontal cortex stimulation in the present study was applied centrally, and would need to travel to the upper extremity, elicit the

muscular perturbation and begin the transcortical reflex which would delay this reflex outside the time window of interest.

A more likely mechanism for the PMRs exhibited by rIFC and preSMA stimulation would be subcortical activation of the basal ganglia via frontostriatal connections or the hyperdirect pathway (Bingham et al., 2023; Gillies & Willshaw, 1998; Nambu et al., 2002). These regions and circuits have been identified and implicated frequently within the response inhibition and negative motor network literature. Indeed, single-pulse TMS of rIFC could activate the STN through the hyperdirect pathway, thus producing broad inhibition of the motor system. DES delivered to NMAs generally results in arrest of movement while current is being applied (Borggraefe et al., 2016; Breshears et al., 2019; Viganò et al., 2021). Given that we only applied single-pulse stimulation, it is possible we only caused a brief interruption of motor output and lacked sensitivity to identify this temporary inhibition. Assuming this is the case, the PMR we have outlined above may be a resumption of motor activity as participants continued their contraction. Alternatively, this PMR could be a product of rebound excitation from downstream effects of the hyperdirect pathway on thalamocortical circuits (Kim et al., 2017). To expand on this, optogenetic stimulation of inhibitory basal ganglia circuits in a rodent model caused excitatory output from thalamus resulting in muscle contractions in the post-inhibitory period. However, we did not include stimulation of rIFC or preSMA at rest, which means there is a possibility that muscular contractions may have been evoked through rebound excitation. Further, the PMRs elicited do not appear to be effector-specific which supports a brief, broad inhibitory effect on motor output via single-pulse TMS (Badry et al., 2009; Cai, Oldenkamp, et al., 2012; Wessel et al., 2013). Unfortunately, the latency in which NMRs present at the muscle following DES is not well described since few studies employ EMG, and none specifically

present this information. Despite this, the timeframe for an inhibitory signal to reach the muscle and for re-initiation of excitatory drive should fall within this 50-150 ms window. The presumed mechanism to support this rationale requires approximately three synapses. Assuming activation of the hyperdirect pathway via cortico-STN-globus pallidus (internal segment)-thalamo-M1 circuit, we estimate approximately twice the latency of an MEP.

There is a potential for clinical application of these methods, however this would hinge on whether this stimulation protocol is sensitive to individual responses to frontal TMS. There are considerable advantages to this approach for mapping frontal cortex considering it is non-invasive, inexpensive and can be performed without medical training. These methods may offer a low trial count identification of NMAs. However, a drawback is one of the primary clinical populations would be epilepsy, and TMS has a chance of inducing seizure. The next step in this process would be devising targeted stimulation based on individual anatomy and this will likely require the use of MRI for site identification.

Limitations

Although the present study explores an exciting novel method for investigating the negative motor system and non-motor TMS of the frontal cortex, there are limitations that should be addressed in future research. One limitation in this experiment was the lack of a sham condition for stimulation, instead opting to use the OCC as a control. OCC pole was chosen as a standard control since there is not expected to be motor connections or responses at the muscle and a sufficient distance from M1, rIFC and preSMA to avoid cortico-cortical confounding effects. As this was an exploratory design, we chose to stimulate with the coil in two orientations to induce current in two directions to account for the varying anatomy of the cortex. Fortunately, most trials were good quality, allowing for meaningful comparisons between conditions and

ROI. A final limitation is not all conditions were matched at the same %RMT intensity. Specifically, M1 was only sampled at 80 and 110% RMT, while the ROI were sampled at 110, 120, and 130%. CSP durations scale with TMS intensity and the relative intensity of muscular contraction (Wilson et al., 1993) This means we were not able to compare CSP durations and latencies from a matched intensity for the higher stimulation intensities. Although this may not change our interpretation, it was an oversight that can be addressed in future studies. Finally, individual differences is a key point which will need to be addressed in future research. Our study involved generic MNI targets for approximate locations which will not be as precise between individuals as future studies that use individualized anatomy to guide stimulation.

Conclusions

Here, we aimed to explore the result of single-pulse TMS delivered to candidate NMAs in the frontal cortex while participants sustained steady contraction of four contralateral upper-limb muscles. We predicted a brief arrest of motor activity in the recorded muscles. Contrary to our prediction, we identified PMRs that occurred during the approximate time window of CSPs. rIFC stimulation produced a greater motor response than stimulation of the preSMA or the OCC control target. The observed transient increase in motor activity may result from a brief interruption of motor activity, followed by the re-initiation of the ongoing muscle contraction, or an inhibitory-excitatory basal ganglia-mediated rebound mechanism. Given the link between rIFC, response inhibition and the hyperdirect pathway, these evoked responses may be mediated through brief activation of the fronto-subthalamic stopping network followed by voluntary contraction.

REFERENCES CITED

Alderson, R. M., Rapport, M. D., & Kofler, M. J. (2007). Attention-deficit/hyperactivity disorder and behavioral inhibition: A meta-analytic review of the stop-signal paradigm. *Journal of Abnormal Child Psychology*, *35*, 745–758.

Aron, A. R., Behrens, T. E., Smith, S., Frank, M. J., & Poldrack, R. A. (2007). Triangulating a cognitive control network using diffusion-weighted magnetic resonance imaging (MRI) and functional MRI. *Journal of Neuroscience*, *27*(14), 3743–3752.

Aron, A. R., & Poldrack, R. A. (2006). Cortical and Subcortical Contributions to Stop Signal Response Inhibition: Role of the Subthalamic Nucleus. *The Journal of Neuroscience*, *26*(9), 2424–2433. https://doi.org/10.1523/JNEUROSCI.4682-05.2006

Badry, R., Mima, T., Aso, T., Nakatsuka, M., Abe, M., Fathi, D., Foly, N., Nagiub, H., Nagamine, T., & Fukuyama, H. (2009). Suppression of human cortico-motoneuronal excitability during the Stop-signal task. *Clinical Neurophysiology*, *120*(9), 1717–1723.

Bingham, C. S., Petersen, M. V., Parent, M., & McIntyre, C. C. (2023). Evolving Characterization of the Human Hyperdirect Pathway. *Brain Structure & Function*, *228*(2), 353–365. https://doi.org/10.1007/s00429-023-02610-5

Bissett, P. G., Logan, G. D., van Wouwe, N. C., Tolleson, C. M., Phibbs, F. T., Claassen, D. O., & Wylie, S. A. (2015). Generalized Motor Inhibitory Deficit in Parkinson's Disease Patients who Freeze. *Journal of Neural Transmission (Vienna, Austria : 1996)*, *122*(12), 1693–1701. https://doi.org/10.1007/s00702-015-1454-9

Borchers, S., Himmelbach, M., Logothetis, N., & Karnath, H.-O. (2012). Direct electrical stimulation of human cortex—The gold standard for mapping brain functions? *Nature Reviews Neuroscience*, *13*(1), Article 1. https://doi.org/10.1038/nrn3140

Borggraefe, I., Catarino, C. B., Rémi, J., Vollmar, C., Peraud, A., Winkler, P. A., & Noachtar, S. (2016). Lateralization of cortical negative motor areas. *Clinical Neurophysiology*, *127*(10), 3314–3321.

Breshears, J. D., Molinaro, A. M., & Chang, E. F. (2015). A probabilistic map of the human ventral sensorimotor cortex using electrical stimulation. *Journal of Neurosurgery*, *123*(2), 340–349. https://doi.org/10.3171/2014.11.JNS14889

Breshears, J. D., Southwell, D. G., & Chang, E. F. (2019). Inhibition of Manual Movements at Speech Arrest Sites in the Posterior Inferior Frontal Lobe. *Neurosurgery*, *85*(3), E496–E501. https://doi.org/10.1093/neuros/nyy592

Cai, W., George, J. S., Verbruggen, F., Chambers, C. D., & Aron, A. R. (2012). The role of the right presupplementary motor area in stopping action: Two studies with event-related

transcranial magnetic stimulation. *Journal of Neurophysiology*, *108*(2), 380–389. https://doi.org/10.1152/jn.00132.2012

Chen, W., Hemptinne, C. de, Miller, A. M., Leibbrand, M., Little, S. J., Lim, D. A., Larson, P. S., & Starr, P. A. (2020). Prefrontal-Subthalamic Hyperdirect Pathway Modulates Movement Inhibition in Humans. *Neuron*, *106*(4), 579-588.e3. https://doi.org/10.1016/j.neuron.2020.02.012

Coxon, J. P., Impe, A. V., Wenderoth, N., & Swinnen, S. P. (2012). Aging and Inhibitory Control of Action: Cortico-Subthalamic Connection Strength Predicts Stopping Performance. *Journal of Neuroscience*, *32*(24), 8401–8412. https://doi.org/10.1523/JNEUROSCI.6360-11.2012

Cushing, H. (1909). A Note Upon the Faradic Stimulation of the Postcentral Gyrus in Conscious Patients.1. *Brain*, *32*(1), 44–53. https://doi.org/10.1093/brain/32.1.44

Dubey, O., Petrie, M. A., & Shields, R. K. (2025). Adaptation of Transcortical Responses in Upper Extremity Movements During an Elbow Visuomotor Tracking Task in Humans. *Journal of Functional Morphology and Kinesiology*, *10*(4), 368. https://doi.org/10.3390/jfmk10040368

Di Lazzaro, V., Profice, P., Ranieri, F., Capone, F., Dileone, M., Oliviero, A., & Pilato, F. (2012). I-wave origin and modulation. *Brain Stimulation*, *5*(4), 512–525. https://doi.org/10.1016/j.brs.2011.07.008

Evans, A. C., Kamber, M., Collins, D. L., & MacDonald, D. (1994). An MRI-based probabilistic atlas of neuroanatomy. *Magnetic Resonance Scanning and Epilepsy*, 263–274.

Filevich, E., Kühn, S., & Haggard, P. (2012). Negative motor phenomena in cortical stimulation: Implications for inhibitory control of human action. *Cortex*, *48*(10), 1251–1261. https://doi.org/10.1016/j.cortex.2012.04.014

Foerster, O. (1931). The cerebral cortex in man. *Lancet*, *2*, 309–312.

Foerster, O. (1936). The motor cortex in man in the light of Hughlings Jackson's doctrines. *Brain*, *59*(2), 135–159.

Fornia, L., Puglisi, G., Leonetti, A., Bello, L., Berti, A., Cerri, G., & Garbarini, F. (2020). Direct electrical stimulation of the premotor cortex shuts down awareness of voluntary actions. *Nature Communications*, *11*(1), 705.

Fornia, L., Rossi, M., Rabuffetti, M., Leonetti, A., Puglisi, G., Viganò, L., Simone, L., Howells, H., Bellacicca, A., Bello, L., & Cerri, G. (2020). Direct Electrical Stimulation of Premotor Areas: Different Effects on Hand Muscle Activity during Object Manipulation. *Cerebral Cortex*, *30*(1), 391–405. https://doi.org/10.1093/cercor/bhz139

Fried, I., Katz, A., McCarthy, G., Sass, K. J., Williamson, P., Spencer, S. S., & Spencer, D. D. (1991). Functional organization of human supplementary motor cortex studied by electrical stimulation. *Journal of Neuroscience*, *11*(11), 3656–3666.

Gillies, A. J., & Willshaw, D. J. (1998). A massively connected subthalamic nucleus leads to the generation of widespread pulses. *Proceedings. Biological Sciences*, *265*(1410), 2101–2109. https://doi.org/10.1098/rspb.1998.0546

Groppa, S., Oliviero, A., Eisen, A., Quartarone, A., Cohen, L. G., Mall, V., Kaelin-Lang, A., Mima, T., Rossi, S., Thickbroom, G. W., Rossini, P. M., Ziemann, U., Valls-Solé, J., & Siebner, H. R. (2012). A practical guide to diagnostic transcranial magnetic stimulation: Report of an IFCN committee. *Clinical Neurophysiology*, *123*(5), 858–882. https://doi.org/10.1016/j.clinph.2012.01.010

Hampshire, A., Chamberlain, S. R., Monti, M. M., Duncan, J., & Owen, A. M. (2010). The role of the right inferior frontal gyrus: Inhibition and attentional control. *Neuroimage*, *50*(3–3), 1313–1319. https://doi.org/10.1016/j.neuroimage.2009.12.109

Ikeda, A., Lüders, H. O., Burgess, R. C., Sakamoto, A., Klem, G. H., Morris, H. H., & Shibasaki, H. (1995). Generator locations of movement-related potentials with tongue protrusions and vocalizations: Subdural recording in human. *Electroencephalography and Clinical Neurophysiology*, *96*(4), 310–328. https://doi.org/10.1016/0168-5597(95)00002-a

Ikeda, A., Luders, H. O., Burgess, R. C., & Shibisaki, H. (1992). Movement-related Potentials Recorded from Supplementary Motor Area and Primary Motor area: Role of Supplementary Motor area in Voluntary Movements. *Brain*, *115*(4), 1017–1043. https://doi.org/10.1093/brain/115.4.1017

Ikeda, A., Lüders, H. O., Burgess, R. C., & Shibasaki, H. (1993). Movement-related potentials associated with single and repetitive movements recorded from human supplementary motor area. *Electroencephalography and Clinical Neurophysiology*, *89*(4), 269–277. https://doi.org/10.1016/0168-5597(93)90106-y

Jackson, N., & Greenhouse, I. (2019). VETA: An Open-Source Matlab-Based Toolbox for the Collection and Analysis of Electromyography Combined With Transcranial Magnetic Stimulation. *Frontiers in Neuroscience*, *13*. https://www.frontiersin.org/articles/10.3389/fnins.2019.00975

JASP Team. (2020). *JASP* (Version 0.16.3) [Computer software]. https://jasp-stats.org

Krause, F. (1912). *Surgery of the brain and spinal cord: Based on personal experiences* (Vol. 2). Rebman.

Lim, S. H., Dinner, D. S., Pillay, P. K., Lüders, H., Morris, H. H., Klem, G., Wyllie, E., & Awad, I. A. (1994). Functional anatomy of the human supplementary sensorimotor area: Results of

extraoperative electrical stimulation. *Electroencephalography and Clinical Neurophysiology*, *91*(3), 179–193.

Luders, H. (1987). Negative motor responses elicited by stimulation of the human cortex. *Advonces in Epileptology*, *16*, 229–231.

Lüders, H. O., Dinner, D. S., Morris, H. H., Wyllie, E., & Comair, Y. G. (1995). Cortical electrical stimulation in humans. The negative motor areas. *Advances in Neurology*, *67*, 115–129.

Mahon, B. Z., Miozzo, M., & Pilcher, W. H. (2019). Direct electrical stimulation mapping of cognitive functions in the human brain. *Cognitive Neuropsychology*, *36*(3–4), 97–102. https://doi.org/10.1080/02643294.2019.1630375

Mikuni, N., Oharac, S., Ikeda, A., Hayashi, N., Nishida, N., Taki, J., Enatsu, R., Matsumoto, R., Shibasaki, H., & Hashimoto, N. (2006). Evidence for a wide distribution of negative motor areas in the perirolandic cortex. *Clinical Neurophysiology*, *117*, 33–40.

Monticelli, M., Zeppa, P., Altieri, R., Veneziani Santonio, F., Cofano, F., Melcarne, A., Junemann, C. V., Zenga, F., Sabatino, G., La Rocca, G., Della Pepa, G. M., Ducati, A., & Garbossa, D. (2020). Exploring the anatomy of negative motor areas (NMAs): Findings in awake surgery. *Journal of Clinical Neuroscience*, *73*, 219–223. https://doi.org/10.1016/j.jocn.2020.01.049

Nambu, A., Tokuno, H., & Takada, M. (2002). Functional significance of the cortico–subthalamo–pallidal 'hyperdirect'pathway. *Neuroscience Research*, *43*(2), 111–117.

Numssen, O., van der Burght, C. L., & Hartwigsen, G. (2023). Revisiting the focality of non-invasive brain stimulation – Implications for studies of human cognition. *Neuroscience and Biobehavioral Reviews*, *149*, None. https://doi.org/10.1016/j.neubiorev.2023.105154

Ojemann, G. A. (1991). Cortical organization of language. *Journal of Neuroscience*, *11*(8), 2281–2287.

Ojemann, G., Ojemann, J., Lettich, E., & Berger, M. (1989). Cortical language localization in left, dominant hemisphere. An electrical stimulation mapping investigation in 117 patients. *Journal of Neurosurgery*, *71*(3), 316–326. https://doi.org/10.3171/jns.1989.71.3.0316

Parmigiani, S., & Cattaneo, L. (2018). Stimulation of the Dorsal Premotor Cortex, But Not of the Supplementary Motor Area Proper, Impairs the Stop Function in a STOP Signal Task. *Neuroscience*, *394*, 14–22. https://doi.org/10.1016/j.neuroscience.2018.10.005

Penfield, W. (1938). The cerebral cortex in man: I. The cerebral cortex and consciousness. *Archives of Neurology & Psychiatry*, *40*(3), 417–442.

Penfield, W. (1949). VOCALIZATION AND ARREST OF SPEECH. *Archives of Neurology And Psychiatry*, *61*(1), 21. https://doi.org/10.1001/archneurpsyc.1949.02310070027002

Penfield, W., & Boldrey, E. (1937). Somatic Motor and Sensory Representation in the Cerebral Cortex of Man as Studied by Electrical Stimulation1. *Brain*, *60*(4), 389–443. https://doi.org/10.1093/brain/60.4.389

Penfield, W., & Jasper, H. (1954). *Epilepsy and the functional anatomy of the human brain.*

Penfield, W., & Welch, K. (1951). The supplementary motor area of the cerebral cortex: A clinical and experimental study. *AMA Archives of Neurology & Psychiatry*, *66*(3), 289–317.

Pinson, H., Van Lerbeirghe, J., Vanhauwaert, D., Van Damme, O., Hallaert, G., & Kalala, J.-P. (2022). The supplementary motor area syndrome: A neurosurgical review. *Neurosurgical Review*, *45*(1), 81–90. https://doi.org/10.1007/s10143-021-01566-6

Rech, F., Duffau, H., Pinelli, C., Masson, A., Roublot, P., Billy-Jacques, A., Brissart, H., & Civit, T. (2017). Intraoperative identification of the negative motor network during awake surgery to prevent deficit following brain resection in premotor regions. *Neurochirurgie*, *63*(3), 235–242. https://doi.org/10.1016/j.neuchi.2016.08.006

Rech, F., Herbet, G., Moritz-Gasser, S., & Duffau, H. (2014). Disruption of bimanual movement by unilateral subcortical electrostimulation. *Human Brain Mapping*, *35*(7), 3439–3445.

Schaum, M., Pinzuti, E., Sebastian, A., Lieb, K., Fries, P., Mobascher, A., Jung, P., Wibral, M., & Tüscher, O. (2021). Right inferior frontal gyrus implements motor inhibitory control via beta-band oscillations in humans. *eLife*, *10*, e61679. https://doi.org/10.7554/eLife.61679

Schluter, N. D., Rushworth, M. F., Passingham, R. E., & Mills, K. R. (1998). Temporary interference in human lateral premotor cortex suggests dominance for the selection of movements. A study using transcranial magnetic stimulation. *Brain: A Journal of Neurology*, *121*(5), 785–799.

Schucht, P., Moritz-Gasser, S., Herbet, G., Raabe, A., & Duffau, H. (2013). Subcortical electrostimulation to identify network subserving motor control. *Human Brain Mapping*, *34*(11), 3023–3030. https://doi.org/10.1002/hbm.22122

Siebner, H. R., Funke, K., Aberra, A. S., Antal, A., Bestmann, S., Chen, R., Classen, J., Davare, M., Di Lazzaro, V., Fox, P. T., Hallett, M., Karabanov, A. N., Kesselheim, J., Beck, M. M., Koch, G., Liebetanz, D., Meunier, S., Miniussi, C., Paulus, W., … Ugawa, Y. (2022). Transcranial magnetic stimulation of the brain: What is stimulated? – A consensus and critical position paper. *Clinical Neurophysiology*, *140*, 59–97. https://doi.org/10.1016/j.clinph.2022.04.022

Simone, L., Fornia, L., Viganò, L., Sambataro, F., Rossi, M., Leonetti, A., Puglisi, G., Howells, H., Bellacicca, A., Bello, L., & Cerri, G. (2020). Large scale networks for human hand-

object interaction: Functionally distinct roles for two premotor regions identified intraoperatively. *NeuroImage*, *204*, 116215. https://doi.org/10.1016/j.neuroimage.2019.116215

Spampinato, D. A., Ibanez, J., Rocchi, L., & Rothwell, J. (2023). Motor potentials evoked by transcranial magnetic stimulation: Interpreting a simple measure of a complex system. *The Journal of Physiology*, *601*(14), 2827–2851. https://doi.org/10.1113/JP281885

Swann, N. C., Cai, W., Conner, C. R., Pieters, T. A., Claffey, M. P., George, J. S., Aron, A. R., & Tandon, N. (2012). Roles for the pre-supplementary motor area and the right inferior frontal gyrus in stopping action: Electrophysiological responses and functional and structural connectivity. *Neuroimage*, *59*(3), 2860–2870.

Swann, N., Tandon, N., Canolty, R., Ellmore, T. M., McEvoy, L. K., Dreyer, S., DiSano, M., & Aron, A. R. (2009). Intracranial EEG reveals a time-and frequency-specific role for the right inferior frontal gyrus and primary motor cortex in stopping initiated responses. *Journal of Neuroscience*, *29*(40), 12675–12685.

Viganò, L., Fornia, L., Rossi, M., Howells, H., Leonetti, A., Puglisi, G., Conti Nibali, M., Bellacicca, A., Grimaldi, M., Bello, L., & Cerri, G. (2019). Anatomo-functional characterisation of the human "hand-knob": A direct electrophysiological study. *Cortex*, *113*, 239–254. https://doi.org/10.1016/j.cortex.2018.12.011

Viganò, L., Howells, H., Fornia, L., Rossi, M., Conti Nibali, M., Puglisi, G., Leonetti, A., Simone, L., Bello, L., & Cerri, G. (2021). Negative motor responses to direct electrical stimulation: Behavioral assessment hides different effects on muscles. *Cortex; a Journal Devoted to the Study of the Nervous System and Behavior*, *137*, 194–204. https://doi.org/10.1016/j.cortex.2021.01.005

Wessel, J. R., & Aron, A. R. (2013). Unexpected Events Induce Motor Slowing via a Brain Mechanism for Action-Stopping with Global Suppressive Effects. *Journal of Neuroscience*, *33*(47), 18481–18491. https://doi.org/10.1523/JNEUROSCI.3456-13.2013

Wilson, S. A., Lockwood, R. J., Thickbroom, G. W., & Mastaglia, F. L. (1993). The muscle silent period following transcranial magnetic cortical stimulation. *Journal of the Neurological Sciences*, *114*(2), 216–222. https://doi.org/10.1016/0022-510X(93)90301-E

Yazawa, S., Ikeda, A., Kunieda, T., Ohara, S., Mima, T., Nagamine, T., Taki, W., Kimura, J., Hori, T., & Shibasaki, H. (2000). Human presupplementary motor area is active before voluntary movement: Subdural recording of Bereitschaftspotential from medial frontal cortex. *Experimental Brain Research*, *131*(2), 165–177. https://doi.org/10.1007/s002219900311

Yokoyama, R., Enatsu, R., Kanno, A., Suzuki, H., Suzuki, Y., Sasagawa, A., Hirano, T., Arihara, M., Kuribara, T., Ochi, S., & Mikuni, N. (2020). Negative motor networks: Electric cortical

stimulation and diffusion tensor imaging. *Revue Neurologique*, *176*(7–8), 592–600. https://doi.org/10.1016/j.neurol.2019.12.005

Zhou, Y., Zhao, Z., Zhang, J., Hameed, N. U. F., Zhu, F., Feng, R., Zhang, X., Lu, J., & Wu, J. (2021). Electrical stimulation–induced speech-related negative motor responses in the lateral frontal cortex. *Journal of Neurosurgery*, *137*(2), 496–504. https://doi.org/10.3171/2021.9.JNS211069

CHAPTER IV

NEURO-NAVIGATED TRANSCRANIAL MAGNETIC STIMULATION TO RIGHT INFERIOR FRONTAL CORTEX AND DORSOLATERAL PREFRONTAL CORTEX ELICITS AN ELECTROMYOGRAPHIC RESPONSE IN CONTRALATERALLY CONTRACTED MUSCLES

Introduction

Negative motor areas (NMAs) are regions of the cortex that cause interruptions or arrest of motor processes when stimulated (Lüders, 1987; Lüders et al., 1995). NMAs and results of their stimulation has almost exclusively been studied in the context of intraoperative surgery. In this context, the primary focus is mapping the cortex for functional regions to avoid during resective procedures. Study of NMAs is a secondary or tertiary priority in surgical mapping with direct electrical stimulation (DES), therefore the mechanisms and pathways in which the negative motor system functions are not well understood. Currently, there are no published studies investigating NMAs with non-invasive methods of stimulation

There is evidence resection of NMAs can result in bimanual motor control deficits (Rech et al., 2014), or development of other neurological conditions which may impact speech, muscle weakness and other motor functions (Pinson et al., 2022). Given the relation of NMAs to motor control, it is intriguing that several identified NMAs are shared with the response inhibition network, particularly the right inferior frontal cortex (rIFC). The rIFC has frequently been identified as a region that elicits negative motor responses (NMRs) during surgical mapping (Borggraefe et al., 2016; Breshears et al., 2015; Ikeda et al., 1995; Monticelli et al., 2020; Penfield, 1949), along with other frontal regions, primarily the pre-supplementary motor area (Fried et al., 1991; Monticelli et al., 2020a; Rech et al., 2019; Zhou et al., 2021). The rIFC is also

established as a critical region in the response inhibition network, along with the preSMA and the primary motor cortex (M1) (Aron, 2007; Aron & Poldrack, 2006; Swann et al., 2009; Swann et al., 2012).

A prominent model of the inhibitory control system involves a cortico-basal ganglia thalamacortical circuit. It is likely that an integral part of this network is a monosynaptic white matter fiber tract connecting the rIFC with regions of the basal ganglia, specifically the subthalamic nucleus (STN) (Aron, et al., 2007; Chen et al., 2020; Nambu et al., 2002). Upon excitation, it is thought the STN functions by broadly exciting inhibitory output nuclei of the basal ganglia projecting to motor nuclei of the thalamus to suppress planned movements or cancel ongoing actions. One of the methods for studying this global suppression is using transcranial magnetic stimulation (TMS) in the context of response inhibition paradigms such as the stop signal task (SST). It has been found successful cancellation of movements (Badry et al., 2009), eye saccades (Wessel et al., 2013), and vocalizations (Cai et al., 2012) reduces the excitability of the corticospinal tract, as evidenced by reduced amplitude of motor-evoked potentials (MEPs) via TMS of M1.

A valuable behavioral metric from response inhibition investigations is the stop signal reaction time (SSRT), which is an estimate of the speed of stopping. Successful stopping at the behavioral level ultimately is the absence of a response (e.g. no button pressed on a successful movement cancellation), which makes it difficult to determine the timing of inhibitory influence on the motor system. SSRT allows for estimating the approximate time an individual takes to inhibit a response based on a distribution of their go reaction times (RTs), the stop signal delay (SSD), a variable time between the go cue and stop signal and the probability of responding on stop trials.

There is considerable evidence regarding the stopping network and given the overlap of cortical regions shared between response inhibition and identified NMAs, it is likely they share inhibitory effects on the motor system. Based on the intersection of these research trajectories, there is motivation to identify whether relationships exist between stimulation of NMAs and behavioral measures of response inhibition. Currently, there are no intraoperative studies comparing NMRs with response inhibition, which also reinforces the need to identify non-invasive methods for studying the negative motor system.

Here, we refined our methods from Chapter III to continue investigating electromyographic (EMG) responses to single-pulse TMS of rIFC with contralaterally contracted muscles. We included the occipital pole (OCC), and dorsolateral prefrontal cortex (DLPFC) as control targets. OCC was selected because it is not expected to have motor functions. DLPFC was selected as a separate frontal cortex target because it is approximately equi-distant from M1 as rIFC is to M1 to control for possible TMS spread to M1 and confounding our data. We used a neuro-navigated approach for more precise stimulation of individual anatomy. Navigated TMS (nTMS) is used to improve accuracy and precision of TMS positioning by co-registering a participant's structural magnetic resonance imaging (MRI) scan, and providing real-time feedback of TMS coil position relative to anatomical targets (Caulfield et al., 2022). We hypothesized nTMS of rIFC would increase the likelihood of eliciting electromyographic events. Additionally, we hypothesized individual differences in rIFC TMS-derived EMG markers would relate to behavioral performance (SSRT) on a SST. This hypothesis was motivated by NMA and response inhibition studies identifying rIFC as an important node in each network.

Methods

Participants

Twenty-sex healthy right-handed (self-reported) adults were recruited for this experiment (13 male, 13 female; mean age 25.7 ± 5.1 years). All participants were screened for contraindications to TMS and MRI before data collection. After screening, participants provided written informed consent according to the institutional review board at the University of Oregon.

Magnetic Resonance Imaging

Anatomical MRI was acquired for each participant at the Lewis Center for Neuroimaging on The University of Oregon's campus with a 3T Siemens Prisma scanner utilizing a 32-channel head coil. A 3-dimensional structural scanning protocol used high-resolution T1-weighted magnetization prepared rapid gradient echo (MPRAGE) imaging (1.0 x 1.0 x 1.0 mm^3, total acquisition time (TA) = 5:59 min:sec; TR = 2500 ms, TE = 3.43 ms, TI = 1100 ms, flip angle = 7°; 176 slices acquired; imaged volume = 256 x 256 x 176 mm^3; GRAPPA parallel imaging with a phase encoded acceleration factor of 2).

Electromyography & Task

Electromyography was recorded during TMS and behavioral task visits. Surface EMG was recorded with bipolar Ag-AgCL surface electrodes (Delsys Incorporated, Natick, MA, USA). TMS and behavioral testing occurred within a copper Faraday cage to reduce electrical noise in EMG recordings. During the TMS visit, electrodes were place on the left first dorsal interosseous (FDI), abductor pollicis brevis (APB), extensor carpi radialis (ECR) and anterior deltoid (DELT). An additional electrode was placed on the C7 vertebra of the neck for recording TMS artefacts, and a shared ground electrode was set on the distal (acromial) end of the clavicle. During the behavioral task, EMG was collected from the left and right FDI and grounded on the

dorsal aspect of the left hand. EMG activity was amplified (1000x), bandpass filtered (20-450 Hz), baseline-corrected to 0 mV and sampled at 5000 Hz with a Bagnoli-8 amplifier (Delsys Incorporated) connected to a BNC-2090A terminal block (National Instruments). EMG data were recorded and monitored on each trial using the MATLAB-based VETA toolbox (Jackson & Greenhouse, 2019) and stored for offline analyses.

Participants were then trained to simultaneously contract each of the four muscles with EMG electrodes by assuming the posture in **fig 3.1B**. The participants were asked to activate their FDI by laterally pressing their finger into their thumb and to activate their APB by pressing their thumb medially in a modified pinch grip. Activating these two muscles in this pinch grip is like rotating a radio dial to the left. At the same time, participants would extend their wrist for activation of the ECR and lift their arm in the sagittal plane by flexing their anterior deltoid. Live EMG was displayed on a screen in front of the participants to give them feedback on how to best contract each of the muscles in a consistent manner. We included a condition in which we stimulated rIFC without activation of DELT muscle (FDI, APB, ECR were contracted as described above). This was to address two considerations: whether the posture of lifting the arm for DELT contraction elicited a hysteresis-like rebound through the distal muscles, and to address whether the TMS pulse was causing a startle effect. This condition allowed us to compare FDI, APB and ECR muscles without potential DELT influence.

Once the participants were practiced at resuming this posture from rest, we assessed their maximum voluntary contractions (MVC). This was done by asking the participant to maximally contract their muscles four times with EMG collected using a custom MATLAB script. The difference of the maximum and minimum values was calculated, and 10% of this value was stored for each muscle. This MVC value was used during the TMS visit in this study. A figure

was shown to participants after each trial that overlaid the 10% MVC value on each EMG channel to provide feedback and guide the participant to maintain a steady contraction. The experimenter would monitor the EMG activity and inform the participant to increase or decrease the contraction of any muscle based on visual feedback of the MVC reference lines.

MRI-Guided Transcranial Magnetic Stimulation

The T1 MPRAGE files were used for targeting three regions of interest (ROI): rIFC, DLPFC, and OCC. Two independent raters identified the three targets for each participant prior to further testing. Targeting was performed on anterior commissure – posterior commissure (ACPC) aligned scans using FSL. DLPFC and OCC targets were determined using the original T1-weighted image in FSL EYES (Smith et al., 2004). All targets were selected according to individual participant anatomy. IFC targets were identified using the skull-stripped image created with the FSL BET toolbox. The DLPFC target was identified using a previously published approach (Pommier et al., 2017). In brief, the planes immediately superior and anterior to the corpus collosum were determined in the axial and coronal planes, respectively. The intersection of these planes was then projected to the cortical surface on the right hemisphere. The OCC target was determined by identifying the most posterior aspect of the occipital lobe along the AC-PC line when viewing the sagittal plane. The IFC was determined using the 3D-rendered skull-stripped brain and identifying the most prominent gyrus immediately anterior to the precentral sulcus and inferior to the inferior frontal sulcus. Disagreement between raters > 5 mm would result in the raters meeting to refine the target placement.

Prior to the TMS visit, the participant's T1 MRI was loaded into the Brainsight navigation system software (Brainsight TMS Frameless Navigation System; Rogue Research Inc., Montreal, Quebec, Canada), and the target ROIs described above were marked virtually.

These targets were used for positioning the TMS coil. During the TMS visit, participants were positioned in a chair facing a computer monitor, and in the field of view of an infrared optical tracking system. The TMS coil and the participant were tracked using reflective markers positioned on the coil and attached to a headband worn by the participant. Landmarks were used to coregister the participant to the MR image. The standard landmarks used for participants were the glabella, tip of nose, bilateral lateral canthus of the eye and the most lateral point of the tragus of each ear. TMS was delivered using a 70 mm figure-of-eight coil connected to a MagStim 200^2 stimulator (MadStim Ltd, Whitland, UK).

TMS hotspotting was performed to identify the optimal coil positioning to elicit MEPs from the left FDI. To identify the hotspot, the TMS coil was first positioned 2 cm anterior and 5 cm to the right of the vertex of the head, angled ~45° to the midline to produce a posterior-anterior current over M1. The coil was repositioned incrementally by ~1 cm until reliable MEPs were observed in the left FDI EMG recording. The position coordinates for the FDI hotspot were saved as a target in the Brainsight software throughout the experiment. Resting motor thresholds (RMTs) were determined over 16 trials utilizing an adaptive threshold-hunting maximum-likelihood parameter estimation (PEST) procedure without a priori information (Awiszus, 2003). PA RMTs were found to be 43.7 ± 7.7% of max stimulator output. All stimulation for the remainder of the TMS visit was at 130% of the RMT (56.8 ± 10.0% of max stimulator output). Participants wore earplugs for the remainder of the TMS visit due to the increased TMS intensity.

With hotspotting and thresholding complete, the DLPFC, rIFC, OCC, and M1 targets were tested in a random order. We delivered 30 – 40 single-pulse TMS to these targets in five blocks ~ 5 – 10 seconds between pulses. The trials were initiated when bother experimenter and

participant were ready (i.e. experimenter with coil in appropriate position, participant maintaining task posture. The participant could request a pause if they became fatigued with the task contraction. Typically, most stimulation blocks were completed in increments of 15-20 trials before a break. Breaks would last 3 – 5 min. Participants maintained the task posture with FDI, APB, ECR and DELT contracted at 10% MVC throughout stimulation blocks. Each participant completed a second rIFC stimulation block without a DELT contraction. The purpose of this condition was to address the possibility that effects of stimulation were due to maintaining a posture against gravity. This condition also allowed us to examine patterns of activity in the same muscle when it was contracted versus during contraction and at rest.

Stop Signal Task

During the final visit, participants completed a choice selective stop signal task (SST). Participants were seated in front of the same computer setup as during the TMS session. Visual stimuli for behavioral tasks were presented on the computer monitor using the Selective Stopping Toolbox (SeleST; Wadsley et al., 2023) run in Python. Participants were positioned so their forearms could rest comfortably on the desk, and their hands were placed palm down, approximately shoulder-width apart. Responses were made by laterally moving the index fingers towards the midline of the body to press a button on either side of a box. The buttons were interfaced with a MakeyMakey circuit board (JoyLabz LLC) to collect low-latency (1-2 ms) responses. EMG was collected via the VETA toolbox (Jackson & Greenhouse, 2019) from each FDI muscle to provide electrophysiological supplement to the behavioral task.

The SST consisted of 12 blocks of 36 trials (432 total) with a stop signal rate of 1/3. The stop trials were divided into 3 categories: stop-both (SB), stop-right (SR) and stop-left (SL). Each block was pseudorandomized to include 24 go trials and 12 stop trials (4 of each category).

Each trial of the SST was 1.25 s long, had an intertrial interval (ITI) of 0.5 s and a feedback period of 0.5 s. There were two practice blocks to familiarize the participants with the task. The first practice block was 36 go trials, and the second practice block was 36 trials with 1/3 stop signal rate (identical to blocks that would be completed for the remainder of the task).

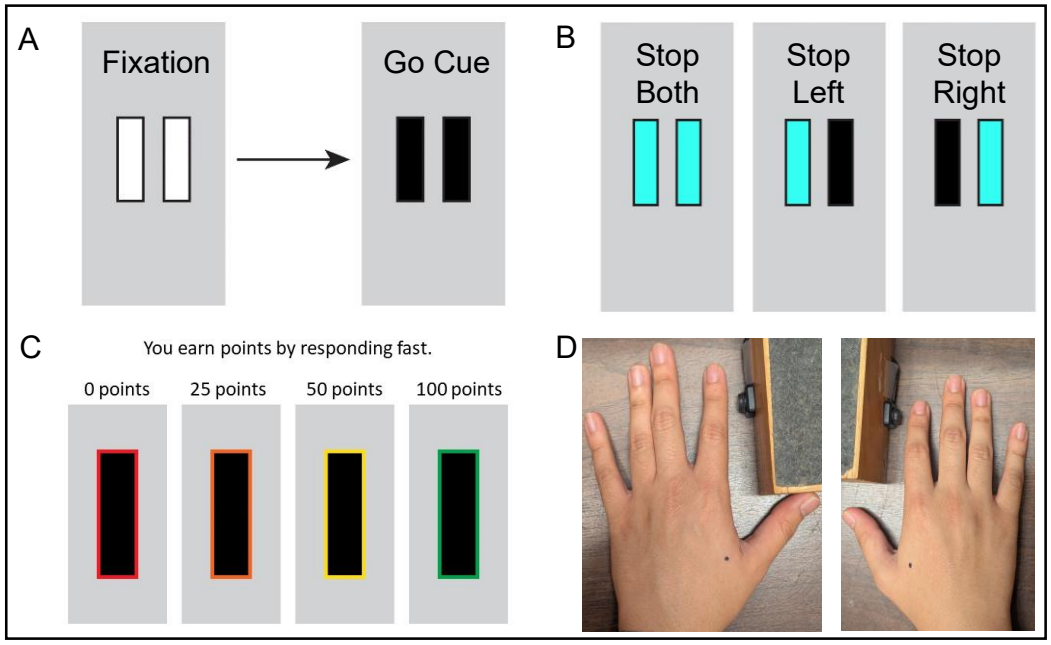

Figure 4.1. Stop signal task (SST) visuals and response input. A) Each trial began with a .5 – 1 s variable fixation cue followed by a go cue prompting participants to respond. B) Presentation of stop signals that would appear in three conditions. If both rectangles changed to cyan, participants attempted to stop both responses. If either the right or left bar turned cyan, participants attempted to stop the appropriate effector while continuing with the response with the other effector. C) Distribution of points awarded based on response speed: green = 100 points: RT < 400 ms, or a successful stop; yellow = 50 points: RT 401 – 500 ms; orange = 25 points: RT 501 – 600 ms; red = 0 points: > 600 ms or failed stop. D) Participant hand position relative to response button. Participant moved their index finger toward the midline when cued to respond with a press button.

The trial began with a 0.5 – 1 s variable fixation period **fig. 4.1a** displaying two vertical white rectangles with black borders on a grey background. Following this, the go cue was presented (two vertical black bars 1.5 cm wide and 5 cm tall) centrally on the screen. On stop trials, the go cue was replaced with a stop cue (bar color changed from black to cyan). The

initial stop signal delay (SSD) was 175 ms for each stop condition. The SSD incremented by a step size of 25 ms, increasing after successful stop trials (no button press), and decreasing after failed stop trials (button pressed). Participants were asked to respond as quickly as possible to go cues and to attempt to stop themselves from pressing the button(s) when a stop cue was presented. Participants received trial-by-trial and block-by-block feedback on their performance throughout the task. There is a tendency for participants to strategically slow their responses to improve their chances of success on stop trials (Verbruggen et al., 2013; Verbruggen & Logan, 2009). Slow responses may affect calculations of stopping speed. Assigning feedback via points is a way to gamify the task for increased engagement. Points were awarded with visual feedback on each trial based on the timing of the RT for the responses (green = 100 points: RT < 400 ms, or a successful stop; yellow = 50 points: RT 401 – 500 ms; orange = 25 points: RT 501 – 600 ms; red = 0 points: > 600 ms or failed stop). Feedback points for the block as well as the total for the task were displayed at the end of each block. During the inter-trial interval (ITI), a grey screen was presented with a jitter from 0.5 – 1 s. One participant was removed from SST behavioral analysis due to poor stopping performance (stopping success rate < 30%).

EMG Data Preprocessing & Visualization

EMG data were preprocessed and visualized using the VETA toolbox in MATLAB (Jackson & Greenhouse, 2019). Data from each trial were visualized to ensure that participants maintained sufficient levels of tonic EMG in each muscle. Whole trials or channels from a trial were removed from analysis based on visual determination of the EMG deflection outside the expected range. Trials were noted to be removed during data collection when participants failed to maintain the posture during a trial. Two total participants were removed from TMS analysis. The first was removed due to large artifact signal contaminating time epochs of interest. The

other was removed due to difficulty sustaining the task posture resulting in < 10 trials available for analysis, per condition. For the rIFC stimulation condition, participants (n = 24) contributed an average ± std of 35.5 ± 1.6 (98.5 ± 2.6 % of total) trials for analysis. For the rIFC stimulation condition without DELT activation, participants contributed an average ± std of 35.7 ± 2.0 (99.4 ± 1.4 % of total) trials for analysis. In the DLPFC condition, participants contributed an average ± std 34.8 ± 1.8 (99.8 ± 0.8 % of total) trials for analysis. Finally, for the OCC condition, participants contributed an average ± std of 31 ± 1.8 (99.2 ± 1.6% of total) trials for analysis.

Replicating work from Chapter III, we assessed the evoked responses from rIFC and DLPFC, by measuring the peak-to-peak amplitude and area under the curve (AUC) at the participant level. In essence, we averaged accepted trials from a given condition time-locked to TMS onset, for a participant. Then performed peak-to-peak and AUC measures (using trapz.m function in MATLAB). This is a similar approach to an electroencephalographic event related potential (ERP) and may be more sensitive to EMG characteristics since it is assessed at the participant level, rather than the trial level. As assessed in Chapter III, peak-to-peak amplitude was assessed on raw, baseline-corrected data (**fig 4.2A)** in a 100 ms pre-stimulation window (105 ms to 5 ms pre-stimulation), and a matched 100 ms post-stimulation window (from 25 ms to 125 ms post-stimulation). The post-stimulation to pre-stimulation proportion was calculated from these values and used to evaluate whether the post-stimulation window exhibited a greater EMG response than the pre-stimulation window. AUC was assessed in the same time epochs on baseline-corrected, raw, rectified data (**fig 4.2B, fig 4.4)**.

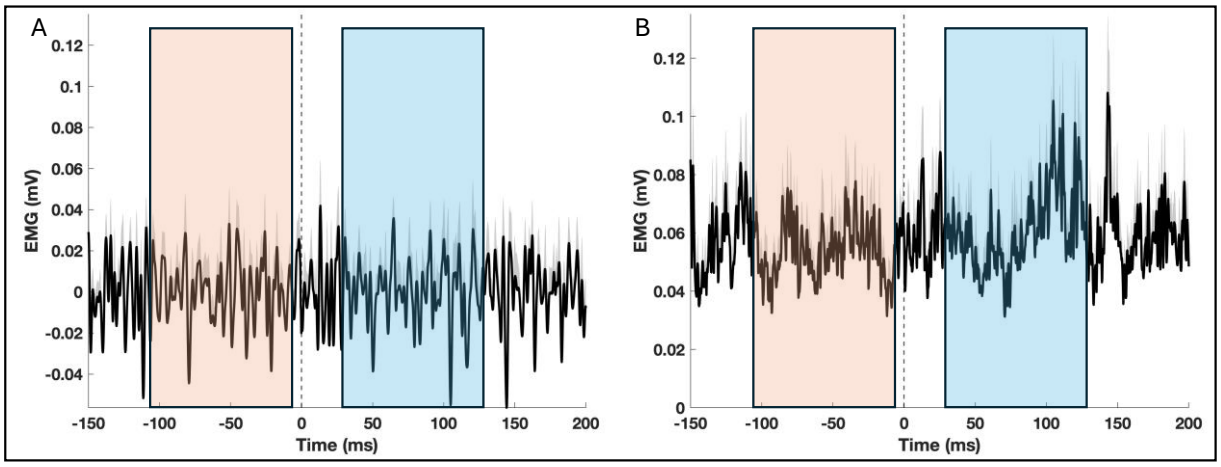

Figure 4.2. Example participant level EMG traces time locked to TMS stimulation with positive shaded error displayed. The red and blue shaded regions indicate the pre- and post-stimulation epochs, respectively. Pre-stimulation epoch was -105 to -5 ms from stimulation, and post-stimulation epoch was 25 to 125 ms after stimulation. These epochs were analyzed for peak-to-peak and area under curve. A) Raw averaged EMG signal from an example participant with positive shaded error. B) Raw, rectified averaged EMG signal from the same participant, also with positive shaded error.

For data visualization, we also generated participant level root mean square (RMS) smoothed time series data (**fig 4.3)**. RMS was calculated on each accepted trial, and data were smoothed in MATLAB (movRMS via the DSP System Toolbox) with a sliding window of 30 sample points, equivalent to 2.4 ms. Trials contributing to these time series data were averaged at the participant level, then averaged at the group level for plotting.

Behavioral Measures

Behavioral metrics of interest were calculated for each task condition in the SST. These included means and standard deviations of button Go RT, mean SSD, mean stopping accuracy (%), integration SSRT (Verbruggen et al., 2019), and means and standard deviations of failed stop button RT. Behavioral measures of interest are displayed in Table 4.1.

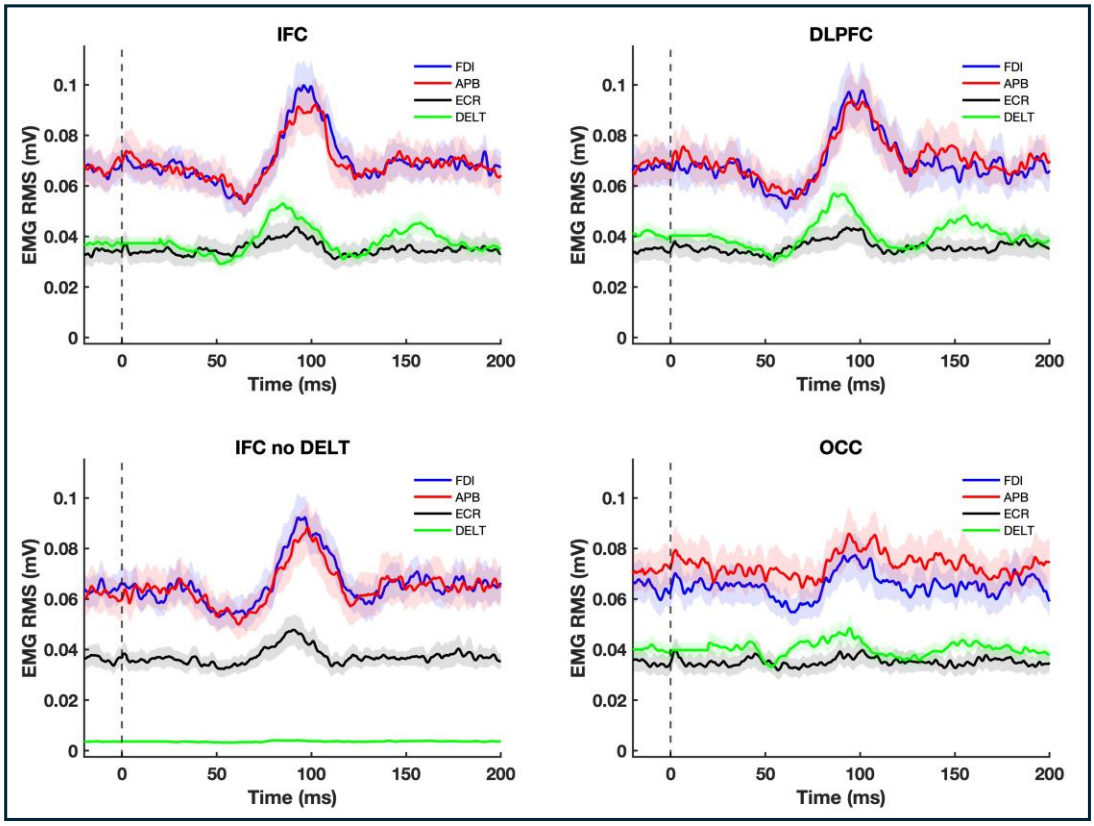

Figure 4.3. Time series root mean square plots locked to TMS stimulation for rIFC (top left), DLPFC (top right), rIFC with relaxed DELT (bottom left), and OCC (bottom right). Each plot has a trace ± standard error (shaded region) for each muscle. Blue trace is FDI, red trace is APB, black trace is ECR, and green trace is DELT. RMS is calculated on each trial, then averaged for each subject, then averaged for the group (n = 23).

Statistical Tests

Statistical tests were primarily performed in JASP (JASP 0.16.3). Peak-to-peak and AUC measures were represented as a proportion of the post-stimulation epoch relative to the pre-stimulation baseline.

A repeated-measures ANOVA with the factors ROI (rIFC, DLPFC, and OCC), and muscle (FDI, APB, ECR, and DELT) tested for differences in peak-to-peak and AUC measures. Another set of repeated-measures ANOVA with the factors ROI (rIFC, DLPFC, OCC, and rIFC

resting DELT condition), and muscle (FDI, APB, and ECR) tested for differences in peak-to-peak and AUC measures. We used this test to determine whether DELT contraction influenced

Table 4.1. Behavioral measures from the choice response SST (n = 23). All data presented as mean ± std (in parentheses). RT = reaction time, SSD = stop signal delay, SSRT = stop signal reaction time.

Choice SST Behavioral Measures	
Go Both RT (ms)	408.9 (74.4)
Stop Both Fail RT (ms)	359.1 (51.2)
Partial Stop Fail RT (ms)	359.4 (51.8)
Stop Both SSRT (ms)	210.1 (42.6)
Partial Stop SSRT (ms)	195.6 (36.4)
Stop Both SSD (ms)	203.4 (76)
Partial Stop SSD (ms)	201.0 (73.2)
Go Both Accuracy (%)	98.0 (1.9)
Stop Both Accuracy (%)	43.6 (7.6)
Selective Stop Accuracy (%)	51.1 (4.8)

EMG evoked responses. Sphericity violations were corrected with Greenhouse-Geisser and significant effects were evaluated with Bonferroni-corrected post hoc tests, alpha level set to 0.05. Statistical test results are provided with the corrected non-integer degrees of freedom unless otherwise noted.

Bayesian paired t-tests were used to compare pre- and post-stimulation peak-to-peak and AUC measures in the rIFC condition with DELT at rest. We hypothesized if startle was the source of DELT activation, then we would see increased EMG following TMS even when the muscle was at rest. Alternatively, we hypothesized the pre- and post-stimulation epochs would be statistically similar, meaning we didn't expect an evoked response in the resting DELT that differed from baseline. We also performed Bayesian repeated-measures ANOVA for peak-to-peak and AUC with factors ROI (rIFC, and rIFC resting DELT), and muscle (FDI, APB, and ECR). We hypothesized evoked responses in the peripheral muscles in both rIFC stimulation

conditions would be equivalent. This would indicate that the engagement of the DELT to maintain the arm's posture against gravity was not the cause of the EMG pattern following TMS.

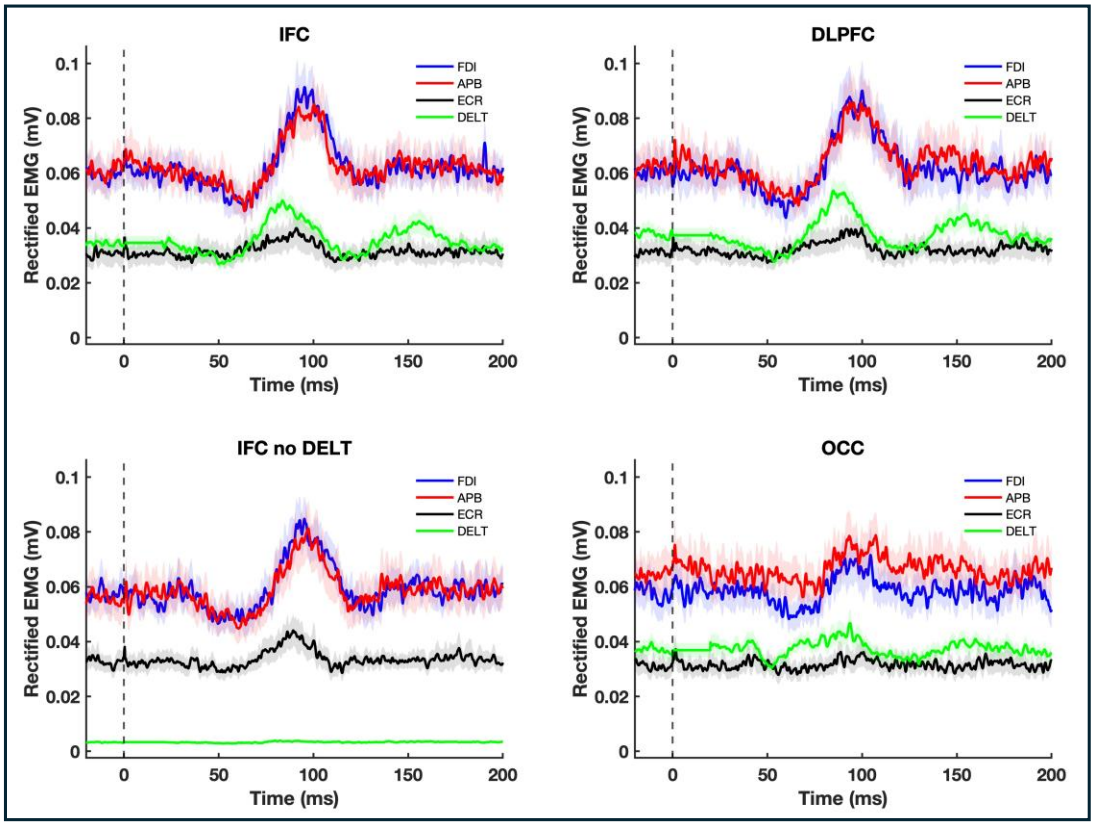

Figure 4.4. Time series raw, rectified plots locked to TMS stimulation for rIFC (top left), DLPFC (top right), rIFC with relaxed DELT (bottom left), and OCC (bottom right). Each plot has a trace ± standard error (shaded region) for each muscle. Blue trace is FDI, red trace is APB, black trace is ECR, and green trace is DELT. Data is averaged for each subject, then averaged for the group (n = 23).

Finally, we tested whether subject level peak-to-peak and AUC measures of the evoked responses were related to stopping performance. We hypothesized stimulation of rIFC would evoke an EMG response and given the relevance of rIFC to the stopping network, believed the magnitude of the response would correlate with SSRT across participants. We predicted individuals with larger evoked responses would exhibit faster SSRTs. We tested this hypothesis by calculating Pearson correlations between rIFC and OCC FDI peak-to-peak and AUC proportional measures with SSRT estimates from the SST.

Results

Participant Level Peak-to-peak and AUC Comparisons

A primary aim of this study was to extend our findings from Chapter III using our nTMS approach to examine differences in evoked EMG responses between frontal ROI (rIFC and DLPFC) and control (OCC) stimulation. Mean peak-to-peak and AUC were calculated on averaged EMG traces at the subject level on baseline corrected raw EMG, and baseline corrected rectified EMG, respectively. For peak-to-peak amplitudes (**fig 4.5, right panel**), there was a significant main effect of ROI, [$F(1.794, 41.265) = 7.31$, $p < .05$, $\eta^2_p = .241$], and muscle [$F(1.668, 38.366) = 11.81$, $p < .001$, $\eta^2_p = .339$]. Post hoc t tests for ROI revealed significantly greater peak-to-peak amplitudes for rIFC compared to OCC ($t = 3.0$, $d = .45$, $p < .05$), and for DLPFC compared to OCC ($t = 3.6$, $d = .55$, $p < .05$). AUC (**fig 4.5, left panel**) showed no main effect of ROI (rIFC, DLPFC, and OCC) [$F(1.887, 43.391) = 2.93$, $p = .07$, $\eta^2_p = .113$], or muscle [$F(2.080, 47.838) = 0.96$, $p = .42$, $\eta^2_p = .040$]. These results partially replicate our findings in Chapter III and show participant level peak-to-peak measures on raw averaged EMG signal may be a reliable method for measuring evoked responses via frontal cortex stimulation. Surprisingly, navigated TMS, and a larger sample did not increase our sensitivity to differences in our EMG AUC measure.

Another aim for this study was to determine if DELT contraction influenced the contraction of distal muscles. We considered stimulation of frontal ROI may cause a brief interruption, or startle, and DELT posture resumption could have resulted in a hysteresis-like effect influencing the state of FDI, APB and ECR muscles. To test this, we included an rIFC stimulation block with DELT at rest allowing us to compare FDI, APB and ECR muscles with and without potential DELT influence. A 2 x 3 Bayesian repeated measures ANOVA was used

to compare peak-to-peak and AUC measures between ROI (rIFC with and without DELT contraction) and muscle (FDI, APB, and ECR). Participant level peak-to-peak $BF_{01} = 4.1$ suggests moderate evidence for no difference, and participant level AUC $BF_{01} = 1.2$ suggests anecdotal evidence for no difference in ROI between resting and contracting DELT during rIFC stimulation.

The DELT rest condition also allowed for testing of equivalence in the resting DELT condition to determine if stimulation of rIFC would evoke responses at rest relative to the pre-stimulation baseline. We analyzed the same pre- and post-stimulation epochs for peak-to-peak and AUC in the resting DELT muscle using paired samples Bayesian *t*-tests to determine whether there was a proportional change in resting muscular activity due to stimulation. Participant level peak-to-peak returned a $BF_{01} = 0.69$, which suggests weak evidence for no difference. Participant level AUC returned a $BF_{01} = 3.0$, suggesting anecdotal evidence for no difference between baseline EMG and post-stimulation.

Relationship Between SSRT and TMS-Evoked EMG Responses

The rIFC is implicated as a crucial region the stopping network and has been identified as a NMA from intraoperative stimulation studies. Given both processes are likely inhibitory in nature, we sought to explore the link between the evoked EMG responses from TMS stimulation of the rIFC and participant's ability to stop (SSRT). To explore the link between rIFC and stopping, we correlated the SSRT from our SST with participant level FDI muscle AUC and peak-to-peak proportions from rIFC and OCC stimulation (**fig 4.6**). The FDI muscle was selected as relevant since it is the primary muscle for mobilizing the index finger in the SST. The rIFC was our primary ROI due to the connections with stopping and NMAs, and the OCC was selected as a control since this target is not expected to engage the response inhibition network.

No relationships were observed between SSRT and rIFC or OCC stimulation measurements (all *p*s > .05).

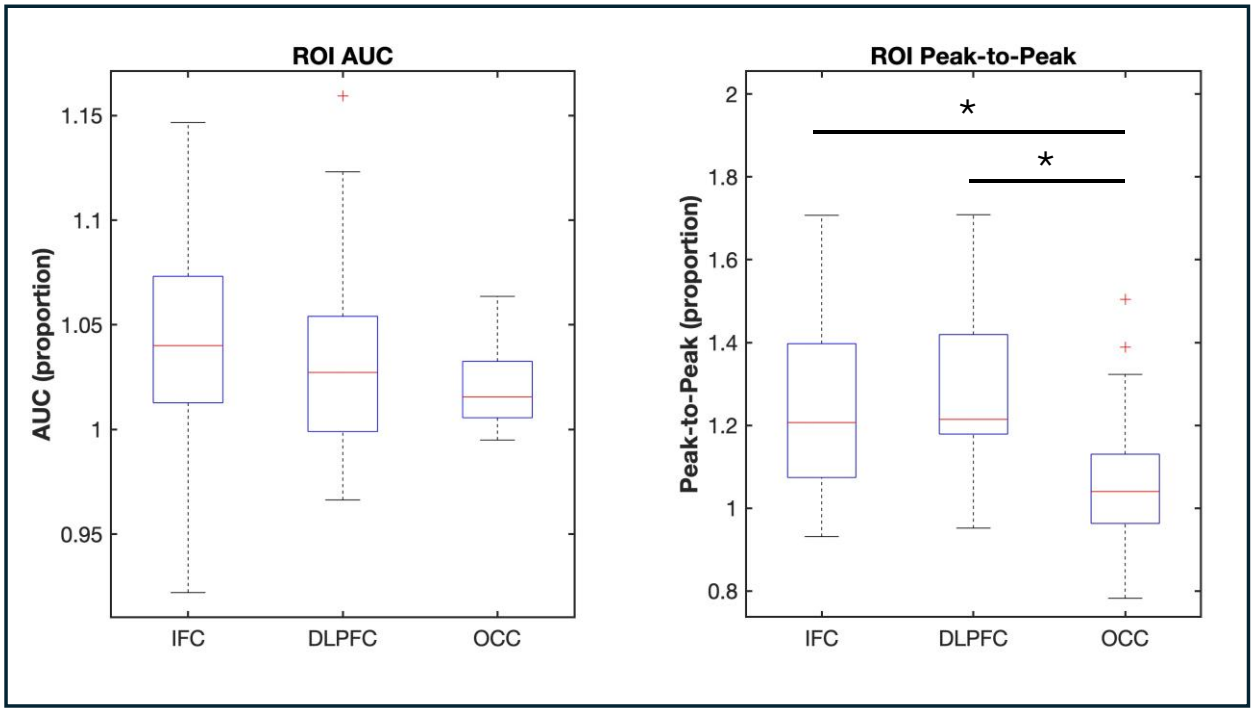

Figure 4.5. Box and whisker plots (mean, 25-75%, full range, + = outliers) displaying pre- and post-stimulation proportions for area under the curve (AUC, left panel), and peak-to-peak proportions (right panel), calculated at the participant level (n = 23). The three regions of interest (ROI) are right inferior frontal cortex (IFC), dorsolateral prefrontal cortex (DLPFC) and occipital cortex (OCC). * indicates $p < .05$.

Discussion

In the present study, we used nTMS to anatomically target rIFC. Based on our previous study, we predicted nTMS of rIFC would elicit evoked responses in the ongoing muscular contractions, and we hypothesized tailoring stimulation to individual anatomy would result in more consistent patterns across participants to yield more robust effects. This hypothesis was motivated by findings in Chapter III, in which we elicited motor responses via single-pulse TMS of rIFC and preSMA. Based on previous evidence suggesting overlap between a fronto-basal ganglia response inhibition network and frontal cortical NMAs, we also hypothesized

characteristics of the rIFC TMS-evoked responses would correlate with SSRT, a behavioral estimate of a participant's speed of stopping.

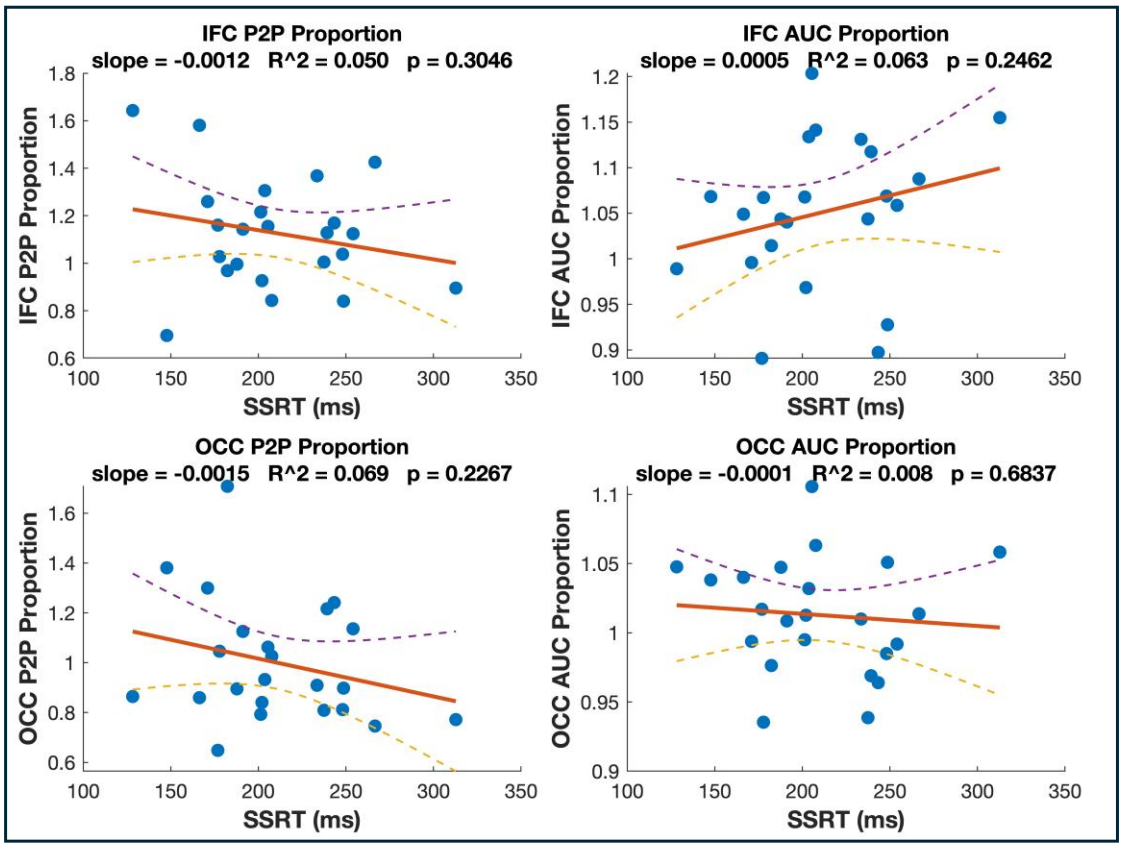

Figure 4.6. Displays a correlation matrix for relationships between stop signal reaction time (SSRT) and metrics of TMS-evoked responses in the first dorsal interosseous (FDI) muscle from stimulation of right inferior frontal cortex (IFC) and occipital cortex (OCC). Left side panels display the peak-to-peak amplitude as a proportion of post- relative to pre-stimulation from participant level averaged raw EMG signal for IFC (top) and OCC (bottom) plotted against SSRT. Right side panels display the post- relative to pre-stimulation area under the curve (AUC) proportion from participant level averaged raw rectified EMG signal for IFC (top) and OCC (bottom) plotted against SSRT. All comparisons with n = 23.

We partially replicated our TMS evoked response results from Chapter III. Specifically, evaluating rIFC pre- to post-stimulation peak-to-peak proportion in the 25 – 125 ms post-stimulation epoch was significantly different from OCC. Whereas AUC proportion to compare rIFC and OCC in the same epoch was not significant. This result indicates stimulation over the

rIFC produces a larger positive motor response than OCC stimulation and suggests peak-to-peak measurements are more sensitive to frontal cortical stimulation effects than AUC.

Our experimental design allowed for investigation of rIFC stimulation with and without DELT contraction. This is important to rule out the potential influence of proximal muscle activation on distal muscle activity when sustaining a posture against gravity. Bayesian tests indicated there was anecdotal to moderate evidence for no difference in rIFC TMS evoked responses in distal muscles with and without DELT contraction, which suggests DELT contraction does not influence evoked responses in distal muscles. We were also able to test the effect of rIFC stimulation at rest in the DELT muscle. Bayesian tests revealed weak and anecdotal evidence to suggest no difference between pre- and post- stimulation EMG for peak-to-peak and AUC measures, respectively. This suggests effects of stimulation over non-motor areas are only observable in the presence of tonic muscle activity.

Finally, to address the possible overlap of the response inhibition network with NMAs, we correlated participant SSRT with FDI AUC and peak-to-peak measures from rIFC and OCC stimulation and found no relationship between SSRT and TMS evoked responses. Altogether, these findings contribute to our understanding of how frontal cortex single-pulse TMS influences the motor system and constrain interpretations of TMS-evoked EMG as a marker of inhibitory control.

Extension of Previous EMG Findings

Our peak-to-peak EMG data showed rIFC stimulation evoked greater amplitude responses relative to OCC. This finding is in alignment with our results from Chapter III. Interestingly, DLPFC stimulation also evoked greater peak-to-peak amplitude responses relative to OCC stimulation. Together, these data support the idea that frontal cortex stimulation has a

causal influence on motor output. This may be related to results from Schluter et al., which claim stimulation of premotor cortex disrupts the early stages of movement (1998). Despite our data showing a positive motor response, it is possible this effect may still be a result of activation of the hyperdirect pathway via NMAs. Intraoperative studies show rIFC stimulation leads to motor arrest (Lüders et al., 1995; Mikuni et al., 2006), and our data show measurable peripheral EMG changes. This is not proof of inhibitory engagement but provides evidence that stimulation of frontal cortical regions influences the excitability of distal muscles outside the context of action stopping. However, we did not replicate the participant level finding for AUC in the same window. AUC reflects sustained changes in EMG envelope and may be influenced more by variability.

Notably, it is interesting the nTMS approach did not yield more pronounced effects in the evoked responses. This could possibly indicate anatomically defined targets are not necessarily functionally important. In essence, general stimulation of frontal networks could result in motoric responses. Indeed, there is evidence to suggest TMS-evoked responses may be driven by large-scale network dynamics at the time of stimulation (Momi et al., 2023). Alternatively, this could reflect differences in the samples between the two studies. This finding also suggests individual differences in response to frontal TMS effects may not be attributed to anatomical targets, but some other properties such as the networks each region is involved with. This is an important finding for clinical applications that target stimulation at the frontal cortex (e.g. treatment of depression; (Gaynes et al., 2014), and potentially targeting individual anatomy is less important than other factors.

Importantly, our methods allowed us to address two potential confounding factors. First, in Chapter III, there was no resting condition to compare pre- and post-stimulation effects. Our

rIFC stimulation condition with DELT at rest. The peak-to-peak Bayesian comparison was inconclusive, however the AUC comparison suggested anecdotal evidence for no effect. This result suggests the evoked responses in all muscles was not a result of a startle effect, as it would be expected to see EMG responses in resting muscles within 100 ms of the stimulation time (Valls-Solé et al., 1999). Additionally, startle effect is strongest on proximal muscles (DELT) compared to distal muscles (FDI, APB, ECR). The startle effect cannot be eliminated as a possibility since it is a bilateral effect, and we only collected EMG from contralateral muscles. Regardless, it is unlikely startle effect contributed strongly to our data since participants wore earplugs to reduce noise sensitivity, and received 35 – 40 TMS pulses per condition, and likely would have habituated early on during the TMS session (Phelps et al., 2012).

Relationship Between TMS Effects and Stopping Performance

Next, we evaluated the relationship between participant's stopping ability (SSRT) and peak-to-peak and AUC measures of TMS-evoked responses in FDI muscle EMG. We found no relationships or trends with these comparisons. There are several possible interpretations for why this may be. It's possible there could be a state distinction between the two measures (i.e. within vs outside of SST context). Stimulation of frontal cortex may reflect connectivity within the frontal cortex and the capacity to influence the motor system. Whereas SSRT may relate more directly to task-specific inhibitory control. There are a few other considerations for the TMS-evoked potentials. Our findings indicate a positive motor response, and response inhibition is more likely associated with inhibitory effects (e.g. cortical silent periods; (Cantello et al., 1992). One possibility is the positive motor response is a rebound following a transient inhibition of the contracted muscles. As seen in **Figures 4.3-4.4**, several muscles show a decrease in activity prior to the larger positive motor response. A more precise quantification of this period could reveal a

relationship. Also, there may be a disconnect with the measures we've chosen to correlate. We are using the amplitude of a TMS-evoked EMG response and regressing with a behavioral latency. Potentially, a latency measurement of the evoked responses may be more sensitive to the temporal aspects that determine SSRT.

Limitations

As previously mentioned, a limitation of this study was solely collecting tonic EMG from muscles contralateral to cortical stimulation. Including ipsilateral contracted muscles would have allowed for comparisons between limbs that may have provided support for a widespread EMG response to rIFC stimulation. This would favor the hypothesis that NMA stimulation activates the STN via the hyperdirect pathway and would clarify the potential effects of startle on proximal and distal muscles. A true sham control (i.e. an audible 'click' scaled to the noise level expected for a participant's RMT with no TMS delivered to the cortex) would aid in understanding the differences in the evoked responses from OCC and frontal ROI. Essentially, what is a consequence of stimulation as opposed to some other factors. Finally, due to recruitment constraints and three excluded participants, our sample size for SSRT correlations was lower than anticipated.

Conclusions

The present findings provide novel insight into how frontal cortical TMS of rIFC and DLPFC influences the motor system and begins to address the extent to which TMS-evoked EMG can be used to study inhibitory control outside the context of stopping. Both rIFC and DLPFC stimulation reliably produced larger peak-to-peak EMG responses than OCC stimulation, suggesting a causal influence on motor output. Surprisingly, increasing the sample, number of stimulations and using nTMS for precisely targeting individual anatomy did not

improve our sensitivity to characterize AUC for TMS-evoked EMG responses, compared to the previous study (Chapter III). These findings may support the idea of the stopping network as state-dependent and single-pulse stimulation of rIFC may be insensitive to probing transient inhibitory phenomena in tonic EMG. Alternatively, we may have used the wrong measures for comparison in our data. More work is needed to explore if other features of TMS-evoked response are related to behavioral stopping. The present work helps refine how non-invasive stimulation can be used to probe the neural mechanisms of inhibitory control.

REFERENCES CITED

Aron, A. R., Durston, S., Eagle, D. M., Logan, G. D., Stinear, C. M., & Stuphorn, V. (2007). Converging Evidence for a Fronto-Basal-Ganglia Network for Inhibitory Control of Action and Cognition. *Journal of Neuroscience*, *27*(44), 11860–11864. https://doi.org/10.1523/JNEUROSCI.3644-07.2007

Aron, A. R., Herz, D. M., Brown, X. P., Forstmann, B. U., & Zaghloul, K. (2016). Frontosubthalamic Circuits for Control of Action and Cognition. *The Journal of Neuroscience*, *36*(45), 11489–11495.

Aron, A. R., & Poldrack, R. A. (2006). Cortical and Subcortical Contributions to Stop Signal Response Inhibition: Role of the Subthalamic Nucleus. *The Journal of Neuroscience*, *26*(9), 2424–2433. https://doi.org/10.1523/JNEUROSCI.4682-05.2006

Awiszus, F. (2003). Chapter 2 TMS and threshold hunting. In *Supplements to Clinical Neurophysiology* (Vol. 56, pp. 13–23). Elsevier. https://doi.org/10.1016/S1567-424X(09)70205-3

Badry, R., Mima, T., Aso, T., Nakatsuka, M., Abe, M., Fathi, D., Foly, N., Nagiub, H., Nagamine, T., & Fukuyama, H. (2009). Suppression of human cortico-motoneuronal excitability during the Stop-signal task. *Clinical Neurophysiology*, *120*(9), 1717–1723.

Borggraefe, I., Catarino, C. B., Rémi, J., Vollmar, C., Peraud, A., Winkler, P. A., & Noachtar, S. (2016). Lateralization of cortical negative motor areas. *Clinical Neurophysiology*, *127*(10), 3314–3321.

Breshears, J. D., Molinaro, A. M., & Chang, E. F. (2015). A probabilistic map of the human ventral sensorimotor cortex using electrical stimulation. *Journal of Neurosurgery*, *123*(2), 340–349. https://doi.org/10.3171/2014.11.JNS14889

Breshears, J. D., Southwell, D. G., & Chang, E. F. (2019). Inhibition of Manual Movements at Speech Arrest Sites in the Posterior Inferior Frontal Lobe. *Neurosurgery*, *85*(3), E496–E501. https://doi.org/10.1093/neuros/nyy592

Cai, W., Oldenkamp, C. L., & Aron, A. R. (2012). Stopping speech suppresses the task-irrelevant hand. *Brain and Language*, *120*(3), 412–415.

Cantello, R., Gianelli, M., Civardi, C., & Mutani, R. (1992). Magnetic brain stimulation: The silent period after the motor evoked potential. *Neurology*, *42*(10), 1951–1959. https://doi.org/10.1212/wnl.42.10.1951

Caulfield, K. A., Fleischmann, H. H., Cox, C. E., Wolf, J. P., George, M. S., & McTeague, L. M. (2022). Neuronavigation maximizes accuracy and precision in TMS positioning: Evidence from 11,230 distance, angle, and electric field modeling measurements. *Brain Stimulation*, *15*(5), 1192–1205. https://doi.org/10.1016/j.brs.2022.08.013

Chen, W., de Hemptinne, C., Miller, A. M., Leibbrand, M., Little, S. J., Lim, D. A., Larson, P. S., & Starr, P. A. (2020). Prefrontal-subthalamic hyperdirect pathway modulates movement inhibition in humans. *Neuron*, *106*(4), 579–588.

Fried, I., Katz, A., McCarthy, G., Sass, K. J., Williamson, P., Spencer, S. S., & Spencer, D. D. (1991). Functional organization of human supplementary motor cortex studied by electrical stimulation. *Journal of Neuroscience*, *11*(11), 3656–3666.

Momi, D., Wang, Z., & Griffiths, J. D. (2023). TMS-evoked responses are driven by recurrent large-scale network dynamics. *eLife*, *12*, e83232. https://doi.org/10.7554/eLife.83232

Ikeda, A., Lüders, H. O., Burgess, R. C., Sakamoto, A., Klem, G. H., Morris, H. H., & Shibasaki, H. (1995). Generator locations of movement-related potentials with tongue protrusions and vocalizations: Subdural recording in human. *Electroencephalography and Clinical Neurophysiology*, *96*(4), 310–328. https://doi.org/10.1016/0168-5597(95)00002-a

Jackson, N., & Greenhouse, I. (2019). VETA: An Open-Source Matlab-Based Toolbox for the Collection and Analysis of Electromyography Combined With Transcranial Magnetic Stimulation. *Frontiers in Neuroscience*, *13*. https://www.frontiersin.org/articles/10.3389/fnins.2019.00975

Luders, H. (1987). Negative motor responses elicited by stimulation of the human cortex. *Advances in Epileptology*, *16*, 229–231.

Lüders, H. O., Dinner, D. S., Morris, H. H., Wyllie, E., & Comair, Y. G. (1995). Cortical electrical stimulation in humans. The negative motor areas. *Advances in Neurology*, *67*, 115–129.

Mikuni, N., Oharac, S., Ikeda, A., Hayashi, N., Nishida, N., Taki, J., Enatsu, R., Matsumoto, R., Shibasaki, H., & Hashimoto, N. (2006). Evidence for a wide distribution of negative motor areas in the perirolandic cortex. *Clinical Neurophysiology*, *117*, 33–40.

Momi, D., Wang, Z., & Griffiths, J. D. (2023). TMS-evoked responses are driven by recurrent large-scale network dynamics. *eLife*, *12*, e83232. https://doi.org/10.7554/eLife.83232

Monticelli, M., Zeppa, P., Altieri, R., Veneziani Santonio, F., Cofano, F., Melcarne, A., Junemann, C. V., Zenga, F., Sabatino, G., La Rocca, G., Della Pepa, G. M., Ducati, A., & Garbossa, D. (2020). Exploring the anatomy of negative motor areas (NMAs): Findings in awake surgery. *Journal of Clinical Neuroscience*, *73*, 219–223. https://doi.org/10.1016/j.jocn.2020.01.049

Nambu, A., Tokuno, H., & Takada, M. (2002). Functional significance of the cortico–subthalamo–pallidal 'hyperdirect'pathway. *Neuroscience Research*, *43*(2), 111–117.

Penfield, W. (1949). VOCALIZATION AND ARREST OF SPEECH. *Archives of Neurology And Psychiatry*, *61*(1), 21. https://doi.org/10.1001/archneurpsyc.1949.02310070027002

Phelps, B. J., Doyle-Lunders, L., Harsin-Waite, A., Hofman, N., & Knutson, L. M. (2012). Demonstrating habituation of a startle response to loud noise. *The Behavior Analyst Today*, *13*(1), 17–19. https://doi.org/10.1037/h0100714

Pinson, H., Van Lerbeirghe, J., Vanhauwaert, D., Van Damme, O., Hallaert, G., & Kalala, J.-P. (2022). The supplementary motor area syndrome: A neurosurgical review. *Neurosurgical Review*, *45*(1), 81–90. https://doi.org/10.1007/s10143-021-01566-6

Pommier, B., Vassal, F., Boutet, C., Jeannin, S., Peyron, R., & Faillenot, I. (2017). Easy methods to make the neuronavigated targeting of DLPFC accurate and routinely accessible for rTMS. *Neurophysiologie Clinique/Clinical Neurophysiology*, *47*(1), 35–46. https://doi.org/10.1016/j.neucli.2017.01.007

Rech, F., Herbet, G., Moritz-Gasser, S., & Duffau, H. (2014). Disruption of bimanual movement by unilateral subcortical electrostimulation. *Human Brain Mapping*, *35*(7), 3439–3445.

Schluter, N. D., Rushworth, M. F., Passingham, R. E., & Mills, K. R. (1998). Temporary interference in human lateral premotor cortex suggests dominance for the selection of movements. A study using transcranial magnetic stimulation. *Brain*, *121*(5), 785–799. https://doi.org/10.1093/brain/121.5.785

Smith, S. M., Jenkinson, M., Woolrich, M. W., Beckmann, C. F., Behrens, T. E., Johansen-Berg, H., & Matthews, P. M. (2004). Advances in functional and structural MR image analysis and implementation as FSL technical report TR04SS2. *Neuroimage*, *23*(S1), 208–219.

Swann, N. C., Cai, W., Conner, C. R., Pieters, T. A., Claffey, M. P., George, J. S., Aron, A. R., & Tandon, N. (2012). Roles for the pre-supplementary motor area and the right inferior frontal gyrus in stopping action: Electrophysiological responses and functional and structural connectivity. *NeuroImage*, *59*(3), 2860–2870. https://doi.org/10.1016/j.neuroimage.2011.09.049

Swann, N., Tandon, N., Canolty, R., Ellmore, T. M., McEvoy, L. K., Dreyer, S., DiSano, M., & Aron, A. R. (2009). Intracranial EEG reveals a time-and frequency-specific role for the right inferior frontal gyrus and primary motor cortex in stopping initiated responses. *Journal of Neuroscience*, *29*(40), 12675–12685.

Valls-Solé, J., Rothwell, J. C., Goulart, F., Cossu, G., & Muñoz, E. (1999). Patterned ballistic movements triggered by a startle in healthy humans. *The Journal of Physiology*, *516*(Pt 3), 931–938. https://doi.org/10.1111/j.1469-7793.1999.0931u.x

Verbruggen, F., Chambers, C. D., & Logan, G. D. (2013). Fictitious Inhibitory Differences: How Skewness and Slowing Distort the Estimation of Stopping Latencies. *Psychological Science*, *24*(3), 352–362. https://doi.org/10.1177/0956797612457390

Verbruggen, F., & Logan, G. D. (2009). Models of response inhibition in the stop-signal and stop-change paradigms. *Neuroscience & Biobehavioral Reviews*, *33*(5), 647–661.

Wadsley, C. G., Cirillo, J., Nieuwenhuys, A., & Byblow, W. D. (2023). Comparing anticipatory and stop-signal response inhibition with a novel, open-source selective stopping toolbox. *Experimental Brain Research*, *241*(2), 601–613. https://doi.org/10.1007/s00221-022-06539-9

Wessel, J. R., Reynoso, H. S., & Aron, A. R. (2013). Saccade suppression exerts global effects on the motor system. *Journal of Neurophysiology*, *110*(4), 883–890. https://doi.org/10.1152/jn.00229.2013

Zhou, Y., Zhao, Z., Zhang, J., Hameed, N. U. F., Zhu, F., Feng, R., Zhang, X., Lu, J., & Wu, J. (2021). Electrical stimulation–induced speech-related negative motor responses in the lateral frontal cortex. *Journal of Neurosurgery*, *137*(2), 496–504. https://doi.org/10.3171/2021.9.JNS211069

CHAPTER V

SUMMARY AND CONCLUSIONS

Summary of Results and Findings

This dissertation sought to clarify when and how cortically mediated inhibition manifests in electromyographic events, whether endogenously driven during behavioral stopping or exogenously through non-invasive stimulation of negative motor areas (NMAs). Motivation for this work was the potential to determine electrophysiological signatures of inhibition in peripheral muscles, and to develop novel methods for interrogating the response inhibition network (for review: Aron et al., 2016). We addressed these questions across a series of behavioral, electromyographic (EMG) and non-invasive stimulation paradigms. A primary aim of this dissertation was to characterize inhibition in peripheral EMG associated with fronto-basal ganglia networks, whether recruited during task performance or through non-invasive brain stimulation. Specifically, we focused on EMG events to begin exploring whether the two different approaches tap into the same underlying mechanism(s). We first tested a novel response inhibition setup in which participants sustained tonic muscular contractions with a muscle on one hand while performing a stop signal task (SST) with the opposite hand (Chapter II). The task setup allowed us to examine EMG signatures of inhibition during SST performance. In two experiments, we found EMG returns to baseline much quicker on failed stop trials compared with go trials. This suggests inhibitory influence arrives at the muscles, but too late to prevent movement completion. The dissertation direction then shifted to non-invasively investigating the negative motor system. We used transcranial magnetic stimulation (TMS) delivered to candidate NMAs while participants sustained tonic contractions with contralateral effectors (Chapter III). Then we performed a follow-up investigation in a larger sample to refine these methods with a

neuro-navigated stimulation technique (Chapter IV). In Chapter IV, we also administered a behavioral SST to determine if there are correlations between TMS-evoked EMG responses and stopping behavior.

Chapter II employed two versions of a SST (simple and choice) that participants completed with one hand while simultaneously contracting a homologous effector on the opposite hand. We designed the task on the premise of detecting global suppression of the motor system in peripheral muscles. Based on previous TMS work, successfully inhibiting responses results in a reduction in corticospinal activity (Badry et al., 2009; Cai et al., 2012; Wessel et al., 2013). Our work examined electromyographic signatures during stop task performance. We revealed patterns that 1) activity associated with going predicted failed stopping, and 2) suggest inhibitory mechanisms continue to influence the motor system even in the face of completed responses during failed stopping. Thus, during trials in which participants failed to inhibit a response, we found evidence to suggest inhibitory processes run to completion despite arriving too late.

Chapters III & IV examined the effects of TMS over frontal cortical areas implicated in reactive response inhibition and identified as NMAs. NMAs and their electrical stimulation evoked negative motor responses (NMRs) have been primarily studied in surgical settings with the aim of preserving functional areas prior to resection. Electrical stimulation of NMAs is observed to cause interruptions and / or arrest of movements and vocalizations. We developed and refined a novel protocol for non-invasively stimulating frontal NMAs in two experiments. We collected EMG from four muscles on the contralateral hand and arm while participants maintained tonic contractions throughout stimulation. The first experiment was exploratory and included stimulation at multiple intensities, and with the TMS coil oriented in two opposing

directions to determine if a given method was optimal for evoking responses. The first experiment used generalized Montreal Neurological Institute (MNI) coordinates for targeting. The second experiment refined this method by using individual participant MRI with a neural navigation system to precisely stimulate targets. In both experiments, we revealed positive motor events following frontal stimulation. These events occur distinctly after the typical latency for motor-evoked potentials (MEPs), which are elicited from primary motor cortex stimulation. Instead, these positive motor events occur in the typical window for cortical silent periods (CSPs), which represent the manifestation of neurophysiological inhibitory processes in EMG signal. These results offer new insight into the role non-motor frontal cortical regions function within the motor and inhibitory response system. We also provide a novel method for stimulation of NMAs in healthy populations. These methods may be useful for translation to clinical populations.

In summary, the methods and results of these studies show the potential of critically analyzing EMG events within the context of stopping, and in the context of non-motor area brain stimulation. We have shown the utility of these methods for investigating the timing and duration in which inhibitory processes influence muscular dynamics (Chapter II & bridge). We have developed new methods for probing the negative motor system, an understudied branch of cognitive inhibitory control research (Chapters III & IV). These methods can be used to identify electrophysiological signatures of inhibition, and further probe the relationships between frontal cortical stimulation, response inhibition and the negative motor system.

Limitations

A significant limitation in Chapter II was only using one type of response inhibition paradigm. We used simple and choice versions of standard SSTs to investigate the influence of

stopping from tonically active muscles in the opposite hand. We believe performing these tasks in a unimanual fashion influenced the cognitive control of action. Essentially, asking the participants to do separate activities with each of their hands may have created a dual task environment which could have washed out evidence of inhibitory influence in the tonically active, task-irrelevant muscle. We addressed this in a follow-up study led by an undergraduate mentee, Isaiah Mills. We collaborated with Isaiah to design a bimanual response inhibition task with tonically active, task-irrelevant muscles in both hands. I mentored Isaiah throughout this process, and his work was published in eNeuro (Mills et al., 2025).

Our first attempt at evaluating TMS of NMAs involved several limitations (Chapter III). We lacked neuroanatomical targeting, had a relatively small sample size, and our analysis was a first pass at processing tonic EMG data in this manner. Other alternative approaches should be explored. We also did not include secondary behavioral measurements to evaluate the relationship to stopping. In our second attempt at evaluating TMS of NMAs (Chapter IV), we addressed the sample size and performed anatomically precise targeting of frontal cortical regions of interest. However, we did not functionally define the areas we targeted (e.g. through fMRI localization). A general limitation for Chapters III and IV is that we only used magnitude (peak-to-peak amplitude and area under curve) of EMG markers for quantification of evoked responses. This leaves open questions concerning latency of these events.

Recommendations for Future Work

This thesis provides methods and insight for assessing inhibitory control in the context of stopping. We also provide a framework and novel methods for investigating the negative motor system, and its relation to the inhibitory control network outside of the surgical suite. The

experiments in Chapters III & IV are early entries into an exciting new area of research that has clinical applications.

Future work from Chapters III & IV could explore many directions. A primary focus in the field of response inhibition is to understand the latencies and timings in which inhibitory control manifests peripherally. This warrants further inspection of the time course and patterns of TMS-evoked responses from frontal cortex stimulation. Given we did not see a more pronounced effect from frontal stimulation in the navigated TMS, follow-up studies should discern whether targeted stimulation is different from stimulation in general areas of the frontal cortex in the same sample. To build on this, it would be worthwhile to stimulate a variety of targets in the frontal cortex with bimanual contractions to determine whether this is effect occurs bilaterally, or just contralaterally. An extension of that investigation should include left frontal cortex stimulation which would aid in understanding the spread of these events and whether they can be evoked from frontal cortices of both hemispheres. Lastly, the NMA experiments were designed with the intention of offering mapping alternatives for patients undergoing resective surgery. There are a multitude of experiments which could be designed to bridge this gap and compare frontal cortex stimulation effects pre-, during and post-surgery.

REFERENCES CITED

Aron, A. R., Herz, D. M., Brown, X. P., Forstmann, B. U., & Zaghloul, K. (2016). Frontosubthalamic Circuits for Control of Action and Cognition. *The Journal of Neuroscience*, *36*(45), 11489–11495.

Badry, R., Mima, T., Aso, T., Nakatsuka, M., Abe, M., Fathi, D., Foly, N., Nagiub, H., Nagamine, T., & Fukuyama, H. (2009). Suppression of human cortico-motoneuronal excitability during the Stop-signal task. *Clinical Neurophysiology*, *120*(9), 1717–1723.

Cai, W., Oldenkamp, C. L., & Aron, A. R. (2012). Stopping speech suppresses the task-irrelevant hand. *Brain and Language*, *120*(3), 412–415.

Mills, I., Fisher, M., Wadsley, C. G., & Greenhouse, I. (2025). Failed stopping transiently suppresses the electromyogram in task-irrelevant muscles. *Eneuro*, *12*(1). https://www.eneuro.org/content/12/1/ENEURO.0166-24.2025.abstract

Wessel, J. R., Reynoso, H. S., & Aron, A. R. (2013). Saccade suppression exerts global effects on the motor system. *Journal of Neurophysiology*, *110*(4), 883–890. https://doi.org/10.1152/jn.00229.2013